Two-dimensional turbulence

1980 Rep. Prog. Phys. 43 547

(http://iopscience.iop.org/0034-4885/43/5/001)

Rep. Prog. Phys., Vol. 43, 1980. Printed in Great Britain

Two-dimensional turbulence

ROBERT H KRAICHNAN† and DAVID MONTGOMERY‡

† Dublin, New Hampshire 03444, USA
‡ Department of Physics, The College of William and Mary, Williamsburg, Virginia 23185, USA

Abstract

The theory of turbulence in two dimensions is reviewed and unified and a number of hydrodynamic and plasma applications are surveyed. The topics treated include the basic dynamical equations, equilibrium statistical mechanics of continuous and discrete vorticity distributions, turbulent cascades, predictability theory, turbulence on a rotating sphere, turbulent diffusion, two-dimensional magnetohydrodynamics, and superfluidity in thin films.

This review was received in October 1979.

0034-4885/80/050547+73 $06.50

Contents

1. Introduction

Fluid and plasma turbulence is ubiquitous in nature, at all scales from coffee cup to universe. Two-dimensional turbulence has the special distinction that it is nowhere realised in nature or the laboratory but only in computer simulations. Its importance is two-fold: first, that it idealises geophysical phenomena in the atmosphere, oceans and magnetosphere and provides a starting point for modelling these phenomena; second, that it presents a bizarre and instructive statistical mechanics. Phenomena characteristic of two-dimensional turbulence also play essential roles in the confinement of thermonuclear plasmas and in superfluid and superconductive behaviour of thin films. The latter subject has had an intense recent development.

The intent of this review is to present in a unified way the dynamical equations and statistical-mechanical behaviour, both equilibrium and non-equilibrium, of turbulent two-dimensional flows described by either continuous vorticity distributions or by the interaction of collections of discrete vortices. Then the applications of the basic phenomena, and their modifications under certain departures from strict two-dimensionality, are surveyed. We mean by turbulence disordered fluid flows which are mathematically represented by stochastic initial conditions or stochastic driving forces. The mathematical development in §§2 and 3 is given in considerable detail, more or less *ab initio*, in order to provide sufficient framework to discuss in some depth the peculiarities of the two-dimensional flow system. Later sections are less mathematical and, we hope, do not require digestion of §§2 and 3 to be understandable. The treatment in §2 is similar to that of Batchelor (1967), who gives a more extended treatment of some of the topics.

The review is incomplete both in thoroughness of coverage of the applications treated and, regrettably, by the total omission of some topics. Among the latter are numerical methods (see, for example, Orszag 1976, 1977), two-dimensional shear layers (see, for example, Saffman and Baker 1979, Aref and Siggia 1980) and recent studies of few-vortex systems (see, for example, Novikov 1975, 1978b, Aref 1979).

The treatment is phrased in the language of hydrodynamics (except for §7 which deals explicitly with magnetohydrodynamics). But much of the statistical-mechanical development applies equally well to the partly homologous problems of the guiding-centre plasma (Taylor and McNamara 1971) and the two-dimensional Coulomb gas. Some limitations on this homology are stated in §3.4.

No attempt is made to develop three-dimensional turbulence theory, except to point out contrasts between two and three dimensions. Some textbook references for three-dimensional turbulence are Tennekes and Lumley (1972), Hinze (1975) and Monin and Yaglom (1975).

An incompressible fluid differs from systems usually treated in statistical mechanics in that it is non-Hamiltonian. The energy expression is a simple sum of squares of normal-mode amplitudes and carries no hint of the non-linear dynamics expressed by the equations of motion. Nevertheless, a Liouville theorem holds in the absence of viscosity and provides the basis for an equilibrium statistical mechanics. In the two-dimensional fluid the equilibrium statistics has a most interesting structure, despite the simplicity of the energy expression, because there is an additional important constant of motion: the enstrophy, or integrated square of the vorticity.

The enstrophy constant leads to equilibria in which a large fraction of the energy is condensed into the largest spatial scales of motion, a situation closely analogous to the Einstein–Bose condensation in an ideal boson gas. But the present condensation involves negative (higher than infinite) temperatures.

Flows consisting of discrete vortices, with vorticity present only in finite concentrated cores, display an additional condensation phenomenon: a collapse into 'molecules' or bound pairs of oppositely signed vortices at low temperature. The discrete vortex system shares the negative-temperature condensation with the continuum. The phase space for a discrete vortex system in a finite volume is finite. Infinite temperature corresponds to complete statistical independence of the vortices. Higher energy states than this, in which vortices of like sign clump together, correspond to negative temperatures. At a critical value of negative temperature there is evidence for a supercondensation phenomenon, not shared with the continuum solutions: the cores of all vortices of the same sign become essentially coincident.

Like all classical fields a velocity field obeying the inviscid Navier–Stokes (Euler) equation exhibits an ultraviolet catastrophe. Normalisable inviscid equilibrium states are obtained only if the system is truncated by eliminating high-wavenumber modes. In three dimensions most of the energy in equilibrium lies in the high-wavenumber modes of the truncated system. In a non-equilibrium state in the presence of viscosity the fluid seems to seek equilibrium: energy cascades to higher wavenumbers (smaller spatial scales) until it reaches wavenumbers high enough that viscous dissipation dominates. In two dimensions, where enstrophy as well as energy are constants of inviscid motion, the equilibria are importantly different and so are the cascades in disequilibrium. Excitation of the fluid at intermediate wavenumbers results simultaneously in a cascade of energy to *lower* wavenumbers and a cascade of enstrophy to higher wavenumbers. The energy cascade to lower wavenumbers can have the result that random excitation at intermediate wavenumbers drives the (necessarily coherent) largest spatial scales of the system. Thus the two-dimensional fluid flow has a self-organising character.

In three dimensions the degree of disequilibrium in actually encountered turbulence is large. The dynamics of cascade and evolution of the statistical state are all-important and the equilibrium states are of interest only in pointing out the direction of energy cascade. In two dimensions the equilibrium solutions can be much closer to realistic states of the fluid. For some flows, and in particular for certain almost two-dimensional flows over a boundary surface with height variations, computer simulations seem well explained by an equilibrium solution in which the enstrophy is spread over all wavenumbers (to effective infinity) while the energy is trapped in low-lying modes (§5). Quasi-equilibrium solutions for the discrete vortex system are relevant to the dynamics of superfluidity in thin films (§8).

Strictly two-dimensional flow in a layer of fluid requires that the velocity vector everywhere lie in a given plane and that there be no variation of the velocity field perpendicular to that plane. Realisation of such a flow would require plane parallel, perfectly slippery boundary planes (say, horizontal) and something to inhibit vertical motion and variation. If the fluid layer is thin compared to its horizontal extent, large-scale motions are necessarily horizontal, but this does not prevent vertical variation of the horizontal motion. The latter is inhibited by sufficient viscosity but also, and importantly for geophysics, by rotation about a vertical axis. The rotation, discussed further in §5, gives an effective stiffness against vertical variations so that they can be rapidly equilibrated. In the Earth's atmosphere, which is a thin layer

on large scales, the effects of rotation are complicated by the curvature of the surface and by buoyancy effects. A vertical magnetic field in a horizontal layer of plasma has a stiffening effect similar to that of rotation (§7). Thin superfluid films (§8) would seem an ideal situation for the realisation of truly two-dimensional flow. But in fact the substrate cannot be considered a plane boundary. The gap between ideal two-dimensionality and geometries which occur in the real world must always be kept in mind when applying the theory reviewed in this paper.

2. Some equations of incompressible hydrodynamics

2.1. Three-dimensional inviscid equations of motion

The evolution of an incompressible, non-viscous fluid of constant density ρ is given by Euler's equation (Lamb 1945, Landau and Lifshitz 1959)

$$\partial \boldsymbol{u}/\partial t + \boldsymbol{u}.\nabla \boldsymbol{u} + \nabla p/\rho = 0 \tag{2.1}$$

where $\boldsymbol{u}(\boldsymbol{x}, t)$ is the velocity field, $p(\boldsymbol{x}, t)$ is the pressure field and incompressibility is expressed by

$$\nabla . \boldsymbol{u} = 0. \tag{2.2}$$

Euler's equation is a local statement of momentum conservation, the $\boldsymbol{u}.\nabla \boldsymbol{u}$ term expressing the advection of momentum by the motion. Because of (2.2) the pressure obeys

$$\nabla^2 p + \nabla.(\boldsymbol{u}.\nabla \boldsymbol{u}) = 0 \tag{2.3}$$

and may be eliminated by integration of (2.3) when boundary conditions are specified. Equation (2.1) can be rewritten as

$$\partial \boldsymbol{u}/\partial t - \boldsymbol{u} \times (\nabla \times \boldsymbol{u}) + \nabla(u^2/2 + p/\rho) = 0 \tag{2.4}$$

where $u^2 = \boldsymbol{u}.\boldsymbol{u}$. If the flow is static ($\partial \boldsymbol{u}/\partial t = 0$ everywhere) it follows from (2.4) that $u^2/2 + p/\rho$ is constant along a streamline (a streamline is the trajectory of a fluid element in a static flow).

The vorticity field $\boldsymbol{\omega}(\boldsymbol{x}, t)$ is defined by

$$\boldsymbol{\omega} = \nabla \times \boldsymbol{u}. \tag{2.5}$$

The curl of (2.4) is

$$\partial \boldsymbol{\omega}/\partial t = \nabla \times (\boldsymbol{u} \times \boldsymbol{\omega}) = -\boldsymbol{u}.\nabla \boldsymbol{\omega} + \boldsymbol{\omega}.\nabla \boldsymbol{u} \tag{2.6}$$

in which p does not appear. In a region of flow where $\omega = 0$, we may write

$$\boldsymbol{u} = \nabla \phi \qquad \nabla^2 \phi = 0 \tag{2.7}$$

and ϕ is called the velocity potential. Flows with $\omega \neq 0$ are called non-potential or rotational.

In most of this review we shall take cyclic boundary conditions on the surface of a rectangular domain or else require that the normal component of velocity vanish on the boundary surface, parts of which may be at infinity. In either case, or with a combination of the two kinds of boundary conditions, a number of conservation laws follow from (2.1) and (2.2). First are the overall conservation laws (the integrations are over the entire domain):

$$\text{total momentum: } \rho \int \boldsymbol{u}\, \mathrm{d}^3x = \text{constant} \tag{2.8(a)}$$

$$\text{total energy: } \tfrac{1}{2}\rho \int u^2\, \mathrm{d}^3x = \text{constant} \tag{2.8(b)}$$

$$\text{total vorticity: } \int \boldsymbol{\omega}\, \mathrm{d}^3x = \text{constant}. \tag{2.8(c)}$$

Equation (2.8(a)) assumes zero momentum transfer to the walls.

There are in addition an infinity of constants of motion of the form

$$\oint \boldsymbol{u}.\mathrm{d}\boldsymbol{l} = \text{constant} \tag{2.9}$$

where the integral is around any closed circuit that moves with the fluid. The left-hand side of (2.9) is called the circulation about the circuit and (2.9) expresses Kelvin's circulation theorem (Lamb 1945, Landau and Lifshitz 1959). By Stokes' theorem

$$\oint \boldsymbol{u}.\mathrm{d}\boldsymbol{l} = \int \boldsymbol{\omega}.\mathrm{d}\boldsymbol{S} \tag{2.10}$$

where $\mathrm{d}\boldsymbol{S}$ is an element of the surface bounded by the circuit. Thus (2.9) implies constancy of the total vorticity flux enclosed by a circuit that moves with the fluid.

The quantity $\int \boldsymbol{u}.\boldsymbol{\omega}\ \mathrm{d}^3x$ is called the helicity of the flow. The integrand measures the 'swirliness' about the local direction of flow. Moffatt (1969) shows that a further consequence of (2.9) is

$$\int \boldsymbol{u}.\boldsymbol{\omega}\ \mathrm{d}^3x = \text{constant} \tag{2.11}$$

and that the value of the helicity is related to the degree of knottedness or linkage of vortex lines. Vortex lines are lines everywhere tangent to $\boldsymbol{\omega}$. Since $\boldsymbol{\nabla}.\boldsymbol{\omega} = 0$, by (2.2), a vortex line either closes on itself or extends to infinity.

2.2. *Two-dimensional inviscid equations of motion*

Let $x_1 = x$, $x_2 = y$, $x_3 = z$ be a right-handed coordinate system. We define two-dimensional motion by

$$u_1(\boldsymbol{x}, t) = u_1(x, y, t) \qquad u_2(\boldsymbol{x}, t) = u_2(x, y, t) \qquad u_3(\boldsymbol{x}, t) = 0. \tag{2.12}$$

The vorticity reduces to the single component ω_3 which may be conveniently expressed in tensor notation as a pseudoscalar:

$$\omega \equiv \omega_3 = \epsilon_{ij}\,\partial u_j/\partial x_i \qquad (i, j = 1, 2) \tag{2.13}$$

with $\epsilon_{12} = 1$, $\epsilon_{ij} = -\epsilon_{ji}$. Equation (2.6) reduces to

$$\partial\omega/\partial t + \boldsymbol{u}.\boldsymbol{\nabla}\omega = 0. \tag{2.14}$$

Equation (2.14) expresses the important fact that ω is constant in time at a point which moves with the fluid. This also can be seen from (2.9) and (2.10) by taking an infinitesimal circuit which bounds a fluid element. Thus, in two-dimensional flow the infinity of constants of motion associated with Kelvin's theorem are the values of ω in every fluid element. Alternatively, we may say that $\int \omega^n\ \mathrm{d}^2x$ is a constant of motion for all n. In particular, there is a quadratic constant of motion

$$\Omega = \int \omega^2\ \mathrm{d}^2x \tag{2.15}$$

which is called the enstrophy of the flow. The energy and the enstrophy appear to be the only quadratic constants of motion for the two-dimensional Euler system while energy and helicity appear to be the only such constants for the three-dimensional system. In two-dimensional flow $\boldsymbol{u}.\boldsymbol{\omega} = 0$ identically.

Let us confine the two-dimensional flow between slippery plane boundaries perpendicular to the z axis and redefine ρ as the density per unit area.

Then the kinetic energy may be written as

$$E=\tfrac{1}{2}\rho\int u^2\,\mathrm{d}^2x. \tag{2.16}$$

The existence of the two constants E and Ω implies a profound difference between the dynamics of two- and three-dimensional turbulence. In the latter the mean-square vorticity can be increased by the stretching of vortex tubes. The constancy of Ω in two dimensions expresses the intrinsic three-dimensionality of the stretching mechanism (Batchelor 1952).

The velocity field can be derived from a pseudoscalar potential ψ called the stream function:

$$u_i(\boldsymbol{x},t)=\epsilon_{ij}\,\partial\psi(\boldsymbol{x},t)/\partial x_j. \tag{2.17}$$

The vorticity is then given by

$$\omega(\boldsymbol{x},t)=-\nabla^2\psi(\boldsymbol{x},t) \qquad (\nabla^2=\partial^2/\partial x^2+\partial^2/\partial y^2). \tag{2.18}$$

The condition that the normal velocity component vanish at a boundary is that ψ be constant on the boundary. In the case of a totally enclosed domain or an infinite domain with localised velocity field it is convenient to take this constant value as zero. In a rectangular domain with rigid slippery walls perpendicular to the y axis and cyclic boundary conditions in the x direction a uniform velocity v in the x direction is described by $\psi=vy+\text{constant}$.

A velocity field corresponding to a given $\omega(\boldsymbol{x},t)$ can be found by inverting (2.18). It is illuminating to do this for more general boundary conditions than we may actually want to use. Consider a simply-connected domain D with a closed boundary which is rigid and slippery except for two straight-line segments parallel to the y axis, each of length W. We require that $\boldsymbol{u}$ and ψ be the same on each segment. This is a generalisation of cyclic conditions for a rectangular channel and if $W=0$ it reduces to a domain totally enclosed by rigid walls. A particular solution of (2.18) is

$$\psi_\omega(\boldsymbol{x},t)=\int G_\psi(\boldsymbol{x},\boldsymbol{x}')\,\omega(\boldsymbol{x}',t)\,\mathrm{d}^2x \tag{2.19}$$

where the integration is over the entire domain and G_ψ satisfies

$$\nabla^2G_\psi(\boldsymbol{x},\boldsymbol{x}')=-\delta(\boldsymbol{x}-\boldsymbol{x}') \qquad (\boldsymbol{x},\boldsymbol{x}'\in D) \tag{2.20}$$

with the boundary condition that $G_\psi(\boldsymbol{x},\boldsymbol{x}')$ vanish for $\boldsymbol{x}$ anywhere on the boundary except for the straight-line segments, where it exhibits the required cyclic variation. An explicit form for G_ψ is

$$G_\psi(\boldsymbol{x},\boldsymbol{x}')=\sum_n\lambda_n^{-2}\,\phi_n(\boldsymbol{x})\,\phi_n(\boldsymbol{x}') \tag{2.21}$$

where the complete orthonormal set of eigenfunctions ϕ_n satisfy $\nabla^2\phi_n+\lambda_n^2\phi_n=0$ and the boundary conditions for G_ψ. Clearly $G_\psi(\boldsymbol{x},\boldsymbol{x}')=G_\psi(\boldsymbol{x}',\boldsymbol{x})$.

The general solution of (2.18) is then

$$\psi(\boldsymbol{x},t)=\psi_\omega(\boldsymbol{x},t)+\psi_\mathrm{p}(\boldsymbol{x},t) \tag{2.22}$$

where $\psi_\mathrm{p}(\boldsymbol{x},t)$, which represents a potential flow, satisfies $\nabla^2\psi_\mathrm{p}=0$ and has zero tangential derivative over all of the boundary except the straight-line segments where it obeys the cyclic conditions. By (2.17) the difference in value of $\psi_\mathrm{p}(\boldsymbol{x},t)$ at the two ends of a straight-line segment gives the rate of flow (integral of u_x) through the segment. $\psi_\omega(\boldsymbol{x},t)$ as given by (2.19)–(2.21) represents zero rate of flow through

the line segments. In the case of a rectangular domain with cyclic conditions on the ends, the ϕ_n are trigonometric functions and $\psi_p = vy + \text{constant}$, corresponding to a uniform velocity v. If $W=0$ (total enclosure by rigid boundaries) ψ_p is identically zero. Whatever the boundary conditions are, if $|\boldsymbol{x}| \ll L$, $|\boldsymbol{x}'| \ll L$ then

$$G_\psi(\boldsymbol{x}, \boldsymbol{x}') \approx -(2\pi)^{-1} \ln (|\boldsymbol{x}-\boldsymbol{x}'|/L) \tag{2.23}$$

where L is some typical distance of the boundary from the coordinate origin. For a domain of arbitrary shape this follows from the approach of the ϕ_n to trigonometric form for large λ_n (Courant and Hilbert 1953).

The kinetic energy can be written in the forms

$$E = \tfrac{1}{2}\rho \int |\nabla\psi|^2 \, \mathrm{d}^2x = \tfrac{1}{2}\rho \int \omega\psi_\omega \, \mathrm{d}^2x + \tfrac{1}{2}\rho \int |\nabla\psi_p|^2 \, \mathrm{d}^2x \equiv E_\omega + E_p. \tag{2.24(a, b)}$$

This follows from (2.16)–(2.18) and $\nabla^2\psi_p = 0$, upon a partial integration and use of the boundary conditions. Note that there are no cross terms in (2.24(*b*)) between the vortical flow and the potential flow. Equations (2.19) and (2.21) give

$$E_\omega = \tfrac{1}{2}\rho \int G_\omega(\boldsymbol{x}, \boldsymbol{x}') \, \omega(\boldsymbol{x}) \, \omega(\boldsymbol{x}') \, \mathrm{d}^2x \, \mathrm{d}^2x' = \tfrac{1}{2}\rho \sum_n \lambda_n^{-2} (\omega_n)^2 \tag{2.25(a, b)}$$

where $\omega_n = \int \omega(\boldsymbol{x}) \, \phi_n(\boldsymbol{x}) \, \mathrm{d}^2x$.

First-order equations of motion for the ω_n follow from (2.14). ψ_p is fixed by the boundary conditions except for a multiplicative constant, which determines the magnitude of the potential velocity field, and a trivial additive constant. Since the walls are rigid, the total kinetic energy of the flow is constant. Therefore the evolution of the potential velocity field satisfies

$$\mathrm{d}E_p/\mathrm{d}t = -\mathrm{d}E_\omega/\mathrm{d}t. \tag{2.26}$$

There is dynamical coupling between the vortical and potential velocity fields even though there is no interaction energy. In the case of a rectangular channel with cyclic conditions on the ends the potential flow is uniform throughout the domain and trivially convects the vortical flow, with $\mathrm{d}E_\omega/\mathrm{d}t = 0$. The uniform flow then is constant in time. We shall discuss the implications of (2.26) more generally in the context of discrete vortices.

If $\psi(\boldsymbol{x}) = \phi_n(\boldsymbol{x})$, (2.17) and (2.18) give $\boldsymbol{u} \cdot \nabla\boldsymbol{\omega} = 0$ so that, by (2.14), the fields are constant in time. Thus the $\phi_n(\boldsymbol{x})$ represent stationary eigensolutions of the equations of motion. ψ_p is also a stationary eigensolution. The general stationary flow has $\omega = f(\psi)$.

2.3. Systems of discrete vortices

If the vorticity is initially confined to small regions separated by irrotational fluid this situation will persist because the vorticity moves with the incompressible flow. The study of systems of such discrete vortices was initiated by Helmholtz in 1858, and other early contributions were made by Lord Kelvin (W Thomson), J J Thomson, Kirchhoff and T von Kármán (Lamb 1945). A comprehensive treatment is given by Lin (1943). In three dimensions the typical localised vortex is the vortex ring (smoke ring). In the two-dimensional flow between parallel plates the typical vortex is a circular cylinder of fluid, with uniform vorticity, extending perpendicularly between the plates and surrounded by vorticity-free fluid. The two-dimensional analogue of the vortex ring is a pair of such cylinders with equal and opposite vorticity.

A single circular (cylindrical) vortex far from boundaries will keep its shape and maintain its position unchanged. This follows from symmetry if there is no flow except that due to the vortex itself. If a number of such vortices are present, each will move in the total velocity field, and gradients in that field will act to distort the vortical cores. If the core diameters are small compared to the separations between vortices the core distortion will be small, and it is further reduced by stability properties (Lamb 1945). We wish now to discuss the dynamics of a system of discrete vortices in the approximation where core distortion is neglected. We limit discussion to the case where all vortices have the same core diameter and distribution of vorticity within the core but allow variation of sign and magnitude of total core vorticity from vortex to vortex.

We want then to consider vorticity fields of the form $\omega(\boldsymbol{x})=\Sigma_i\, q_i\Delta(|\boldsymbol{x}-\boldsymbol{r}_i|)$ where q_i is the circulation about the ith vortex, whose position is $\boldsymbol{r}_i$, and $\Delta(\boldsymbol{x})$ is the core shape function satisfying $\int \Delta(\boldsymbol{x})\, \mathrm{d}^2x=1$. This cannot be done with complete consistency both because there is no way to consistently rule out all close encounters of vortices and because the cores cannot intersect the rigid walls. We shall eventually be interested in the limit of point vortices, for which these problems disappear, but we do not simply take $\Delta(\boldsymbol{x})=\delta(\boldsymbol{x})$ at the outset because, as will appear below, this implies an infinite kinetic energy. Perhaps the cleanest resolution is to restrict $\Delta(\boldsymbol{x})$ by

$$\omega(\boldsymbol{x})=\sum_i q_i\Delta(\boldsymbol{x},\boldsymbol{r}_i) \qquad \Delta(\boldsymbol{x},\boldsymbol{r}_i)=\sum_n f(\lambda_n)\,\phi_n(\boldsymbol{x})\,\phi_n(\boldsymbol{r}_i) \quad (2.27(a,b))$$

where

$$f(\lambda_n)=1\ (a\lambda_n\leqslant 1) \qquad f(\lambda_n)=0\ (a\lambda_n>1) \tag{2.28}$$

and a is a characteristic dimension of the core. If $a\to 0$, $\Delta(\boldsymbol{x},\boldsymbol{r}_i)\to\delta(\boldsymbol{x}-\boldsymbol{r}_i)$. If $a>0$ but is small compared to domain dimensions, (2.28) represents a wavenumber cutoff of $\Delta(\boldsymbol{x},\boldsymbol{r}_i)$ if $\boldsymbol{x}$ and $\boldsymbol{r}_i$ are located at distances much greater than a from the walls, since the high-order eigenfunctions are essentially trigonometric functions away from the walls.

Most recent papers on systems of discrete vortices in hydrodynamics and the guiding-centre plasma have assumed $a=0$ at the start. Finite a is essential in treating vortex dynamics in two-dimensional superfluids.

Because of the orthonormal property of the ϕ_n, it follows from (2.19) and (2.25(a)) that the stream function and the kinetic energy of the vortices are

$$\psi_\omega(\boldsymbol{x})=\sum_i q_i G_\psi'(\boldsymbol{x},\boldsymbol{r}_i) \qquad E_\omega=\tfrac{1}{2}\rho\sum_{ij} q_i q_j G_\psi'(\boldsymbol{r}_i,\boldsymbol{r}_j) \quad (2.29(a,b))$$

where

$$G_\psi'(\boldsymbol{x},\boldsymbol{x}')=\sum_n f(\lambda_n)\,\lambda_n^{-2}\,\phi_n(\boldsymbol{x})\,\phi_n(\boldsymbol{x}') \tag{2.30}$$

is a modified Green function regular everywhere in the domain. Under our approximation that there is no distortion of the cores, the evolution of the system is determined by $\mathrm{d}\boldsymbol{r}_i/\mathrm{d}t=\boldsymbol{u}(\boldsymbol{r}_i,t)$. Thus, by (2.17) and (2.29)

$$\rho q_i\,\mathrm{d}x_i/\mathrm{d}t=\partial E_\omega/\partial y_i \qquad \rho q_i\,\mathrm{d}y_i/\mathrm{d}t=-\partial E_\omega/\partial x_i \tag{2.31}$$

where $\boldsymbol{r}_i=(x_i,y_i)$.

If the boundaries are infinitely removed from the vortex system, symmetry requires that each vortex be unmoved by its own velocity field. Then E_ω in (2.31)

may be replaced by the interaction energy

$$E_{\text{int}} = \rho \sum_{i<j} q_i q_j G_\psi'(\boldsymbol{r}_i, \boldsymbol{r}_j). \tag{2.32}$$

If, in addition, the vortices are separated by distances large compared to a then G_ψ' in (2.32) may be replaced by (2.23). If the cores are exactly circular and wholly localised within a radius a, then this replacement is exact if the cores do not intersect, but except in the limit $a \to 0$ the exactitude is illusory since the cores will not stay precisely circular. The quasi-Hamiltonian formulation (2.31) with E_{int} replacing E_ω was first given for point vortices by Kirchhoff (Lamb 1945).

If a single vortex is near a slippery rigid boundary it will move in its own velocity field. In analogy to electromagnetic theory, this can be interpreted as motion of the vortex in the field of an induced image vortex which has equal and opposite circulation and is symmetrically placed on the far side of the boundary. By symmetry the combined fields of the two vortices satisfy the boundary condition of zero normal velocity. The contribution of the self-energy term ($j=i$) in E_ω to (2.31) may be interpreted as image velocity field. If the boundaries have arbitrary shape, an image contribution $\Delta G_\psi(\boldsymbol{x}, \boldsymbol{x}')$ to the point-vortex Green function may be defined by (see (2.23))

$$G_\psi(\boldsymbol{x}, \boldsymbol{x}') = -(2\pi)^{-1} \ln\left(|\boldsymbol{x}-\boldsymbol{x}'|/L\right) + \Delta G_\psi(\boldsymbol{x}, \boldsymbol{x}'). \tag{2.33}$$

$\Delta G_\psi(\boldsymbol{x}, \boldsymbol{x}')$ satisfies Laplace's equation (Lin 1943).

The kinetic energy of a single vortex far from boundaries with a core of diameter a may be obtained by using (2.23) to compute the velocity field external to the core and noting that the velocity goes to zero at the centre of the core. This gives

$$E_i = (\rho/4\pi)\, q_i^2 \left[\ln\,(L/a) + \mathrm{O}(1)\right]. \tag{2.34}$$

Next consider a pair of equal and opposite vortices separated by a distance r_{ij} and far from boundaries. Using (2.23) in (2.32) we have

$$E_{ij} = (\rho/2\pi) q^2 \ln\,(r_{ij}/L) \qquad (q_i q_j = -q^2) \tag{2.35(a)}$$

$$E_i + E_{ij} + E_j = (\rho/2\pi) q^2 \left[\ln\,(r_{ij}/a) + \mathrm{O}(1)\right] \tag{2.35(b)}$$

for the interaction energy and total energy of the pair. If a vortex is a distance l from a rigid boundary plane, and other boundaries are far away, we may apply (2.35(b)) to the pair formed by the vortex and its image. This gives

$$E_i = (\rho/4\pi) q_i^2 \left[\ln\,(2l/a) + \mathrm{O}(1)\right] \tag{2.36}$$

for the kinetic energy of the actual vortex, where we note that half the pair energy is in the image space. Since the velocity field of an isolated vortex is everywhere perpendicular to the radius vector, an isolated pair of equal and opposite vortices maintain a constant distance apart and travel with velocity of magnitude $q/2\pi r_{ij}$ perpendicular to the line joining them. This result also applies to a vortex-image pair. If a pair of equal and opposite vortices are separated by r_{ij} and a distance l from a boundary plane, (2.35(b)) is valid if $r_{ij} \ll l \ll L$. The effects of the boundary on E_i and E_j exhibited in (2.36) are cancelled by effects on E_{ij}.

A correspondence between continuous and discrete representations of vorticity may be set up as follows. Divide up a continuous vorticity distribution into sub-areas such that each contains vorticity of one sign only and the magnitude of vorticity in each sub-area is the same. Then concentrate the vorticity of each sub-area into

a concentrated core occupying a small fraction f of the sub-area and located at the centre of gravity of the latter. Now consider a limit in which the number of sub-areas increases indefinitely with f constant. In the limit the total self-energy of all the concentrated vortices goes to zero and their interaction energy (which is independent of f if $f \ll 1$) equals the kinetic energy of the continuous distribution. Optimum correspondences (in a statistical sense) between continuous vorticity and a finite number of discrete vortices are considered in §3.3.

2.4. Vortex momentum and the Magnus force

The vortex flows described by (2.19) or (2.29) have zero momentum; there is instantaneously no net flow through either of the boundary segments with cyclic boundary conditions. This follows immediately from the condition that $\psi_\omega(\boldsymbol{x})$ vanish on each of the rigid boundary segments. However, the generation of a vortical flow by forces applied to the fluid in general does impart momentum to the fluid. If the boundaries are indefinitely remote from the vorticity, and the forces are local, this momentum has a unique value (Lamb 1945). But in the presence of boundaries the imparted momentum is non-unique; it depends on the distribution of the forces. Vortex flow with momentum is described by adding to $\psi_\omega(\boldsymbol{x})$ a potential-flow contribution $\psi_p(\boldsymbol{x})$.

The creation of a single vortex infinitely far from boundaries is impossible since by (2.34) the energy is infinite. Consider then the creation of the vortex pair whose energy is (2.35(*b*)). Lamb (1945) points out that there is an oval, within which the vortex centres are symmetrically placed, such that the fluid within the oval stays inside and is carried along with the linear motion of the cores, while the fluid outside executes a potential flow identical to what would be induced by the motion of a rigid body that occupied the oval. This is the two-dimensional analogue of the motion of the core of a smoke ring through a fluid. The flow can be started from rest by applying forces confined in the oval which produce the internal spinning about the cores together with the linear motion. Generation of the linear motion requires that an impulse be delivered to the fluid such that the total fluid momentum becomes (i and j denote the two vortices)

$$P_{ijx} = \rho(q_i y_i + q_j y_j) \qquad P_{ijy} = -\rho(q_i x_i + q_j x_j) \qquad (q_i = -q_j). \qquad (2.37(a, b))$$

Lamb shows further that this result is independent of the specific force distribution employed provided that the forces are localised within some finite region containing the cores and that the boundaries are infinitely distant. The result extends to any set of discrete vortices whose strengths add to zero, and to continuous vorticity distributions. Thus

$$P_x = \rho \sum_i q_i y_i \qquad P_y = -\rho \sum_i q_i x_i \qquad \left(\sum_i q_i = 0\right) \qquad (2.38)$$

is the total momentum imparted in the creation of the flow. Since the creation by forces can be imagined to take place anytime in the evolution of the flow, a corollary is that the right-hand sides of (2.38) are constants of motion in the absence of boundaries. The destruction of vortices by local forces imparts momentum of opposite sign to the fluid.

In the presence of a rigid boundary these considerations are importantly changed. A single vortex now has a finite energy (2.36) and can be created by applying the

above pair-creation mechanism to the vortex and its image; that is, by applying forces to a half-oval of fluid bounded by the wall. If there is only a single straight boundary and $\Sigma_i q_i = 0$, it can be seen that the total imparted momentum is the same whether the vortices are created in real pairs or as halves of real-image pairs. But if there are two rigid boundaries, or the boundary is curved, this is not the case. P_x and P_y defined by (2.38) are then not constants of motion in general because of interaction between the real vortices and the images. However, they are constants of motion in a straight-walled channel of uniform width with cyclic (re-entrant) ends. This is because in such a channel there is no possibility of momentum transfer between flow and walls or, in other words, between flow and image flow.

Now consider a vortex pair infinitely far from boundaries. Let the core of vortex i be moved *through* the fluid by an applied force. The rate of change of the imparted momentum (2.37) associated with creation of the flow from rest is

$$F_x = \mathrm{d}P_{ijx}/\mathrm{d}t = \rho q_i[\mathrm{d}y_i/\mathrm{d}t - u_y(\boldsymbol{r}_i)] \qquad F_y = \mathrm{d}P_{ijy}/\mathrm{d}t = -\rho q_i[\mathrm{d}x_i/\mathrm{d}t - u_x(\boldsymbol{r}_i)]. \tag{2.39}$$

$\boldsymbol{F}$ is then the force exerted on the core. (Note that motion of the core with the fluid velocity $\boldsymbol{u}(\boldsymbol{r}_i)$ produces no change in $\boldsymbol{P}_{ij}$.) The reaction on the forcing system $-\boldsymbol{F}$ is called the Magnus or lift force (Lamb 1945, Landau and Lifshitz 1959, Milne-Thomson 1960). It arises from pressure differences on the surface of the core due to interaction of the circulating motion and the motion through the fluid and is independent of whether boundaries are present provided that they are many core diameters distant. Since a pair may be created at a very small separation and then pulled apart by forces on the cores, it follows that (2.37) is valid in the presence of arbitrarily placed and shaped boundaries if the core diameters are small enough and $\boldsymbol{P}_{ij}$ denotes the total impulse delivered to fluid and boundaries. A discussion of the Magnus force on curved vortex cores in three dimensions is given by Huggins (1970).

Suppose that there is initially a uniform flow with velocity $\boldsymbol{v}_0$ directed along the x axis of a rectangular channel of length L and width W with rigid walls and cyclic boundary conditions on the ends. Let a system of vortex pairs be created by nucleation within the channel, that is, each pair is created at very small separation and then spread to some finite separation by forces on the cores. The momentum imparted to the fluid is given by (2.38) and the uniform velocity after creation is $\boldsymbol{v} = \boldsymbol{v}_0 + \boldsymbol{P}/M$ where $M = \rho LW$ is the total mass of fluid in the channel. The total kinetic energy after creation is

$$E = E_\omega + \tfrac{1}{2} M v^2. \tag{2.40}$$

The interaction energy of the created pairs with the pre-existing uniform flow is the contribution $\boldsymbol{P}.\boldsymbol{v}_0$ to $\frac{1}{2}Mv^2$. It should be noted that once creation is complete there is no way to distinguish the individual pair contributions to $\boldsymbol{v}$. Each pair moves in the total $\boldsymbol{v}$. A different result is obtained if the vortices with positive and negative signs of circulation are independently nucleated at the walls as partners in vortex-image pairs and then moved to positions in the fluid by forces on the cores. Then (2.38) must be replaced by the more general form

$$P_x = \rho \sum_i q_i (y_i - y_i^0) \qquad P_y = -\rho \sum_i q_i (x_i - x_i^0) \tag{2.41}$$

where $\boldsymbol{r}_i^0$ is the position of nucleation. If all positive vortices are nucleated at the wall $y=W$ and all negative ones at $y=0$ then $P_x=\rho\Sigma_i q_i(y_i-\frac{1}{2}W)$. In any event P_y is transmitted to the walls and does not appear as fluid motion.

In the channel with straight parallel walls $\boldsymbol{v}$ is constant, independent of the motion of the vortices once they are created. The potential flow is in general not constant if the walls are non-parallel or curved. Consider a long channel with two sections of different width and a smooth transition between them. Suppose that a vortex pair aligned at right angles to and symmetric with respect to the channel axis is convected by potential flow from the wide to the narrow section. If the difference in width is large enough and the original separation y_i-y_j is large enough this must be accompanied by a decrease in separation and a consequent decrease in the kinetic energy of the vortex motion E_ω. By (2.26) the kinetic energy of the potential flow must increase. If the initial velocity of the potential flow is below some critical value the vortex pair cannot enter the constriction and instead is repelled by the image field. This is because the required increase in kinetic energy of the potential flow if the pair were to enter involves more momentum than the system has available by exchange with the walls (images).

2.5. *Viscosity*

If the viscosity is non-zero (2.1) is replaced by the incompressible Navier–Stokes equation (Landau and Lifshitz 1959)

$$\partial\boldsymbol{u}/\partial t+\boldsymbol{u}.\nabla\boldsymbol{u}+\nabla p/\rho=\nu\nabla^2\boldsymbol{u} \tag{2.42}$$

where ν is the coefficient of kinematic viscosity, and (2.14) becomes

$$\partial\omega/\partial t+\boldsymbol{u}.\nabla\omega=\nu\nabla^2\omega. \tag{2.43}$$

Viscosity directly affects only the vortical flow since $\nabla^2\psi_{\mathrm{p}}=0$. But with viscosity it may be physically appropriate to replace slippery boundary conditions by no-slip conditions with the result that vorticity can be generated at the walls in an initially purely potential flow. The viscous term in (2.43) diffuses the vorticity through the fluid so that the vorticity in each fluid element no longer is a constant of motion. The diffusion of vorticity may be interpreted in terms of Magnus forces associated with the viscous stresses (Huggins 1970).

If the flow is localised in an infinite domain or if there are cyclic boundary conditions $\int\omega\,\mathrm{d}^2x$ remains a constant of motion under the action of viscosity since the integral of $\nu\nabla^2\omega$ is then zero. But this is not so if there are slippery rigid boundaries (real and image vorticity can diffuse into each other), and, for any of the boundary conditions, viscosity makes E and Ω decrease with time. The viscous effects on the inviscid constants of motion have a simple expression in terms of the eigenmode amplitudes. In correspondence to (2.25(b)) we have

$$\Omega=\sum_n\omega_n{}^2 \qquad J\equiv\int\omega\,\mathrm{d}^2x=\sum_n\omega_n\int\phi_n(\boldsymbol{x})\,\mathrm{d}^2x \tag{2.44(a, b)}$$

and the decay is given by

$$-\mathrm{d}E_\omega/\mathrm{d}t=\nu\rho\sum_n\omega_n{}^2 \qquad -\mathrm{d}\Omega/\mathrm{d}t=2\nu\sum_n\lambda_n{}^2\omega_n{}^2$$
$$-\mathrm{d}J/\mathrm{d}t=\nu\sum_n\omega_n\lambda_n{}^2\int\phi_n(\boldsymbol{x})\,\mathrm{d}^2x. \tag{2.45(a, b, c)}$$

If the boundary conditions are fully cyclic on a rectangular domain the $\phi_n(\boldsymbol{x})$ are sin and cos functions satisfying $\lambda_n{}^2\int\phi_n(\boldsymbol{x})\,\mathrm{d}^2x=0$, $\phi_0(\boldsymbol{x})=(LW)^{-1/2}$. Then $J=(LW)^{1/2}\omega_0$ and $\boldsymbol{u}$ can be defined only if $J=0$.

3. Absolute statistical equilibrium

3.1. The detailed Liouville theorem

The equilibrium statistical mechanics of a classical system with canonical coordinates q_i and momenta p_i is based upon Liouville's theorem

$$\sum_i (\partial\dot{q}_i/\partial q_i+\partial\dot{p}_i/\partial p_i)=0 \tag{3.1}$$

(Tolman 1938), which expresses the incompressibility of the motion in phase space. The parenthesised expression in (3.1) vanishes individually for each i in consequence of Hamilton's equations

$$\dot{q}_i=\partial H/\partial p_i \qquad \dot{p}_i=-\partial H/\partial q_i. \tag{3.2}$$

We shall call this the detailed Liouville theorem.

A detailed Liouville theorem also exists for the two-dimensional flow system, although this system is not Hamiltonian. It is (Lee 1952)

$$\partial\dot{\omega}_n/\partial\omega_n=0 \tag{3.3}$$

where the ω_n are the eigenfunction amplitudes defined after (2.25). Equation (3.3) is easily derived by a method (Kraichnan 1965a, Salmon *et al* 1976) which uses only the conservation of energy E_ω (2.25(*b*)) and the stationary property of the eigenmodes. Assume to start with that the domain is simply connected, with rigid boundaries, so that there is no potential flow. Then the quadratically non-linear equation of motion (2.14) may be written in the form

$$\dot{\omega}_n=\sum_{rs} A_{nrs}\omega_r\omega_s \qquad (A_{nrs}=A_{nsr}) \tag{3.4}$$

where the coefficients A_{nrs} are constants. By supposing that at some instant only ω_n, ω_r, ω_s are non-zero we see that the conservation of the sum of squares Ω (2.44(*a*)) implies

$$A_{nrs}+A_{rsn}+A_{snr}=0 \tag{3.5}$$

and conservation of E_ω implies

$$\lambda_n{}^{-2}A_{nrs}+\lambda_r{}^{-2}A_{rsn}+\lambda_s{}^{-2}A_{snr}=0. \tag{3.6}$$

Terms in (3.4) with n, r and s all different give no contribution to $\partial\dot{\omega}_n/\partial\omega_n$. The coefficients A_{nss} vanish by the stationary property of the eigenmode $\phi_s(\boldsymbol{x})$. A_{nnn} vanishes in particular, and by (3.6) $A_{nsn}=0$ implies $A_{nsn}=A_{nns}=0$. This exhausts the possibilities and we have (3.3).

Now consider more general boundary conditions which permit a potential flow described by ψ_{p}. We may take fully cyclic boundary conditions, a channel with rigid sides and cyclic ends, or a multiply connected domain with a rigid closed outer boundary that encloses R rigid closed interior boundaries. In the last-named case, which is most general, the stream function for potential flow may be written

$$\psi_{\mathrm{p}}=\sum_i a_i\phi_0{}^{(i)}(\boldsymbol{x}) \qquad (i=1,2,\ldots,R) \tag{3.7}$$

where $\nabla^2\phi_0^{(i)}(\boldsymbol{x})=0$ throughout the domain and $\phi_0^{(i)}(\boldsymbol{x})$ is zero everywhere on the boundaries except that it equals one on the ith internal boundary. The total kinetic energy is (2.24) where

$$E_\mathrm{p}=\frac{\rho}{2}\sum_{ij} D_{ij}a_i a_j \qquad (D_{ij}=D_{ji}) \tag{3.8}$$

and D_{ij}, which has only positive eigenvalues, is a constant matrix which depends on the particular geometry. The $\phi_0^{(i)}(x)$ are a degenerate set of stationary eigenfunctions of the equations of motion (eigenvalue zero), and any linear combination (3.7) is a stationary eigenfunction.

The preceding arguments, using only the quadratic form of the kinetic energy and the stationarity of the eigenfunctions, readily extend to the system with potential flow. They show that the equations of motion for the ω_n and a_i are restricted to the form

$$\dot{\omega}_n=\sum_{rs} A_{nrs}\omega_r\omega_s+\sum_{im} B_{nim}a_i\omega_m \qquad \dot{a}_i=\tfrac{1}{2}\sum_{nm} C_{inm}\omega_n\omega_m \tag{3.9(a, b)}$$

($C_{inm}=C_{imn}$) where (3.5) and (3.6) are augmented by

$$\lambda_n^{-2}B_{nim}+\lambda_m^{-2}B_{min}+\sum_j D_{ij}C_{jnm}=0 \tag{3.10}$$

and $A_{nsn}=A_{nns}=B_{nin}=C_{inn}=0$. Thus (3.3) is replaced by

$$\partial\dot{\omega}_n/\partial\omega_n=0 \qquad \partial\dot{a}_i/\partial a_i=0. \tag{3.11(a, b)}$$

Equations (3.7)–(3.11) continue to apply in the case of a rigid-sided channel with cyclic ends, where ψ_p has only one component and in the case of fully cyclic boundary conditions on a rectangular channel, where ψ_p has two components $\phi_0^{(i)}(\boldsymbol{x})$. In the latter case, or in the case of a rectangular channel, the potential flow is spatially uniform and unaffected by vortex motion, so that all C_{inm} vanish.

It should be emphasised that the detailed Liouville property depends both on the quadratic form of the constant of motion and the stationarity of the eigenfunctions. A rotation to new phase-space coordinates which are linear combinations of the ω_n and which preserve the form of E_ω as a sum of squares in general destroys (3.3) or (3.11). The importance of the detailed Liouville theorem is that the overall Liouville theorem

$$\sum_n \partial\dot{\omega}_n/\partial\omega_n+\sum_i \partial\dot{a}_i/\partial a_i=0 \tag{3.12}$$

holds under a truncation of the dynamical equations in which all terms involving any modes outside an arbitrarily chosen subset are dropped from (3.9).

The detailed Liouville theorem for a system of discrete vortices

$$\partial\dot{x}_i/\partial x_i+\partial\dot{y}_i/\partial y_i=0 \tag{3.13}$$

follows immediately from the pseudo-Hamiltonion equations (2.31) if the domain is simply connected and enclosed by a rigid boundary. Under more general boundary conditions, which permit potential flow, (2.31) is replaced by

$$\rho q_i\dot{x}_i=\partial H/\partial y_i \qquad \rho q_i\dot{y}_i=-\partial H/\partial x_i \qquad H=E_\omega+\sum_i \rho q_i\psi_\mathrm{p}(\boldsymbol{r}_i) \tag{3.14(a, b, c)}$$

and (3.13) continues to hold. Since (3.9(*b*)) is independent of whether the vorticity is concentrated into discrete cores (3.11(*b*)) also continues to hold. H is a Hamiltonian in a limited sense only. The term $\rho q_i \psi_p$ is not part of the kinetic energy, nor can it be used to obtain a Hamiltonian equation for the effect of the vortices on ψ_p.

3.2. Continuum equilibrium states

The ω_n and a_i may be taken as phase-space coordinates. An immediate consequence of (3.11) is that a phase-space probability distribution of the form $f(K)$ is stationary under the equations of motion provided that $K(\omega, a)$ is a constant of motion. The *canonical* distribution with respect to K has the form $f(K) \propto \exp(-\beta K)$ where β is a constant parameter. This distribution has a unique property of invariance or stability under arbitrary perturbations of the equations of motion which preserve the constancy of K. Thus suppose there are two systems with constants of motion K_1 and K_2 and distributions $f_1(K_1)$ and $f_2(K_2)$. Let the two initially independent systems be coupled by arbitrary coupling terms subject only to the constraint that $K_1 + K_2$ is a constant of motion of the coupled systems. The initial joint distribution $f_1(K_1) f_2(K_2)$ can be invariant under the couplings only if

$$f_1(K_1) f_2(K_2) = f(K_1 + K_2). \tag{3.15}$$

Differentiation of (3.15) with respect to argument readily shows that the general solution is $f_1(K_1) \propto \exp(-\beta K_1)$, $f_2(K_2) \propto \exp(-\beta K_2)$. Specialisation of the couplings to particular infinitesimal forms leads to the fluctuation-dissipation relations associated with the canonical distribution (Kraichnan 1959). The arbitrary couplings are an idealised representation of thermal contact.

Now let us take $\beta K = \beta E + \alpha \Omega$, a linear combination of energy and enstrophy. Here we identify β with $1/k_B T$, where k_B is Boltzmann's constant and T is temperature while α is a second parameter associated with enstrophy. Since both E and Ω are additive over the ω_n, the two systems of the preceding paragraph can be taken as subsystems of the actual system, and the arbitrary conservative couplings can be taken as perturbations of the A_{nrs} which obey a suitable linear combination of (3.5) and (3.6).

It is convenient and illuminating to call $(k_B \beta)^{-1}$ the 'energy temperature' and $(k_B \alpha)^{-1}$ the 'enstrophy temperature'. This represents a reversal in the roles of the symbols α and β from the usage in the previously mentioned literature, which we hope will not cause undue confusion.

More conventionally, the canonical distribution for the two-dimensional flow system can be obtained from the microcanonical distribution for a supersystem along the lines laid out by Khinchin (1949). (The microcanonical distribution is confined to and uniform on a surface of constant K in the phase space.) This has been carried out by Montgomery and Joyce (1974) for the discrete vortex system and can be extended to the continuum system. A very large number of (dynamically identical) individual flow systems are weakly and conservatively coupled by terms added arbitrarily to their equations of motion, thereby forming the supersystem. The canonical distribution for an individual flow system is then obtained from the microcanonical distribution for the supersystem by an application of the central limit theorem.

It is important to note that the supersystem cannot be formed by simply taking the flow system of interest as part of a very large volume of fluid. As we shall see,

excitations of the gravest modes of the system, which depend directly upon the dimensions of the fluid, can be very important in equilibrium. In this respect the two-dimensional hydrodynamic equilibrium differs sharply from that of, say, a three-dimensional gas of hard spheres.

The systems usually considered in statistical mechanics are large, with many similar components, with the result that fractional fluctuations in energy are small over the canonical ensemble and low-order averages are nearly the same in canonical and microcanonical distributions. We shall see that this is sometimes not so with two-dimensional flow systems. The microcanonical distribution (for an individual flow system now) is appropriate where there is isolation and the system is ergodic. The canonical ensemble is appropriate where there is weak coupling to an environment. The couplings may be time-dependent (Kraichnan 1959) and arbitrary, thereby forcing ergodicity.

In common with all classical fields, the two-dimensional flow system exhibits an ultraviolet catastrophe. There is a finite energy in equilibrium associated with each of the infinite set of modes ω_n, so that the mean energy of the whole system is infinite for finite β and α. The equilibrium statistical mechanics therefore is meaningful only if the system is truncated. We do this by choosing two cutoff parameters $\lambda_{\min}$ and $\lambda_{\max}$ and retaining only the ω_n such that $\lambda_{\min}{}^2 \leqslant \lambda_n{}^2 \leqslant \lambda_{\max}{}^2$. Every term in (3.9) involving a mode outside this range is dropped. The lower cutoff $\lambda_{\min}$ is not needed to avoid the ultraviolet catastrophe but is included for completeness. Because of (3.5), (3.6) and (3.11) the truncated system has the conservation and Liouville properties of the full system.

The equilibrium statistics which we shall now discuss do not have a direct pertinence to typical turbulence, which is far from absolute equilibrium (but see §§5 and 8). But the equilibrium states do appear to represent states toward which the actual turbulent states tend to relax and thereby are of value in predicting the direction and structure of the exchange of energy among the modes (Novikov 1974).

The average value $\langle g \rangle$ of any function in the canonical distribution for the truncated system is given by

$$\langle g \rangle = \int g \exp(-\beta E + \alpha\Omega) \Pi \, \mathrm{d}\omega \Pi \, \mathrm{d}a / Z \tag{3.16}$$

where Z is the partition function

$$Z = \int \exp(-\beta E + \alpha\Omega) \Pi \, \mathrm{d}\omega \Pi \, \mathrm{d}a. \tag{3.17}$$

These formulae yield

$$\bar{E}_n \equiv \tfrac{1}{2}\rho \langle \omega_n \rangle^2 \lambda_n{}^{-2} = \tfrac{1}{2}(\beta + 2\alpha\lambda_n{}^2/\rho)^{-1} \qquad \bar{\Omega}_n \equiv \langle \omega_n{}^2 \rangle = \lambda_n{}^2/(\rho\beta + 2\alpha\lambda_n{}^2)^{-1} \tag{3.18(a, b)}$$

$$\langle a_i a_j \rangle = (\rho\beta)^{-1} D_{ij}{}^{-1} \qquad E_{\mathrm{p}} \equiv \tfrac{1}{2}\rho \sum_{i,j} D_{ij} \langle a_i a_j \rangle = \tfrac{1}{2} R/\beta \tag{3.19(a, b)}$$

where $D_{ij}{}^{-1}$ is the inverse matrix to D_{ij}. The averaged total energy and enstrophy are

$$\bar{E} = \bar{E}_\omega + \bar{E}_{\mathrm{p}} = \sum_n \bar{E}_n + \bar{E}_{\mathrm{p}} \qquad \bar{\Omega} = \sum_n \bar{\Omega}_n. \tag{3.20(a, b)}$$

If $\alpha = 0$, (3.18) and (3.19) give simple equipartition of energy among the modes of the vortical and potential flow. The general case with $\alpha \neq 0$ has a much richer structure. Unless $R = 0$ (singly connected domain enclosed by a rigid boundary), the requirement that $\bar{E}_{\mathrm{p}}$ be finite and non-negative implies $\beta > 0$. α can be negative

as well as positive but is restricted by $\rho\beta+2\alpha\lambda_{\max}{}^2>0$. For any given values $\bar{E}$ and $\bar{\Omega}$ there are values of α and β which satisfy these bounds. Very large values of $\lambda_c{}^2\equiv\rho\bar{\Omega}/2\bar{E}$ correspond to the negative α values and characterise equilibria with strong excitation of the modes with the highest λ_n (note that $\lambda_c\leqslant\lambda_{\max}$). Very small λ_c (the minimum value is $\lambda_c=0$ if $R>0$) corresponds to positive α and very small β. As $\beta\to0$ ($T\to\infty$), $\bar{E}$ increases without limit and is dominated by $\bar{E}_p$.

If $R=0$ (singly connected enclosed domain) there is no potential flow and negative β (negative temperatures) are possible. Equilibria of this type are also possible for the rectangular channel with cyclic ends and for fully cyclic boundary conditions on a rectangle provided that the potential flow degrees of freedom are deleted from the dynamics. Such deletion has the justification that the C_{inm} in (3.9) vanish for these conditions so that an initially zero potential flow remains unexcited. The negative β continuum equilibrium states have been discussed by Kraichnan (1967, 1975), Deem and Zabusky (1971), Cook and Taylor (1972), Seyler *et al* (1975) and Fox and Orszag (1973). The general properties are most simply discussed for the case of fully cyclic boundary conditions (potential flow deleted), where the eigenmodes are trigonometric and λ_n becomes an eigenwavenumber k_n. Suppose to start that $k_{\min}$ is sufficiently large compared to the lowest eigenwavenumber k_0 that the summations in (3.20) can be replaced by integrations over the two-dimensional wavevector space. Then (3.18) yields

$$\bar{E}/L^2=(\pi\rho/8\alpha)\ln\left[(\rho\beta+2\alpha k_{\max}{}^2)(\rho\beta+2\alpha k_{\min}{}^2)^{-1}\right]\qquad(L=\text{box size}) \tag{3.21(a)}$$

$$\bar{\Omega}/L^2=(\pi/4\alpha)(k_{\max}{}^2-k_{\min}{}^2)-(\pi\rho\beta/8\alpha^2)\ln\left[(\rho\beta+2\alpha k_{\max}{}^2)(\rho\beta+2\alpha k_{\min}{}^2)^{-1}\right]. \tag{3.21(b)}$$

Three regimes may be distinguished by the signs of α and β and by the value of $k_c{}^2=\rho\bar{\Omega}/2\bar{E}$. Let

$$k_a{}^2=\tfrac{1}{2}(k_{\max}{}^2-k_{\min}{}^2)\ln(k_{\max}/k_{\min})^{-1}\qquad k_b{}^2=\tfrac{1}{2}(k_{\max}{}^2+k_{\min}{}^2).$$

Then the three regimes are

(i) $k_{\min}{}^2<k_c{}^2<k_a{}^2$ $\qquad\alpha>0,\ -2\alpha k_{\min}{}^2<\rho\beta<0$

(ii) $k_a{}^2<k_c{}^2<k_b{}^2$ $\qquad\alpha>0,\ \beta>0$

(iii) $k_b{}^2<k_c{}^2<k_{\max}{}^2$ $\qquad\beta>0,\ -\rho\beta<2\alpha k_{\max}{}^2<0.$

The energy-equipartition state $\alpha=0$ and the enstrophy-equipartition state $\beta=0$ separate the three regimes. There is no discontinuity of any sort in passing from one regime to the next. Decrease of β corresponds to increase of energy and this increase is smooth as β passes from positive to negative values. Because Ω is present in (3.16), $\beta=0$ (infinite T) corresponds to finite energy. The negative β states may be thought of as being at temperatures higher than infinity. Further details are given by Fox and Orszag (1973), Seyler *et al* (1975) and Kraichnan (1975). In no sense is there a sharp phase transition between regimes. The correlation length for vorticity fluctuations is $\sim k_c{}^{-1}$. As β goes from $+\infty$ to zero and then to its most negative value $-2\alpha k_{\min}{}^2/\rho$, this correlation length goes smoothly from $\sim k_{\max}{}^{-1}$ to $\sim k_{\min}{}^{-1}$, expressing the fact that more complete segregation of positive and negative vorticity regions corresponds to higher energy.

Now suppose that we take $k_{\min}=k_0$, the gravest mode of the cyclic box (excluding $k=0$). The discreteness of the low-lying modes now is important in the negative β states. As $(k_c-k_0)/k_0\to 0$, the kinetic energy condenses into the (degenerate) mode k_0 (the exponential in (3.16) is relatively very large for this mode) so that in the limit it carries all the energy. The condensation involves *only* the gravest mode. For $k=2k_0$ the denominator of (3.18(*a*)) is insignificantly different from its value at $\beta=0$. The gravest mode consists of a single pair of counter-rotating vortices in the cyclic box. The gravest mode with rigid boundary conditions is a single vortex if $J\neq 0$, a pair of opposed vortices if $J=0$.

The inviscid flow system before truncation has an infinite number of constants of motion, including the vorticity of each fluid element. Truncation alters these constants (while preserving energy and enstrophy as constants) but cannot do away with them all; the number remaining must be the order of the number of degrees of freedom. The canonical distribution discussed above represents an ensemble or else a long-time average over a single system so coupled to a fixed-α-and-β reservoir that the extra constants do not disrupt the equilibrium. Two important questions now arise: (i) to what extent are averages over the canonical distribution close to averages over the microcanonical (sharp E and Ω) ensemble; (ii) to what extent does the system exhibit mixing and ergodic properties which imply that the microcanonical averages represent long-time averages for an isolated single system.

These questions have been investigated numerically and analytically by Seyler *et al* (1975), Basdevant and Sadourny (1975), Fornberg (1977) and Kells and Orszag (1978). Computer simulations of (3.4) described in these papers indicate that, with $k_{\min}=k_0$ and $k_{\max}$ large enough to give the order of at least twenty or so modes altogether, the time-averaged spectra in individual realisations do indeed evolve to the canonical form (3.18) for k_c in any of the three regimes. Figures 1 and 2 illustrate this equilibration for two runs by Seyler *et al*, one with k_c corresponding to condensation with 70% of the energy in the gravest mode and one with k_c corresponding to the borderline spectrum k^{-2}. The time averaging is over about the final 10% of the evolution time. The authors point out that fluctuations are large when there is substantial concentration of energy in only a few low-lying modes. Figures 3 and 4 show streamline plots of these runs and illustrate the formation of large-scale vortices in the condensed equilibrium.

Basdevant and Sadourny (1975) construct analytical expressions for the mode excitation as a function of k in the microcanonical ensemble, assuming a cyclic box, and compare the results with both the canonical spectra (3.18) and long-time averages of simulations. For systems with at least 16×16 modes, they find close agreement between canonical and microcanonical averages, with $k_{\min}=1$, $k_{\max}=8{\cdot}71$ and $1{\cdot}57<k_c<7{\cdot}34$. They find ergodic behaviour for as few as 8×8 modes. However, the simulations are carried for so many time steps and so few details are given, so the level of numerical error is difficult to assess.

Kells and Orszag (1978) have checked the mixing property by examining time-correlation functions and have compared moments of mode amplitudes through eighth order obtained from simulations, microcanonical ensemble, and canonical ensemble. A model with ten complex modes (twenty real modes) shows excellent agreement among all three sets of moments and decaying time correlations consistent with mixing. Smaller models showed significant differences among the three sets of moments. One of the smaller models yielded forever-oscillating time correlations, a clear indication that mixing fails. Hald (1976) has shown analytically that the latter

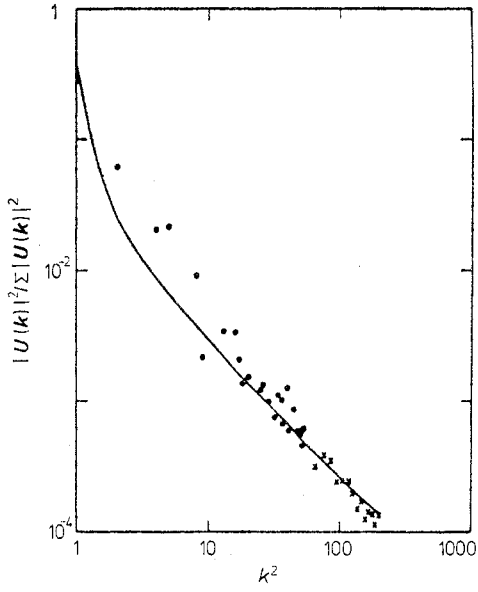

Figure 1. Normalised modal energies, averaged over 100 time steps, from the numerical solution to equation (3.4) (from Seyler *et al* 1975). Full curve is the theoretical prediction, equation (3.18). Different values of $\boldsymbol{k}$ corresponding to the same k^2 have been averaged over. This run corresponds to a negative β regime with 70% of the energy in the fundamental $k_{\min}$.

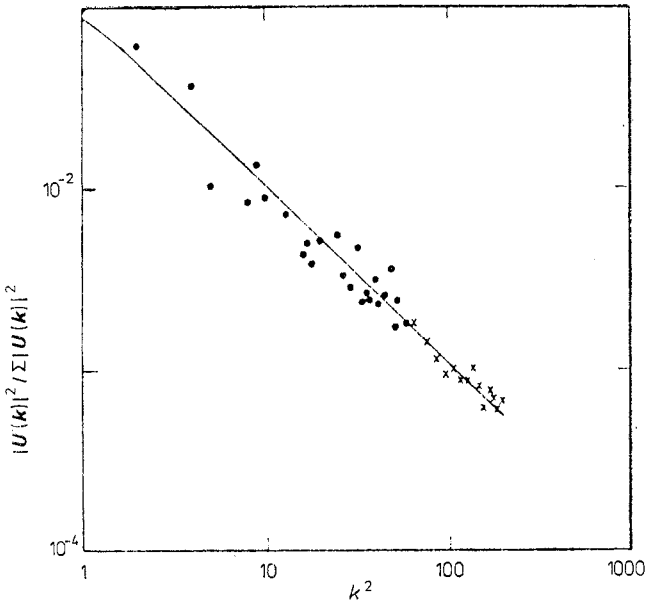

Figure 2. Normalised modal energies, averaged over 200 time steps, from the numerical solution to equation (3.4) (from Seyler *et al* 1975). Full curve is the theoretical prediction, equation (3.18). Different values of $\boldsymbol{k}$ corresponding to the same k^2 have been averaged over. This run corresponds to the transition regime $\beta = 0$.

model and other sufficiently small truncations have isolating integrals in addition to energy and enstrophy.

If the truncation involves only a few Fourier modes, the system may not be ergodic and mixing, but even if it is ergodic and mixing, low-order truncations may lead to differing predictions from the canonical and microcanonical ensembles (Kells and Orszag 1978). The differences become significant for the higher moments, though insignificant differences were observed in the spectra. The minimum number of modes required to obtain ergodic or mixing behaviour is not known precisely though the results of Basdevant and Sadourny (1975) and Kells and Orszag (1978) suggest that 16×16 modes are 'many'.

Figure 3. Contours of constant stream function corresponding to the situation shown in figure 1. The times corresponding to the three (instantaneous) sets of streamlines are the initial time, a time halfway through the run, and a time at the end of the run (from left to right).

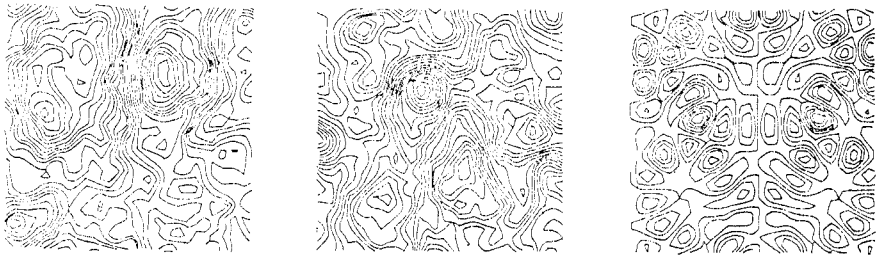

Figure 4. Contours of constant stream function corresponding to the situation shown in figure 2. The times corresponding to the three (instantaneous) sets of streamlines are the initial time, a time halfway through the run, and a time at the end of the run (from left to right).

All the ensembles considered above have zero mean vorticity $\bar{J}$ (2.44(b)). In this case the equilibria are extensive in the following sense. Let the area A of the domain increase without limit. Then, given *any* finite positive values of the energy density $\bar{E}/A$ and enstrophy density $\bar{\Omega}/A$, these values are realised by a canonical ensemble (3.16) such that β tends to a finite *positive* limit. We assume that $k_{\max}$ (more generally $\lambda_{\max}$) is kept constant so that the number of degrees of freedom is $\propto A$ as $A \to \infty$. The negative β states, on the other hand, are intrinsically non-extensive. They exist only for systems with finite A and involve a vorticity correlation length the order of the system size. The transition between $\beta < 0$ and $\beta > 0$ at fixed A is smooth.

If $\bar{J} \neq 0$, the total energy increases logarithmically as $A \to \infty$ with constant $\bar{J}/A$, so that in this case there is not extensive behaviour even for positive β.

3.3. Equilibrium states for discrete vortices

The Liouville theorem and conservation properties for a system of discrete vortices again permit the construction of standard equilibrium distributions: the microcanonical, canonical and grand canonical distributions. The statistical mechanics of the discrete-vortex system was first treated by Onsager (1949). Since then there have been a large number of papers in the contexts of classical hydrodynamics and the homologous problem of the guiding-centre plasma (Montgomery *et al* 1972, Montgomery and Tappert 1972, Joyce and Montgomery 1973, Mongomery 1975a,b). The statistical mechanics of discrete vortices also play a central role in recent theories of superfluidity in thin films. In the present subsection we wish to give some simple qualitative and analytical discussion of the discrete-vortex system, emphasising the similarities and differences with respect to the truncated continuum. Then we shall describe the formal analytical approaches to the statistical mechanics, and computer experiments which test the theories. The application to superfluidity will be discussed in §8.

The canonical distribution describes a fixed number of vortices interacting with the potential-flow field and in contact with a reservoir in thermal equilibrium, with which it is free to exchange energy. The partition function, to be compared with (3.17), is

$$Z_N = \int \exp\left[-\beta(E_\omega + E_\mathrm{p})\right] \prod_{i=1}^{N} (\rho \, \mathrm{d}x_i \, \mathrm{d}y_i) \tag{3.22}$$

where N is the number of vortices, E_ω is given by (2.29(*b*)) and E_p is given by (3.8). The factor ρ^N in (3.22) does not affect averages at constant ρ and is included, as will be explained later (§3.4), to give correctly the pressure associated with the vortices. Note that the total energy $E_\omega + E_\mathrm{p}$ is what appears in (3.22), not the pseudo-Hamiltonian (3.14(*c*)). It is $E_\omega + E_\mathrm{p}$ that is conserved.

In the case of a multiply connected domain, where E_p does not vanish trivially, its presence in (3.22) restricts β to positive values, as with the continuum equilibria. But in a singly connected domain enclosed by a rigid boundary, or in a fully cyclic domain or a uniform channel with cyclic ends, the potential flow either vanishes or is unaffected by the vortex motion, and can be excluded from the system. Then both $\beta > 0$ and $\beta < 0$ are possible. The integration over $\mathrm{d}x_i \, \mathrm{d}y_i$ in (3.22) is confined to the finite domain and E_ω is finite whatever the configuration, provided that the core diameters are finite and defined by (2.30). If $\beta > 0$ so that the equilibrium is extensive, (3.22) can be derived from the microcanonical ensemble for a very large system of interacting vortices of which the system of interest forms a small part. This derivation can be extended to the non-extensive $\beta < 0$ equilibria by forming a supersystem of many flow systems, each with N interacting vortices in an area A, such that the vortices within a system interact with each other according to (2.29(*b*)) and distinct systems are weakly coupled (Montgomery and Joyce 1974).

If there is a mechanism for creation and destruction of vortices the appropriate ensemble is the grand canonical ensemble, a weighted average over canonical ensembles with different N (Tolman 1938, Fowler 1936). Creation and destruction is important in the superfluidity problem (§8). Provided that $\bar{N}$ is large, averages over the grand canonical ensemble that do not involve fluctuations in N will be closely approximated by averages over the canonical ensemble with $N = \bar{N}$.

Suppose there are equal numbers of plus and minus vortices and all have equal strengths and ψ_p vanishes. The $\beta = 0$ (infinite temperature) state is immediately soluble: (3.22) weights all configurations equally and any position of a vortex is

independently equally probable. If the vortices are arbitrarily assigned to plus-minus pairs, each pair sees the zero mean field of the others, because of plus-minus symmetry. Then by (2.29(*b*)) and (2.30) the mean energy is a sum over independent pairs:

$$E_\omega(\beta=0)=(N/2)\rho q^2\sum_n f(\lambda_n)(A\lambda_n{}^2)^{-1}\,[1-A\{\phi_n(r)\}^2] \tag{3.23}$$

where $N/2$ is the number of pairs, B is the domain area, $\{\ \}$ denotes spatial average over the domain, and we have used the orthonormality property $A\{\phi_n{}^2(r)\}=1$. Equation (3.23) can be evaluated once the boundary conditions are specified and the eigenfunctions determined. With rectangular fully cyclic boundary conditions, $\{\phi_n(r)\}^2=0$ except $A\{\phi_0(r)\}^2=1$. The surviving part of (3.23) represents the self-energy of the individual vortices plus the interaction energy of each vortex with its own images. The latter interaction energy has been evaluated and discussed in the limit of vanishing core diameter a by a number of authors: Taylor (1972), Joyce and Montgomery (1973), Seyler (1974, 1976) and Pointin and Lundgren (1976). Seyler's treatment perhaps is the clearest.

If the cutoff in $f(\lambda_n)$ is at $\lambda_{\max}$ the mode dependence of the continuum equilibrium (3.18(*a*)) is the same $\lambda_n{}^{-2}$ dependence that occurs in (3.23). More generally, it is plausible that for some range of β on both sides of $\beta=0$ the gas of discrete vortices should act like a continuum and exhibit similar equilibria. But in general it is plausible that $\lambda_{\max}$ should be taken to approximate the reciprocal of the mean spacing between vortices rather than the reciprocal of the core diameter. This would make the number of degrees of freedom the same in continuum and discretum; the possibility of the correspondence of $\lambda_{\max}$ and the cutoff in $f(\lambda_n)$ is then a peculiarity of $\beta=0$ without real significance. Further discussion of the discretum–continuum relation is given by Kraichnan (1975).

The similarity of continuum and discretum equilibria can be expected to break down when close encounters, defined as encounters at much less than the mean vortex spacing, become of importance. When is this to be expected? As β increases to positive values the mean energy decreases, and this implies increasing proximity between plus and minus vortices. As $\beta\to\infty$ we then expect the vortex gas to degenerate into closely bound plus-minus pairs. On the other hand, as β becomes increasingly negative the mean energy increases, corresponding to proximity of vortices of the same sign. As $\beta\to-\infty$ we expect the finite-volume gas to separate into a cluster of all the positive vortices, with their cores very close together and a similar cluster of all the negative vortices, since this gives the maximum energy. We may term these clusters supervortices.

Analysis indicates that both the pair collapse (Salzberg and Prager 1963, May 1967, Knorr 1968, Hauge and Hemmer 1971, Gonzalez and Hemmer 1972, Deutsch and Lavaud 1972, Edwards and Taylor 1974) and the collapse into supervortices (Kraichnan 1975) occur already at finite values of $|\beta|$. Consider first the pair collapse and start by supposing that there is only a single plus-minus pair in the domain, separated by a distance r which satisfies $a\ll r\ll L$, where a is the core size and L is a typical dimension of the domain ($A\sim L^2$). The *a priori* probability that the separation lies between r and $r+\mathrm{d}r$ is $\sim r\,\mathrm{d}r/L^2$. By (2.35(*a*)) the Boltzmann factor has the r dependence $\exp(-\beta E_\omega)\propto(r/L)^{-\beta z}$, where $z=\rho q^2/2\pi$. Therefore in the canonical distribution the equilibrium probability that the vortices have a separation between r and $r+\mathrm{d}r$ is $Q(r)\,\mathrm{d}r$ where

$$Q(r)\propto L^{-1}(r/L)^{1-\beta z}. \tag{3.24}$$

It follows immediately that the critical temperature for collapse of the pair is given by

$$\beta\rho q^2/2\pi = 2. \tag{3.25}$$

If $\beta z < 2$, $\int_a^L Q(r)\,\mathrm{d}r$ is dominated by contributions from $r \sim L$. But if $\beta z > 2$, the integral is dominated by contributions from $r \sim a$.

Next suppose that many pairs are present. If the mean spacing between pairs d satisfies $a \ll d \ll L$, simple estimates based on (2.35(a)) indicate that the interactions between pairs have only a small effect on the pair distribution function $Q(r)$ provided that $\beta z > 2$ (pair collapse region) and $r \ll d$. If $a \to 0$ with fixed q, d and L, the pair collapse becomes a sharp phase transition at $\beta z = 2$ which is first order in the sense that there is a discontinuous change in the mean energy per vortex. The transition temperature is independent of d (that is, independent of the number density of vortices) (Salzberg and Prager 1963, Knorr 1968, Hauge and Hemmer 1971, Deutsch and Lavaud 1972). However, an important characteristic of a phase change is missing: if a is kept finite and $L \to \infty$ with fixed d the transition does not become perfectly sharp in the limit; the energy per vortex varies continuously with β.

A further peculiarity of the pair-collapse transition is that the transition temperature depends on what quantity is being measured. In the condensed state the polarisability of the gas of vortex pairs is $\propto \langle r^2 \rangle$. It follows from (3.24) that $\langle r^2 \rangle$ is dominated by contributions from $r < a$ if $\beta z > 4$. But if $\beta z < 4$, $\langle r^2 \rangle$ is dominated by contributions from $r \sim L$ in the case of a single pair or $r \gtrsim d$ if there are many pairs. If $a \ll d$, $\langle r^2 \rangle$ increases abruptly if βz decreases through the transition value of 4 (Kosterlitz and Thouless 1973, Kosterlitz 1974). Thus the transition temperature for $\langle r^n \rangle$ depends on n. The transition in $\langle r^2 \rangle$ is of special physical importance and will be treated further in §8. In the case of a gas of many pairs, Nelson (1978) finds that $\beta z = 4$ represents a transition in the behaviour of $Q(r)$ itself for $r \gtrsim d$. If $\beta z > 4$, Nelson finds that (3.24) is modified only by ln factors for $r \gg d$, while for $\beta z < 4$ there is an exponential fall-off in $Q(r)$ for $r \gg d$ due to shielding effects in the effective medium of polarised pairs. A consistent definition of $Q(r)$ for all r (plus-minus pairs are not uniquely defined for $r \gtrsim d$) is given by $Q(r) \propto r \langle \omega(\boldsymbol{x})\omega(\boldsymbol{x}+\boldsymbol{r}) \rangle$ with $\int_0^\infty Q(r)\,\mathrm{d}r = 1$ and with the average over all $\boldsymbol{x}$ as well as over ensemble.

The transition in the pressure of the vortex gas is discussed in §3.4, together with the relation between the vortex gas and a gas of massive particles with two-dimensional Coulomb interaction.

We consider next the possibility of the formation of a pair of supervortices, each containing all the vortices of one sign, at sufficiently negative β. If there are $N/2$ vortices in each cluster, their cores contained within a circle of size r, the *a priori* probability of the configuration is $\sim (r/L)^{2N}$. The energy is approximately that of a single pair of vortices, each of strength $Nq/2$. By (2.35(b)) the energy is then $E \sim (\rho/2\pi)(Nq/2)^2 \ln (L/r)$, where r is the effective core size of the supervortex and we assume that the separation of the supervortices is $\sim L$. The Boltzmann factor $\exp(-\beta E)$ favours high energies for $\beta < 0$. The product of Boltzmann factor and *a priori* probability is $\sim (r/L)^\mu$ where $\mu = 2N + \beta N^2 \rho q^2/8\pi$. If $\beta < \beta_s$, where

$$\beta_s = -16\pi/N\rho q^2 \tag{3.26}$$

the product increases without limit as $r \to 0$. We interpret this as meaning that the supervortices do form and that their (collective) core size collapses to $r \sim a$ if $\beta < \beta_s$.

If the domain is bounded by a rigid boundary, there will be maximum-energy positions for the centres of the supervortices (the locations of plus and minus vortices are interchangeable) (Pointin and Lundgren 1976). If the boundary conditions are cyclic, there will be only a maximum-energy separation vector. In the canonical distribution there will be a statistical fluctuation in the positions of the centres. If the supervortices are treated as macro degrees of freedom, an elementary calculation gives $(\sigma/L)^2 \sim L^2/N$ at $\beta \sim \beta_s$, or $\sigma \sim d$, where σ is the dispersion of a centre position and d^2 is the mean domain area per vortex. As $\beta \to -\infty$, $\sigma \to 0$.

A correspondence between the continuum equilibrium of regime (ii) (§3.2) and the discrete-vortex equilibrium between the temperatures of pair collapse and supervortex formation is obtained by taking $k_{\max} \sim 1/d$ and $\alpha \sim d^2/q^2$ (Kraichnan 1975). Then it is found that the pair collapse β corresponds to $\rho\beta \sim \alpha k_{\max}{}^2$; that is, to temperatures high enough to give approximate energy equipartition at $k \sim k_{\max}$ in the continuum equilibrium. All of regime (iii) then is unattainable by the discretum, which instead exhibits pair collapse. The supervortex formation temperature corresponds approximately to the minimum temperature limit $\rho\beta = -2\alpha k_{\min}{}^2$ of the continuum (with $k_{\min} \sim 1/L$). The continuum can reach indefinitely high energies if α is sufficiently close to this negative limit, but the discretum has a maximum possible energy if N and a are finite.

The statistical mechanics of the discrete vortex system appears to be exactly soluble only for $\alpha = 0$ and $\beta = \pm\infty$. (We shall see in §3.4 that the exact equation of state obtained by Salzberg and Prager (1963) for the two-dimensional Coulomb gas for β outside the pair-collapse regime and with $a \to 0$ does not apply to the vortex gas.) However, a number of formal analytical approximation procedures have been brought to bear. The treatment of the pair-collapse regime for $\beta\rho q^2/2\pi > 4$ by renormalisation group and related approaches (Kosterlitz and Thouless 1972, Kosterlitz 1974, Nelson and Kosterlitz 1977, Young 1978, José *et al* 1977, Huberman *et al* 1979, Myerson 1978, and others) will be noted in §8.

If $\beta > 0$ and there is not pair collapse, the behaviour may be approximated by Debye–Hückel theory, which is strictly applicable for $\beta\rho q^2 \ll 1$. In this method the hierarchy of n-body spatial distribution functions is calculable as a perturbation series in powers of the reciprocal of the number of particles inside a Debye square (e.g. Montgomery 1975a). These well-known solutions appear to be valid to $\beta = 0$ and to yield extensive thermodynamic behaviour for $\beta > 0$.

Given the n-body functions, various statistics of $\omega(\boldsymbol{x})$, as given by (2.27), may be calculated. In particular the two-body distribution yields values for the $\langle \omega_n{}^2 \rangle$, which may be compared with the continuum results (3.18). The Debye–Hückel results support our anticipation that the discrete vortex gas behaves like the continuum for $0 < \beta\rho q^2/2\pi < 2$. A similar result for this regime is obtained by a cumulant-discard method (Pointin and Lundgren 1976).

The $\beta < 0$ regime has been studied by random-phase approximations applied to the ω_n as collective coordinates (Taylor 1972, Edwards and Taylor 1974, Lundgren and Pointin 1977a); by discarding pair correlation functions (Montgomery and Joyce 1974, Pointin and Lundgren 1976, Lundgren and Pointin 1977b); and by seeking most probable states under the assumptions of stationarity and slow variation of vortex number density with position (Joyce and Montgomery 1973).

The random-phase approximation can logically be applied only if the set of ω_n is truncated at $\lambda_{\max}$ (or $k_{\max}$) $\sim 1/d$, where d is the mean vortex spacing. This is because the higher modes have strongly correlated phases that express the localisation

of vorticity into the cores of size a. But once the truncation is made, one is no longer really analysing discrete vortices; it is perhaps as satisfactory simply to truncate and make the approximation of identification with the truncated continuum, as already discussed. The truncated random-phase analysis (Taylor 1972) gives a relation between β and E which is consistent with the continuum approximation (Kraichnan 1975).

Both the most-probable-state analysis and the discard of the two-body pair correlations lead to the same final differential equation for the $\beta<0$ mean stationary-state stream function. In the case of equal numbers of plus and minus vortices, all of the same strength, this equation can be written

$$\nabla^2\psi+\gamma^2\sinh(|\beta'|\,\rho q\psi)=0 \tag{3.27}$$

(Joyce and Montgomery 1973, Montgomery and Joyce 1974) where γ and β' are constants and β' has the dimensions of β.

Equation (3.27) results from the substitution of the most probable vorticity expression into (2.18) and assumes the limit of point vortices. β must be less than 0 in the derivation. As β passes through zero, we pass from a state with a spatially uniform one-body distribution (with the interaction energy residing in the Debye–Hückel pair correlation) to a spatially non-uniform state (with the interaction energy residing in the Vlasov limit mean-field solution to (3.27)). If $|\beta'\rho q\psi_{\max}|\ll 1$, (3.27) may be linearised to $\nabla^2\psi+\lambda^2\psi=0$, which is just the equation obeyed by the stationary eigenfunctions $\phi_n(\boldsymbol{x})$ of the continuum.

The non-linear solutions to (3.27) have been studied numerically (McDonald 1974, 1978 private communication, Book *et al* 1975, Pointin and Lundgren 1976, Kriegsmann and Reiss 1978, Montgomery *et al* 1980). They are not unique in the sense that there is a family of non-linear eigenvalues γ for each energy and total vorticity: the solutions are distinguished by the number of local maxima and minima in ψ. However, only one of these actually maximises the original probability functional from which (3.27) is derived: the one with a single maximum and a single minimum in ψ.

The relationship of (3.27) to the exact canonical distributions for the discrete vortex system and the continuum is not fully illuminated in the literature. Moreover, the present authors do not fully agree with each other. One of us (RHK) believes that, within the domain of validity of (3.27), some subclass of its solutions bear the same relation to the discretum canonical distribution as the eigenfunctions $\phi_n(\boldsymbol{x})$ of $\nabla^2\phi_n+\lambda_n^2\phi_n=0$ do to the continuum canonical distribution. A typical realisation of the absolute equilibrium (3.16) for the truncated continuum is instantaneously a random superposition of the $\phi_n(\boldsymbol{x})$ and, by (2.14), ψ fluctuates with time in this realisation. Similarly, an individual solution of (3.27) represents a fluid state in which there is no statistical fluctuation on scales large compared to the vortex spacing; the large-spatial-scale fluctuations in the canonical distribution can be represented by time-varying superposition of such solutions. A similar view has been expressed by Pointin and Lundgren (1976) and Lundgren and Pointin (1977a,b).

What then is the physical meaning of the non-linearity of (3.27) by which, in this interpretation, the continuum and discretum distributions differ at scales large compared to the discretum intervortex spacing? In the continuum states the ϕ_n may appear with arbitrarily large amplitude. But in the discrete case the amplitude of a large-spatial-scale variation in ψ is limited to a maximum value associated with the complete separation of the plus and minus vortices, whose number and strengths are fixed.

If the scale of variation of ψ is $\sim L$, the domain size, then $\psi \sim Nq$, if there is substantially complete separation of plus and minus vortices, so that the total mean vortex strength on the scale L is $\sim Nq$. In this case the condition for linearisability is

$$|\beta'| \ll |\beta_s| \tag{3.28}$$

where β_s is the supervortex condensation temperature (3.26).

An obvious qualitative feature of (3.27) is that the spatial dependence of $-\nabla^2\psi$ (the vorticity) is less smooth than that of ψ. The smoothness assumptions on spatial variation used in deriving (3.27) preclude this equation from describing the ultimate limit of this bunchedness of vorticity: the supercondensation collapse. Seyler (1974, 1976) finds that the random phase approximation with zero core diameter gives infinite energy at $\beta \sim \beta_s$, which suggests that β_s may be a limit for the validity of the derivations of (3.27).

The second author (DCM) wants to register views which depart slightly from those just presented. First, no direct relevance of equation (3.27) to the case of *finite-core* vortices is conceded. The derivation of (3.27) (Joyce and Montgomery 1973, Montgomery and Joyce 1974) makes use of Poisson's equation (2.18) in a fundamental way, and modification of the two-body interaction potential from the Coulomb law will significantly modify (3.27) itself. As it stands, β_s has no meaning for (3.27) directly. Secondly, it is believed that §V of Montgomery and Joyce (1974) does indeed illuminate the relation between (3.27) and the exact canonical distribution for line vortices, in terms which are familiar from the theory of the BBGKY hierarchy (Bogolyubov 1946, Montgomery 1971).

A number of numerical experiments have been carried out in which a set of point vortices in a given geometry move according to the equations of motion. Joyce and Montgomery (1972, 1973) and Montgomery and Joyce (1974) have followed sets of typically 4000 vortices (equal strengths and equal numbers of positive and negative) in a rectangular domain with rigid boundaries with initial conditions corresponding to both positive and negative interaction energies of the vortices. Representative results for high and low energies are shown in figures 5 and 6. Similar calculations have been reported by Edwards and Taylor (1974). Pointin and Lundgren (1976) have simulated sets of 40 vortices in a circular domain. These experiments confirm the general predictions of equilibrium theory. The vortices tend to evolve to configurations which are spatially uniform in the mean, with small-scale spatial fluctuations in locally averaged vorticity, if the interaction energy is negative, corresponding to $\beta > 0$ equilibria. If the interaction energy is positive, corresponding to $\beta < 0$ equilibria, there is evolution into large-scale aggregations of like-signed vortices. The experiments have not been on a large enough scale, or carried out for long enough times of evolution, to shed light on the delicate questions of deviation between continuum and discretum behaviour at large negative β which we have raised above.

Seyler (1976) has used Monte Carlo calculations with a set of 256 vortices to compute the phase-space volume associated with various ranges of system energy. He finds good agreement with equilibrium random phase theory for positive interaction energies ($\beta < 0$) but finds that the random phase approximation underestimates the available phase volume for $\beta > 0$.

3.4. Pressure and entropy

The pressure associated with a distribution of vorticity in an incompressible fluid can be defined by introducing a tiny compressibility. In order not to become involved

with sound waves and related complications, we may assume that compression is carried out slowly and that the only compressive mode excited is the one in which every fluid element experiences the same change in density. If ζ is the change of linear scale associated with the uniform compression, the area of the domain A' and density ρ' after compression are related to initial values by $A'=\zeta^2 A$, $\rho'=\zeta^{-2}\rho$. Kelvin's circulation theorem holds under the compression (Lamb 1945) and the motion is unaffected except for the scale changes

$$\omega'(\boldsymbol{x})=\zeta^{-2}\omega(\zeta^{-1}\boldsymbol{x}) \qquad \boldsymbol{u}'(\boldsymbol{x})=\zeta^{-1}\boldsymbol{u}(\zeta^{-1}\boldsymbol{x})$$

which express conservation of circulation and angular momentum. Here $\boldsymbol{x}$ is measured from the centre of mass of the domain, which is fixed. If there are discrete vortices,

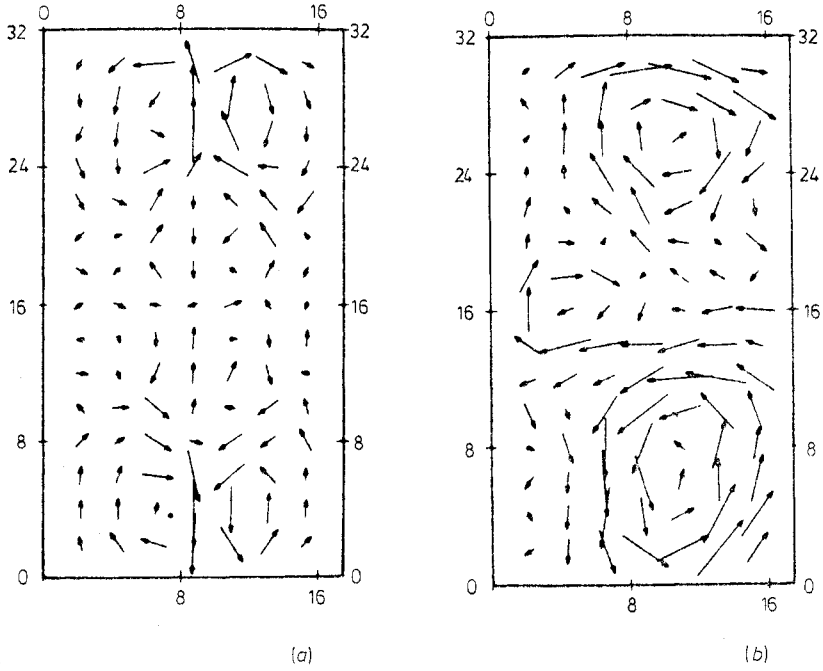

Figure 5. Fluid velocity field initially, and after considerable evolution of the flow, for 4008 point vortices (Montgomery and Joyce 1974). The energy for this case is above the negative temperature threshold. Boundaries are rigid and frictionless. (*a*) Time = 0·0, $v_{\max}=2{\cdot}7845$. (*b*) Time = 160·0, $v_{\max}=1{\cdot}8794$.

the cores compress as well as the rest of the fluid and scale according to $a'=\zeta a$. It follows from these relations that the scaling of the total kinetic energy is $E'=\zeta^{-2}E$ or $E'A'=EA$. Thus the kinetic energy increases as the fluid is compressed (in analogy to the spin-up one experiences upon drawing the arms inward whilst rotating on a piano stool). The two-dimensional pressure $\bar{p}$ (averaged over the boundary) is

$$\bar{p}=-\partial E/\partial A=E/A. \tag{3.29}$$

The standard formula for the pressure associated with a slow (adiabatic) change of volume in the canonical ensemble is (Landau and Lifshitz 1958)

$$\bar{p}=\beta^{-1}(\partial Z/\partial A)_\beta \tag{3.30}$$

where the partial derivative is at constant β. Underlying (3.30) is the fact that the adiabatic compression is isentropic. This is an automatic consequence of the Hamiltonian dynamics for the systems ordinarily considered. But for our non-Hamiltonian flow system the constancy of entropy under compression, and hence a correct result from (3.30), is obtained only if the partition function Z is written in terms of properly chosen variables. Let us confine the discussion now to a singly connected domain with rigid boundary (extension to the general case is not difficult). Then (2.25(*b*)) can be written

$$E_\omega = \tfrac{1}{2}\rho \sum_n u_n^2 \tag{3.31}$$

where $u_n = \lambda_n^{-1}\omega_n$. We have seen above that E and ρ have the same scaling under compression, and it then follows from the similarity of $\omega(\boldsymbol{x})$ and $\omega'(\boldsymbol{x})$ that the u_n are

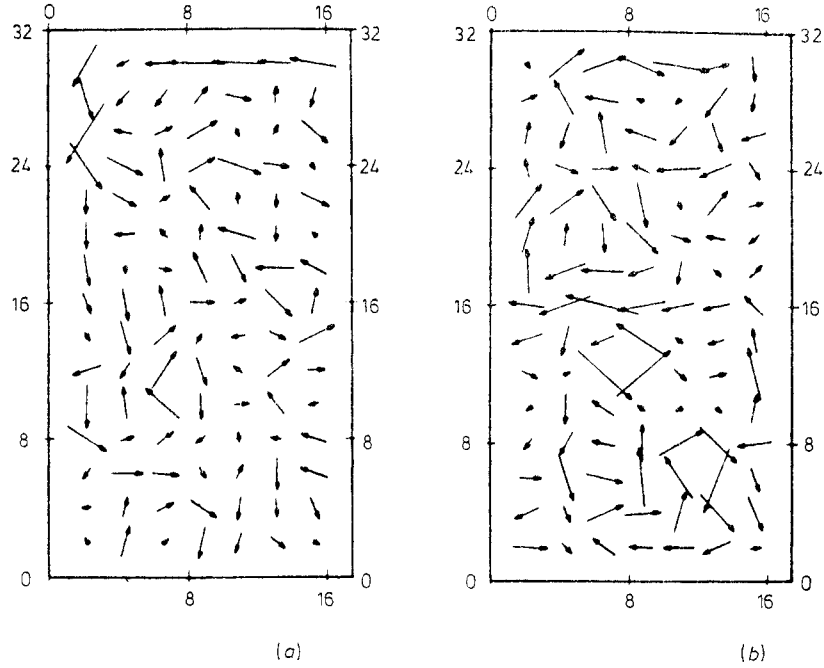

Figure 6. Fluid velocity field initially, and after considerable evolution of the flow, for 4008 point vortices (Montgomery and Joyce 1974). The energy for this case is below the negative temperature threshold. Boundaries are rigid and frictionless. (*a*) Time = 0·0, $v_{\max} = 0{\cdot}8307$, (*b*) Time = 375, $v_{\max} = 0{\cdot}7540$.

invariant under the adiabatic compression. They are the desired variables; the invariance of the u_n is analogous to the invariance of quantum-mechanical eigenstate amplitudes under adiabatic processes (Landau and Lifshitz 1958).

If we now write (3.17), with no potential flow variables a and with $\alpha = 0$, in the form

$$Z = \int \exp(-\beta E_\omega)\Pi \, du \tag{3.32}$$

with E_ω given by (3.31), (3.30) gives immediately the correct result (3.29). In order for the result to remain correct for $\alpha \neq 0$ (a generalisation not usually contemplated

in writing (3.30)) it is necessary to write $\alpha\Omega$ as $\hat{\alpha}\hat{\Omega}$, where $\hat{\Omega}=\Omega/\rho$ is independent of ζ.

Since E in (3.29) is solely kinetic energy, the pressure is always positive.

The pseudo-Hamiltonian relations (3.14) are a guide in choosing correct variables for the discrete vortex system. In writing (3.22) we have therefore taken ρx_l and y_l as a canonical pair (the factor q_l is invariant under compression and we have ignored it) rather than x_l and y_l. Again, (3.30) applied to (3.22) gives the correct result (3.29).

It is essential at this point to distinguish carefully between the vortex system, the two-dimensional Coulomb gas, and the guiding centre plasma; their homology does not extend to pressure. The *potential* energy of the Coulomb gas is what has the same form as the *kinetic* energy of the vortex system. In addition, the Coulomb gas has kinetic energy of the particles. The contribution of this kinetic energy to the pressure is recovered from (3.22) by *omitting* the ρ factors in the area elements. This is correct for the Coulomb gas because the canonical pairs there are (x_i, p_{ix}) and (y_i, p_{iy}); the momentum $\boldsymbol{p}$ does not enter the vortex gas problem.

The difference in behaviour of the pressure for the vortex gas and the Coulomb gas is especially sharp at and below the pair-collapse temperature (3.25). If a is small enough, the energy of the vortex gas in the pair collapse regime is a small fraction of its value just above transition so that, by (3.29), there is a corresponding collapse of pressure. In the case of the Coulomb gas, an exact equation of state can be obtained above transition for $a\to\infty$ (Salzberg and Prager 1963). In the pair-collapse regime, there remains the perfect-gas pressure contribution from the bound pairs (Hauge and Hemmer 1971, Gonzalez and Hemmer 1972), one-half that of free particles.

4. Spectral transport of energy and enstrophy

4.1. Relaxation toward equilibrium

The turbulent flows which are generated in nature, in the laboratory, or in computer simulations usually are out of statistical equilibrium in two respects. First, the very existence of hydrodynamic modes with macroscopically significant excitation is a departure from the absolute equilibrium of the fluid considered as a molecular system. Second, the hydrodynamic modes are in disequilibrium among themselves and do not have the equilibrium properties described in §3. In this situation we can expect that the equations of motion mediate a two-fold relaxation toward equilibrium: the hydrodynamic modes dissipate their energy into heat energy of the fluid via the viscosity term, while the non-linear terms give an exchange of energy among the hydrodynamic modes tending to bring the state of motion closer in some way to the equilibrium states of §3. If processes are acting continuously to regenerate the turbulence, the competition between forcing and relaxation may result in a non-equilibrium steady state.

The relaxation toward equilibrium of a non-linear system with many degrees of freedom (or even just several degrees of freedom) can result in a complex interplay of order and disorder. In turbulent shear flow, such as flow in a pipe, the generation of turbulent excitation near the walls involves non-linear instabilities and the creation of characteristic three-dimensional vortex structures. As these structures move away from the wall they become more random in appearance and more isotropic. The eventual breakdown of the turbulence into small-scale structures that are dissipated

by viscosity involves the formation of thin sheets of vorticity which are coherent over distances large compared to their thickness, but which are chaotically oriented and distributed. A review of mechanisms and structures in turbulent shear flow is given by Roshko (1976).

The basic mechanism for the formation of sheets of vorticity operates even when no boundaries are present and the turbulence is statistically isotropic and homogeneous. It has been clearly described by Batchelor (1952). Random motion tends on the average to separate points which move with the fluid; the points execute a random walk constrained by incompressibility. This tends to elongate initially compact fluid elements. In two dimensions the vorticity at each point of the fluid is constant (neglecting viscosity) and the result is that an initial blob of vorticity is drawn out into a filament (or sheet, adding the z dimension). In three dimensions, the enstrophy tends to be enhanced by this process (Batchelor 1952). If viscosity is now included, the effect is to diffuse vorticity thus blurring the edges of the vorticity filaments.

In three-dimensional inviscid incompressible flow, it has been demonstrated that the vorticity-straining mechanism described above, and the concomitant enhancement of vorticity, can lead to singularities in a finite time of evolution (Morf *et al* 1980). In contrast, it has been proved that the two-dimensional Euler equations do not lead to singularities of the velocity field or its derivatives in finite time if the initial conditions are smooth (Wolibner 1933, Frisch and Bardos 1975, Rose and Sulem 1978).

In what follows we shall measure the evolution of non-equilibrium initial ensembles of flows principally by following the evolution of spectra; that is, the values $\langle \omega_n{}^2 \rangle$ as functions of time, or these values in the non-equilibrium steady state. This limitation excludes most of the information about the non-random aspects of the characteristic structures, such as vortex sheets, or local aggregations of like-signed vorticity, which can form during evolution. It is an unfortunate result of the fundamental difficulties that presently exist in giving a satisfactory description of part-random, part-coherent structures. Almost all theoretical studies of turbulence have been limited to spectra, or to equivalent correlation functions, because it has been found very difficult to do more. Fortunately some information about the actual spatial appearance of flow structures has emerged from computer experiments, laboratory experiments, and observations of natural flows. Figure 14 illustrates the evolution of constant vorticity contours in a computer experiment by Lilly (1971) which used random initial conditions on a truncated inviscid system.

In order to obtain an equation for the evolution of the spectral intensities $\bar{\Omega}_n$, or equivalently $\bar{E}_n$, we may start by generalising (3.4) to include the viscous damping term that appears in (2.42) and (2.43):

$$\mathrm{d}\omega_n/\mathrm{d}t + \nu\lambda_n{}^2\omega_n = \sum_{rs} A_{nrs}\omega_r\omega_s. \tag{4.1}$$

Multiplying by $2\omega_n$ and averaging over ensemble we obtain

$$\mathrm{d}\bar{\Omega}_n/\mathrm{d}t + 2\nu\lambda_n{}^2\bar{\Omega}_n = 2\sum_{rs} A_{nrs}\langle \omega_r\omega_s\omega_n \rangle \equiv \sum_{rs} \lambda_n{}^2 T_{nrs} \tag{4.2}$$

where T_{nrs} expresses the mean rate of transfer of excitation into mode n due to its interaction with modes r and s. We omit the easy generalisation to systems with potential flow. The ν term acts to reduce the excitation in each mode independently. By (3.5) and (3.6) the transfer terms satisfy

$$T_{nrs} + T_{rsn} + T_{snr} = 0 \qquad \lambda_n{}^2 T_{nrs} + \lambda_r{}^2 T_{rsn} + \lambda_s{}^2 T_{snr} = 0 \tag{4.3(a, b)}$$

which express conservation of energy and enstrophy, respectively, by the elementary three-mode (triad) interactions. We take $T_{nrs} = T_{nsr}$.

Equations (4.3) imply

$$T_{rsn}/T_{nrs} = (\lambda_s^2 - \lambda_n^2)\,(\lambda_r^2 - \lambda_s^2)^{-1} \tag{4.4}$$

which, with its two cyclic permutations, expresses an important qualitative characteristic of the energy transfer process (Batchelor 1953, Fjørtoft 1953). Suppose that the eigenvalues have the ordering $\lambda_s < \lambda_n < \lambda_r$. Then transfer of energy *out* of mode n requires that this energy be transferred *into both* modes r and s. Only by simultaneous transfer to both higher and lower λ modes can enstrophy and energy conservation be satisfied simultaneously. Whether this process transfers more energy to mode s than to mode r depends on the particular relative magnitudes of λ_s, λ_n and λ_r (Merilees and Warn 1975).

Most of the theoretical and computer-experiment work has been done for the square cyclic box. In this case it is most convenient to write the equations in terms of the complex Fourier coefficients of the velocity or vorticity field, whose real and imaginary parts are the mode amplitudes we have previously considered. If we write $u_i(\boldsymbol{x}, t) = \Sigma_k\, \hat{u}_i(\boldsymbol{k}, t) \exp(\mathrm{i}\boldsymbol{k}.\boldsymbol{x})$, where the sum is over all allowed wavevectors for the cyclic box, then the Navier–Stokes equation (2.42), with the pressure eliminated by the incompressibility condition, can be written as

$$(\partial/\partial t + \nu k^2) u_i(\boldsymbol{k}) = -\mathrm{i}k_m(\delta_{ij} - k_i k_j/k^2) \sum_{\boldsymbol{p}+\boldsymbol{q}=\boldsymbol{k}} u_j(\boldsymbol{p})\, u_m(\boldsymbol{q}) \tag{4.5}$$

where the indices are tensor indices and we have dropped the carets. If the Fourier modes can be considered dense ($k_{\min} \gg 1/L$ where L is the box side or negligible excitation in wavenumbers $\sim 1/L$), then the statistics are greatly simplified by assuming that averages are spatially isotropic and defining continuous isotropic spectrum functions. Thus we define the smooth function $U(k)$ by $U(k) = (L/2\pi)^2 \langle |u(\boldsymbol{k})|^2 \rangle$ at each allowed $\boldsymbol{k}$. Then if $E(k) = \pi k U(k)$, the total mean kinetic energy and enstrophy are

$$\bar{E} = \rho L^2 \int_0^\infty E(k)\, \mathrm{d}k \qquad \bar{\Omega} = 2L^2 \int_0^\infty k^2 E(k)\, \mathrm{d}k. \tag{4.6(a, b)}$$

The equilibrium state (3.18) gives

$$U(k) = 2\pi^2(\rho\beta + 2\alpha k^2)^{-1}. \tag{4.7}$$

Further information about the transformation from discrete to continuous representation is given by Leith and Kraichnan (1972). In the continuous representation we have

$$(\partial/\partial t + 2\nu k^2) E(k) = T(k) \qquad T(k) = \tfrac{1}{2} \int_0^\infty \int_0^\infty T(k, p, q)\, \mathrm{d}p\, \mathrm{d}q \tag{4.8(a, b)}$$

where $T(k, p, q)$ plays the role of T_{nrs} in (4.2) but involves isotropic averaging. We have

$$T(k, p, q) + T(p, q, k) + T(q, k, p) = 0 \tag{4.9(a)}$$

$$k^2 T(k, p, q) + p^2 T(p, q, k) + q^2 T(q, k, p) = 0 \tag{4.9(b)}$$

$$T(p, q, k)/T(k, p, q) = (q^2 - k^2)\,(p^2 - q^2)^{-1} \tag{4.9(c)}$$

with $T(k, p, q) = T(k, q, p)$. Equations (4.9) yield overall conservation of energy and enstrophy by the non-linear interaction:

$$\int_0^\infty T(k)\,\mathrm{d}k = 0 \qquad \int_0^\infty k^2 T(k)\,\mathrm{d}k = 0. \qquad (4.10(a, b))$$

In three-dimensional turbulence (with reflection invariance) the only quadratic constant of motion is energy and the equipartition of energy among all the modes is the only equilibrium state for the truncated system. The two-dimensional equilibrium which we have examined in §3 is more complicated because there are the

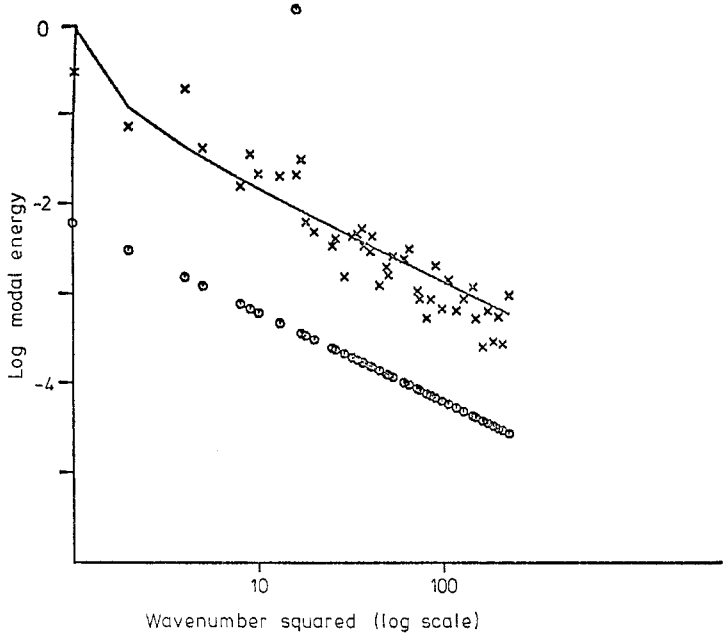

Figure 7. Evolution of a 2D Navier–Stokes run with $\nu = 0$ (equation (3.4)) (from Matthaeus and Montgomery 1980). The initial spectrum (circles) is concentrated in the modes $k^2 = 16$, and evolves to the crosses. The full curve is the modal energy corresponding to equation (3.18) for these initial conditions.

two quadratic constants, energy and enstrophy. The ergodic properties found by Seyler *et al* (1975), Basdevant and Sadourny (1975) and Kells and Orszag (1978) and discussed in §3 imply that any initial energy spectrum in the truncated inviscid system should relax to an equilibrium spectrum. In contrast to three-dimensional turbulence, where the energy transfer that relaxes toward equipartition is primarily to higher wavenumbers, the transfer in two dimensions is importantly toward both higher and lower wavenumbers, as noted by Batchelor (1953) and Fjørtoft (1953). In both three and two dimensions viscosity acts most strongly on the higher wavenumbers. Figures 7 and 8 show the relaxation of the spectrum to equilibrium for two inviscid computer-simulation cases computed by Matthaeus and Montgomery (1980). In each case almost all the initial energy was concentrated in a single wavenumber and the ratio $k_{\max}/k_{\min}$ was 16. A random noise energy of the order of 1% was distributed among the rest of the modes. Comparison of the initial and final

spectra in figure 7 clearly shows an approach to the equilibrium spectrum involving transfer of energy to both higher and lower wavenumbers. Figure 8, on the other hand, shows a case in which both the initial and final spectra have most of the excitation in the gravest modes (condensed equilibrium). The conservation laws render this initial state essentially stable to random perturbations (see Matthaeus and Montgomery 1980).

Figures 9 and 10 show the transfer function $T(k)$ and the enstrophy transfer function $k^2T(k)$ from computer simulations of the system with viscosity presented by Herring *et al* (1974). The initial spectrum was smoothly peaked about $k=8$. Note that the energy transfer is primarily to lower wavenumbers while the enstrophy

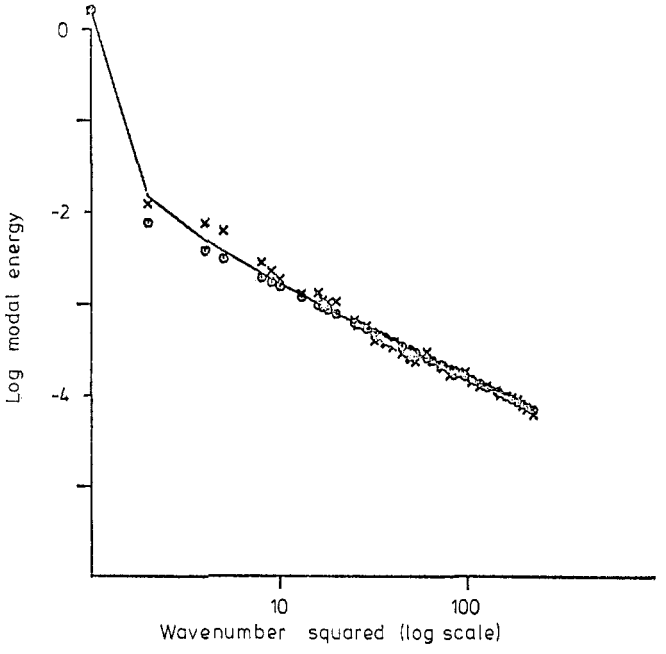

Figure 8. Evolution of a 2D Navier–Stokes run with $\nu=0$ (equation (3.4)) (from Matthaeus and Montgomery 1980). The initial spectrum (circles) is concentrated in the modes $k^2=1$ and evolves to the crosses. Full curve is equation (3.18) for these initial conditions, which in effect lock all the excitation into the $k^2=1$ modes for all time.

transfer, because of the weighting by k^2, is primarily to higher wavenumbers. Again because of the k^2 weighting, the dissipation of enstrophy by viscosity is proportionately greater than that of energy, and this difference is enhanced during evolution by the directions of transfer. Figure 11 shows for contrast the energy transfer $T(k)$ found by Orszag and Patterson (1972) from a three-dimensional simulation with similar initial spectrum.

The absolute equilibrium states are isotropic except for the excitation at wavenumbers low enough that discreteness is important. Herring (1975) has investigated the relaxation toward isotrophy of initially anisotropic states. He finds weaker isotropising effects than in three dimensions.

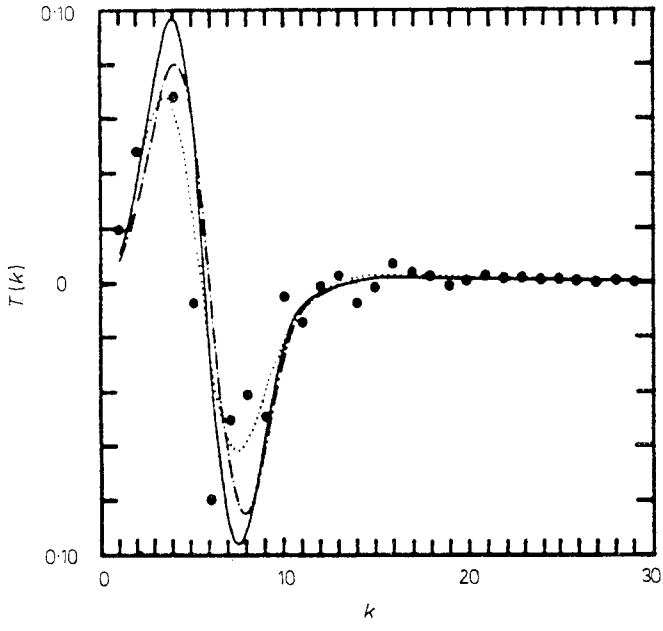

Figure 9. Energy transfer function $T(k)$ (points) for a 2D Navier–Stokes initial spectrum peaked about $k=8$. Full curves are for three different closures, described elsewhere (—, – – –, two versions of TFM; . . ., DIA) (from Herring *et al* 1974).

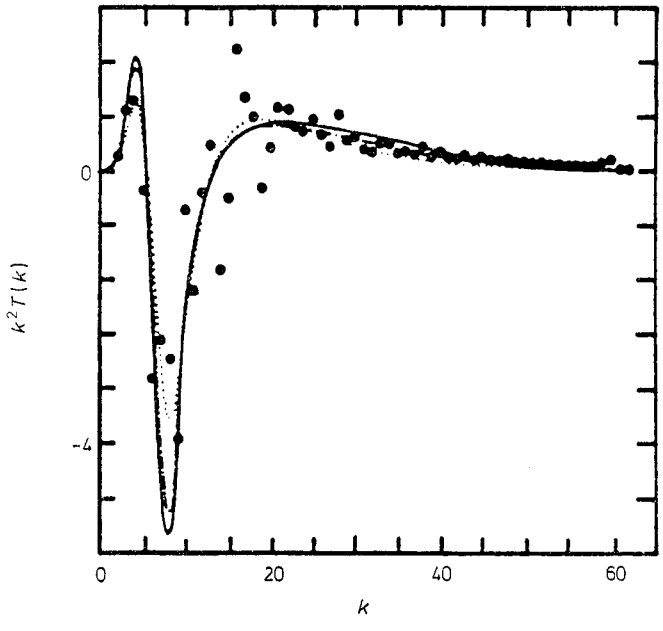

Figure 10. Enstrophy transfer function $k^2T(k)$ (points) for the same 2D Navier–Stokes simulation shown in figure 9 (from Herring *et al* 1974).

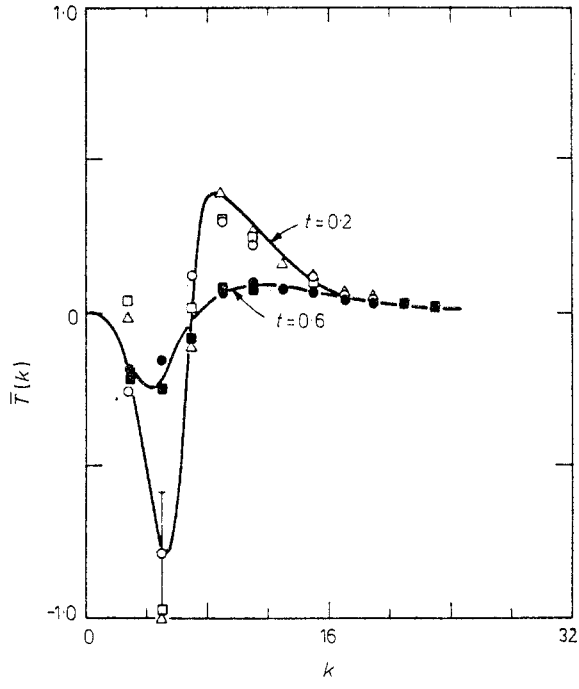

Figure 11. Energy transfer function (points) for a 3D Navier–Stokes simulation (from Orszag and Patterson 1972), with an initial spectrum similar to that for the initial spectrum corresponding to figure 9 for two dimensions. Note the fundamental difference in shape between the 2D and 3D cases. ○, △, □, $t=0{\cdot}2$, ●, ■, $t=0{\cdot}6$.

4.2. Inertial ranges

Kolmogorov's (1941) theory of the inertial range has a central place in the theory of three-dimensional turbulence. Kolmogorov's theory may be stated as follows. Suppose that most of the energy of the turbulence is at wavenumbers $k \sim 1/L$ and that most of the dissipation of turbulent energy into heat by viscosity is at wavenumbers $k \sim k_s \gg 1/L$. Then there is an inertial range of wavenumbers connecting these two regions through which energy is cascaded by non-linear processes to the wavenumbers where it is dissipated. Furthermore, the energy spectrum in the inertial range depends only on k and on the rate ϵ at which energy is cascaded per unit mass. Therefore it has the form (Rose and Sulem 1978)

$$E(k) = C\epsilon^{2/3} k^{-5/3} \tag{4.11}$$

which is the only dimensionally correct combination. Later Kolmogorov (1962) and others proposed corrections to the $-5/3$ exponent because of intermittency effects. A discussion of the theory and its dynamical basis is given by Monin and Yaglom (1975) and Rose and Sulem (1978). A critical appraisal of some of the work on intermittency corrections is attempted by Kraichnan (1974a).

In two-dimensional turbulence there are two conserved quantities, energy and enstrophy, which are candidates for cascades of the Kolmogorov type. The dimensionally determined inertial-range energy spectra for these putative cascades are

(Kraichnan 1967, Leith 1968, Batchelor 1969) (4.11) and

$$E(k) = C' \eta^{2/3} k^{-3} \tag{4.12}$$

where η is the rate of cascade of enstrophy per unit area. C and C' are dimensionless constants.

The inertial-range hypothesis can be formulated analytically by introducing the functions

$$\Pi(k) = \int_k^\infty T(k')\, \mathrm{d}k' \qquad Z(k) = 2 \int_k^\infty (k')^2 T(k')\, \mathrm{d}k' \tag{4.13(a, b)}$$

which are (in view of (4.10)) the rates at which energy and enstrophy, respectively, are transferred from wavenumbers $< k$ to wavenumbers $> k$. By use of the detailed conservation relations (4.9) $\Pi(k)$ and $Z(k)$ can be written as

$$\Pi(k) = \tfrac{1}{2} \int_k^\infty \mathrm{d}k' \int_0^k \int_0^k T(k', p, q)\, \mathrm{d}p\, \mathrm{d}q - \tfrac{1}{2} \int_0^k \mathrm{d}k' \int_k^\infty \int_k^\infty T(k', p, q)\, \mathrm{d}p\, \mathrm{d}q \tag{4.14(a)}$$

$$Z(k) = \int_k^\infty (k')^2\, \mathrm{d}k' \int_0^k \int_0^k T(k', p, q)\, \mathrm{d}p\, \mathrm{d}q - \int_0^k (k')^2\, \mathrm{d}k' \int_k^\infty \int_k^\infty T(k', p, q)\, \mathrm{d}p\, \mathrm{d}q. \tag{4.14(b)}$$

Here $\Pi(k)$ and $Z(k)$ are expressed as differences between the total rate of gain in the range $k' > k$ due to triad interactions with $p, q, < k$ and the total rate of gain in the range $k' < k$ due to triads with $p, q > k$.

Now consider a hypothetical power-law similarity behaviour such that

$$T(ak, ap, aq)/T(k, p, q) = a^{-r} \tag{4.15}$$

where a is an arbitrary scaling factor such that all six wavenumbers in (4.15) lie in the putative inertial range. If (4.15) and (4.9) are used in (4.14) some changes of variable and algebraic manipulations yield the formal results

$$\Pi(k) \propto k^{3-r} \qquad Z(k) \propto k^{5-r} \tag{4.16}$$

(Kraichnan 1967). Thus an energy inertial range in which $\Pi(k)$ is k-independent requires $r = 3$ and an enstrophy inertial range in which $Z(k)$ is k-independent requires $r = 5$. Moreover, and importantly, the analysis shows that if $r = 3$ a coefficient vanishes to give $Z(k) \equiv 0$ while if $r = 5$ a coefficient vanishes to give $\Pi(k) \equiv 0$. Thus there is zero-energy cascade in the formal enstrophy inertial range and vice versa.

So far we have not related the transfer scaling (4.15) to the spectrum forms (4.11) and (4.12). This relation comes through the requirement of localness of the cascade in wavenumber. The formal results for $\Pi(k)$ and $Z(k)$ are meaningful only if the integrations over k', p and q in (4.14) converge at very small and very large argument values. We are then led to ask what constitutes similarity of the local behaviour of T and E. If k, p, q are all the same order of magnitude such similarity requires that $T(k, p, q)$ exhibit the same scaling as the local quantity $[E(k)]^{3/2} k^{-1/2}$, which has the same dimensions. Then (4.15) implies $E(ak)/E(k) = a^{-(2r-1)/3}$, from which we recover (4.11) and (4.12) for $r = 3$ and $r = 5$, respectively. This linking of T and E scaling has the following significance in x space. Suppose the velocity field is band-limited by a filter which passes only wavenumbers within, say, an octave of k. Then the assumed relation of scalings assures that triple moments of the filtered field and its space derivatives are k-independent if they are non-dimensionalised by the needed powers of the mean square of the filtered field and the mean square of its gradients.

The non-linear transfer process arises from the stretching or differential advection of the velocity field by itself. In the energy inertial range, simple estimates based on statistical independence of different wavenumber ranges support the localness of cascade. These estimates show that the effective straining acting on structures of size $\sim 1/k$ is dominated by contributions from components of wavenumbers $\sim k$ if the spectrum is (4.11). These estimates are given a precise mathematical form (but not made much more compelling) by the closure approximations described in §4.3. On the other hand, the enstrophy inertial-range spectrum (4.12) implies equal contributions to the effective strain from each octave in wavenumber that lies below (lower wavenumber) the k of interest. The integrations in (4.14(b)) then diverge logarithmically toward small wavenumbers, if the logarithmic extent of the putative inertial range is infinite.

Kraichnan (1971b) and Leith and Kraichnan (1972) have proposed on the basis of the TFM closure approximation (see §4.3) that the enstrophy inertial range has the corrected form

$$E(k) = C'\eta^{2/3}k^{-3}\,[\ln\,(k/k_1)]^{-1/3} \tag{4.17}$$

where k_1 is a wavenumber at the bottom of the range. According both to the closure approximation and simple estimates this correction makes the integrations in (4.14(b)) convergent and gives $\Pi(k)\to 0$, $Z(k)\to\eta$ for $k/k_1\to\infty$. The strict similarity between T and E is now lost since $E(k)$ has a logarithmic correction and $Z(k)$ does not.

The directions of energy or enstrophy transfer in the putative inertial ranges (i.e. the signs of ϵ and η) must now be considered. The formal analysis of (4.14) shows that individual triad interactions make a negative contribution to ϵ and a positive contribution to η if the mean energy transfer by the triad is *from* the mid-sized wavenumber *to* the extreme wavenumbers. This is also the physically plausible case if the ranges were to arise from the relaxation toward equilibrium of excitation initially placed at $k\sim k_1$. The relaxation would then be mediated by a range (4.11) with $\epsilon<0$ carrying energy to lower wavenumbers and a range (4.17) with $\eta>0$ carrying enstrophy to higher wavenumbers. Some further support for these signs of ϵ and η is provided by an initial-value analysis with power-law $U(k)$ and Gaussian initial distribution (Kraichnan 1967). It is found that the initial transfer is out of the middle wavenumber unless $U(k)$ falls between the power laws k^0 and k^{-2} corresponding to the $\alpha=0$ and $\beta=0$ equilibria of §3. Both (4.11) and (4.12) give $U(k)$ out of those limits (note $E(k)=\pi kU(k)$) and therefore correspond to initial transfer out of the middle wavenumber.

The formal analysis and the support by simple estimates of straining and by closure approximations by no means assure that the inertial ranges actually occur. This is, in fact, a very difficult matter to settle. Computer simulations verify that there does occur transfer of excitation to lower and higher wavenumbers in a manner qualitatively consistent with the simultaneous existence of both the energy and enstrophy inertial ranges. This is illustrated by the spectrum evolution curves in figure 12 obtained by Lilly (1971) (see also Lilly 1969, Fyfe *et al* 1977b, figure 2). However, numerical experiments can include only finite wavenumber ranges and cannot determine asymptotic behaviour, such as the precise power law of the asymptotic infinite k-range spectra. This difficulty is more acute in two dimensions than in three because estimates of the localness of interaction in k space (Kraichnan 1971b) suggest that triad interactions involving wavenumber ratios up to 10:1 are important in the two-dimensional transfer process so that very great wavenumber ranges would be

needed to approximate asymptotic behaviour. The logarithmic correction in (4.17) is particularly difficult to verify. Figure 13 illustrates the difficulty. Here an attempt is portrayed to simulate the enstrophy inertial range with several different wavenumber cutoffs; the results are compared with spectrum curves from integration of the test-field closure (§4.3) with the same cutoffs. The distorting effects of finite cutoffs is clearly shown. The test-field closure is known analytically to give the asymptotic spectrum (4.17) yet with a finite cutoff and with the effects of viscosity at the included wavenumbers it appears on the plot to yield a spectrum behaviour closer to k^{-4}.

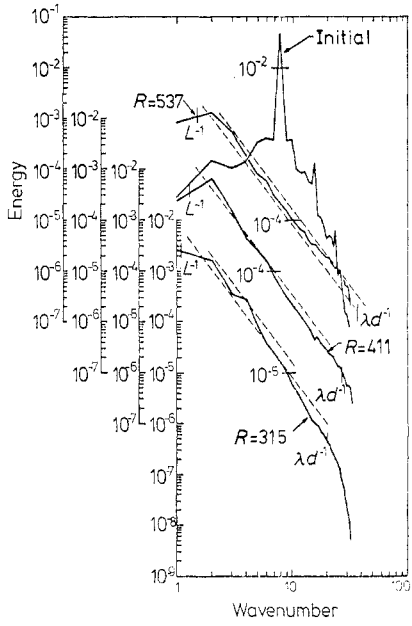

Figure 12. Energy spectrum for three 2D Navier–Stokes decay runs (from Lilly 1971), averaged over 200 time steps, and labelled by Reynolds number. Broken lines have slope -3.

Suppose that energy and enstrophy are steadily fed into the system at $k \sim k_1$ and that viscosity acts but that there is no upper cutoff ($k_{\max} = \infty$). If (4.11) and (4.17) are correct asymptotic forms we expect that, as the input continues, energy is carried toward the gravest modes k_0 by down transfer in the (4.11) range while the (4.17) range carries enstrophy upward and extends to successively higher k as time goes on. The enstrophy transport eventually is interrupted when the enstrophy inertial range has reached sufficiently high wavenumbers that the rate of enstrophy transfer is substantially balanced by the viscous dissipation (Novikov 1978a). As $\nu \to 0$ these wavenumbers become infinite and, in the limit, the enstrophy dissipation approaches a constant rate independent of ν while the energy dissipation rate becomes zero. In contrast to three-dimensional turbulence, where it is supposed that the inertial range can develop to infinite wavenumbers in finite time if $\nu \to 0$, in two dimensions the inertial range exhibits a constant asymptotic logarithmic rate of extension in k, according to closure approximations (Rose and Sulem 1978). The absolute equilibrium state

for $k_{\max}=\infty$ is one of condensation of all the energy in the gravest modes and this suggests that with steady input at k_1 and $\nu\to 0$ a singular excitation of energy in k_0 builds with time (Kraichnan 1967), or that with initial excitation at k_1 and no subsequent input all the initial energy collects eventually in k_0, while the enstrophy not associated with the k_0 excitation is dissipated (Bretherton and Haidvogel 1976, Matthaeus and Montgomery 1980).

The enstrophy range (4.17) corresponds to a spectrum of form k^{-1} for the enstrophy spectrum $2k^2E(k)$, apart from the log correction. This is the same as the spectrum for small-scale blobs of passive scalar passively advected by turbulence

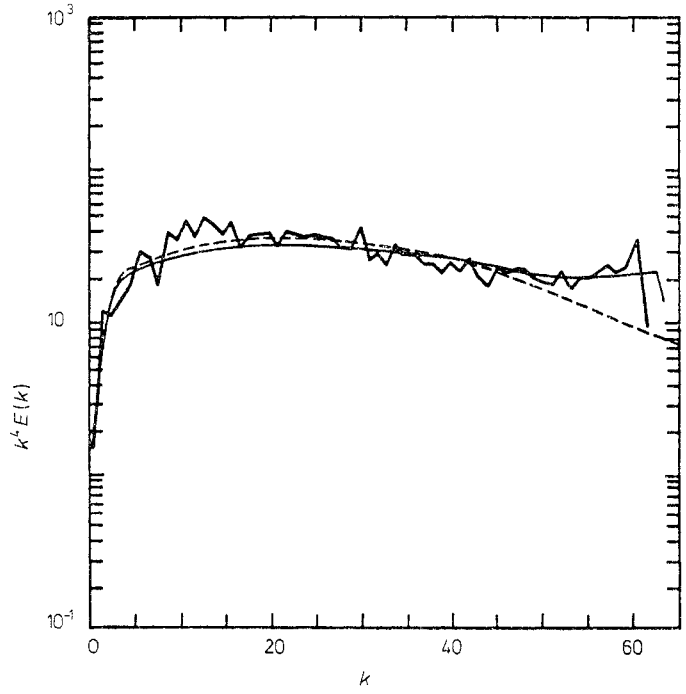

Figure 13. Comparison of $k^4E(k)$ (bold full curve) from a 2D Navier–Stokes decay simulation run ($k_{\max}=63$) with two different test field model runs with $k_{\max}=63$ (full curve) and $k_{\max}=128$ (broken curve) (from Herring *et al* 1974).

(Batchelor 1959, Kraichnan 1974b) and corresponds to the same basic physics: the small blobs (in the present case blobs of vorticity) are drawn out into filaments and the resultant statistical distribution of filament widths gives the k^{-1} spectrum. The log correction reflects the fact that the straining comes equally from all octaves of the enstrophy inertial range. The small-scale vorticity behaves essentially passively because it contributes little to the effective strain compared to the logarithmically larger contribution from lower wavenumbers.

Saffman (1971, 1977) has suggested an alternative to the spectrum forms (4.12) and (4.17). He considers an initial state in which the vorticity is segregated into sharp-edged domains. Fourier transformation of the sharp-edged distribution yields $E(k)\propto k^{-4}$ at high k. Then, since the vorticity in each fluid element is a constant of motion, Saffman argues that the sharp edges will persist and so therefore

will the k^{-4} spectrum except at k so large that viscous dissipation is significant. However, if viscosity is neglected, (4.17) also is consistent with sharp-edged domains; as discussed above, it describes a statistical distribution of widths of vorticity filaments. If the small scales are strained like a passive scalar then, given Saffman's initial condition, we would expect the log-corrected k^{-3} spectrum to spread to ever-higher k (until viscosity interferes) overpowering the k^{-4} spectrum as it does so. If, instead, the k^{-4} spectrum persists this would imply that the vorticity is not drawn out into filaments with statistically distributed widths. Figure 13 suggests that this question will not easily be settled by experiment, computer or otherwise. High-resolution simulations by Orszag (1976) are on the threshold of distinguishing k^{-3} from k^{-4}.

Sulem and Frisch (1975) have shown that if the steady-state rate of enstrophy dissipation approaches a non-zero limit as $\nu \to 0$ then the enstrophy inertial range cannot fall off more steeply than k^{-4}. A later sharpening of this bound (Pouquet 1978) has been found to be invalid by U Frisch, A Pouquet and P-L Sulem (private communication from U Frisch (1979)). Saffman (1977) points out that no such bound can eliminate the *a priori* possibility that the steady-state enstrophy dissipation goes to zero with ν. Orszag (1974) argues that if $\nu = 0$ and initial conditions are smooth then the enstrophy dissipation is zero for all finite time, a conclusion corroborated by Pouquet *et al* (1975) on the basis of the EDQNM closure (§4.4).

In three dimensions there are theoretical and experimental grounds to believe that the $k^{-5/3}$ inertial-range spectrum is modified, to a more negative exponent, by spatial intermittency of the small scales which increases the energy transfer ϵ associated with a given spectrum level $E(k)$ because of the non-linearity of the transfer process. A review of some of the relevant arguments is given by Kraichnan (1974a) and Rose and Sulem (1978). If the small scales of the vorticity field in two dimensions do behave like an advected passive scalar, then the dynamics in the enstrophy inertial range (4.17) are essentially linear, from which it can be argued that no intermittency corrections are to be expected in the spectrum law although gradients of the vorticity field will exhibit intermittency that increases as scale size decreases (Kraichnan 1975). If intermittency effects occur in the two-dimensional $-5/3$ range, the associated increase in transfer efficiency would be expected to make the exponent *less* negative, since the transfer is to smaller wavenumbers (Kraichnan 1975). Existing computer experiments can hardly decide the very existence of the inertial ranges, let alone determine intermittency corrections. However, figure 14 does exhibit increase of intermittency of vorticity gradients as the flow evolves. H Aref and E D Siggia (private communication) have suggested simulation by discrete vortices to explore intermittency effects in the energy inertial range.

4.3. Closure approximations

The non-linearity of the equations of motion makes it impossible to form from them simple closed equations that describe the evolution of given moments. Thus in (4.2) triple moments essentially affect the evolution of second-order moments. Many workers have sought (more or less) logically posed and tractable approximation schemes that yield closed equations useful for the extraction of qualitative features and semiquantitative predictions. Most of the schemes are based in some way on perturbation treatments of the non-linear terms in the equations of motion (e.g. (4.1) or (4.5)), modified or renormalised perturbation expansions for strong non-linearity, or related expansions of given moments as series in successively higher-order moments or cumulants. We shall not attempt to systematically summarise or even reference

this body of work both because of lack of space and because the methods used are not unique to two-dimensional turbulence. Some review articles and entrance points to the literature are Deissler (1977), Bradshaw (1976), Leslie (1973), Monin and Yaglom (1975), Orszag (1970), Kraichnan (1972), Kadomtsev (1965) and Rose and Sulem (1978). Recent efforts to apply perturbation theory to the inertial ranges via the renormalisation group approach are discussed by De Dominicis and Martin (1979).

A central place in the plethora of closure approximations is occupied by the direct interaction approximation (DIA) (Kraichnan 1959). Many other approximations can be obtained from it by various modifications and simplifications. This approximation results in closed equations that involve the two-point, two-time covariance

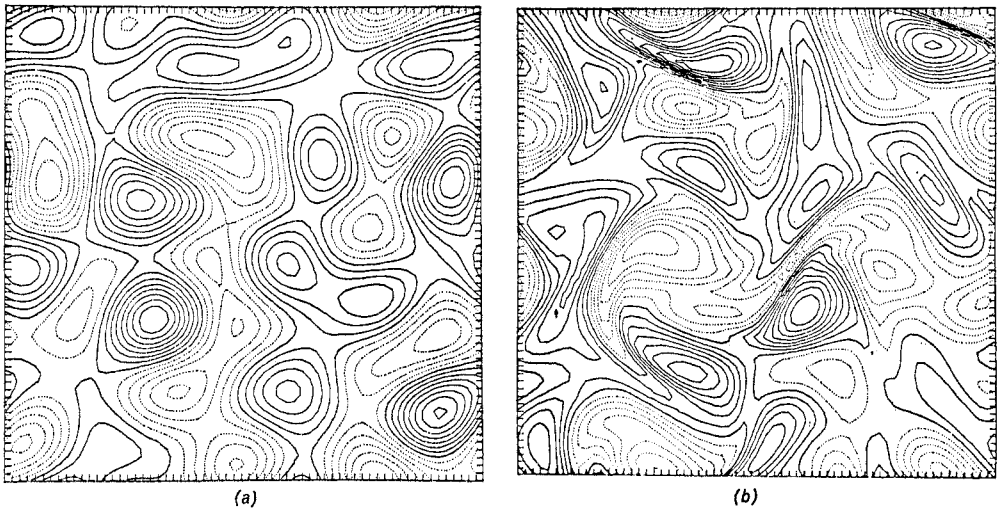

Figure 14. Evolution of the vorticity field for a 2D Navier–Stokes decay run (from Lilly 1971). (*a*) shows the initial vorticity field and (*b*) shows the vorticity field after 100 time steps. Regions of steep vorticity gradients may indicate intermittency.

of the velocity field, the mean response of the velocity amplitude to infinitesimal perturbations, and the mean velocity field if the latter is non-zero. The DIA may be obtained either as the lowest truncation of a renormalised perturbation expansion (Kraichnan 1977a,b) or, in several ways, as the exact statistical description of stochastic models of the actual equations of motion (Kraichnan 1969, Leith 1971, Herring and Kraichnan 1972). The model representation assures that the DIA gives conservation of energy and enstrophy in two dimensions and that it gives correct absolute statistical equilibria of the truncated flow system. It gives rather accurate descriptions of isotropic turbulence decay at low Reynolds numbers (Orszag and Patterson 1972) in three dimensions, but underestimates the efficiency of energy transfer in the three-dimensional inertial range because it cannot separate effects of convection by large scales and effects of internal distortion of small scales upon the rate of time-decorrelation of small scales (Leslie 1973). A modification of the closure that uses Lagrangian rather than Eulerian two-time functions (Kraichnan 1966, 1977a,b, Leslie 1973) gets around this difficulty, yields (4.11) in three dimensions and gives a value of C consistent with experiment.

The DIA has been worked out and evaluated for two-dimensional turbulence by

Seyler *et al* (1975) and Herring *et al* (1974). The Lagrangian modification (LHDIA) has been compared with computer decay experiments in two dimensions by Herring and Kraichnan (1979) who also evaluated a variant of the LHDIA approximation in which the symmetric rate-of-strain field rather than the velocity field is basic (SBLHDIA).

The DIA and LHDIA closures, together with a number of other closure approximations related to (renormalised) second-order perturbation theory, lead to an expression of the following form for the transfer function $T(k, p, q)$:

$$T(k, p, q, t) = C(k, p, q)\,[2\theta_{kpq}(t)E(p, t)E(q, t) - \theta_{pqk}(t)E(k, t)E(q, t) - \theta_{qkp}(t)E(k, t)E(p, t)]. \tag{4.18}$$

Here $C(k, p, q)$ is a time-independent coefficient which is the same for all the closures but which depends on the dimensionality of space; it vanishes unless k, p and q can form a triangle and thus be directly coupled by (4.5). $\theta_{kpq}(t) = \theta_{kqp}(t)$ is a closure-dependent characteristic decorrelation time for the phase coherence of modes k, p and q. In the DIA closure it is an integral over past time of an integrand composed of average response functions and normalised two-time Eulerian correlation functions. In the LHDIA closure it is a similar integral over Lagrangian functions. The structure of $C(k, p, q)$ ensures that $T(k, p, q)$ vanishes in absolute equilibrium states (detailed balance) and that (in two dimensions) (4.9) is satisfied identically.

In the test-field-model closure (TFM) $\theta_{kpq}(t)$ is related to the characteristic times of pressure forces that maintain $\nabla . \boldsymbol{u} = 0$ (Kraichnan 1971a,b, 1972, Leith and Kraichnan 1972). Its evolution is fixed by an ordinary differential equation in t with the result that the TFM closure is Markovian: the change of $E(k, t)$ depends only on current values instead of essentially involving integrals over past history as in the DIA closure. Another Markovian closure is the Markovianised eddy-damped quasi-normal (EDQNM) approximation (Orzsag 1970, 1977, Rose and Sulem 1978) in which $\theta_{kpq}(t)$ is determined by scaling arguments. In contrast to the DIA and LHDIA closures, the Markovian closures involve disposable constants.

Figures 15 and 16 compare the decay of isotropic two-dimensional turbulence according to computer simulations and several closure approximations.

The closure approximations and the perturbation expansions which underlie them can be used to investigate formally the dependence of cascade dynamics on a *continuous* dimensionality parameter d. Frisch *et al* (1976) and Fournier and Frisch (1978) have used the TFM and EDQNM closures and simple Taylor expansions in time to examine behaviour in the neighbourhood of $d = 2$. They find unphysical behaviour for $d < 2$ and a $k^{-5/3}$ energy cascade range for $d \geqslant 2$. If $2 \leqslant d < d_c$, where $d_c \sim 2{\cdot}05$, the energy flow in this range is to lower wavenumbers while for $d > d_c$ the flow is to higher wavenumbers. The enstrophy inviscid constant of motion exists only for $d = 2$. However, for $2 \leqslant d < d_c' \sim 2{\cdot}06$ there exists a zero-energy-transfer inertial range whose exponent depends on d and which goes into the enstrophy inertial range at $d = 2$.

Forster *et al* (1976, 1977) and De Dominicis and Martin (1979) have studied the d dependence of turbulence forced at all wavenumbers by white noise stirring with prescribed spectral forms. They again find unphysical behaviour for $d < 2$ and anomalous effects at $d = 2$. We shall discuss the latter in §4.4. These papers employ interesting applications of renormalisation group techniques to turbulence theory. Fournier *et al* (1978) have examined the limit of infinite d.

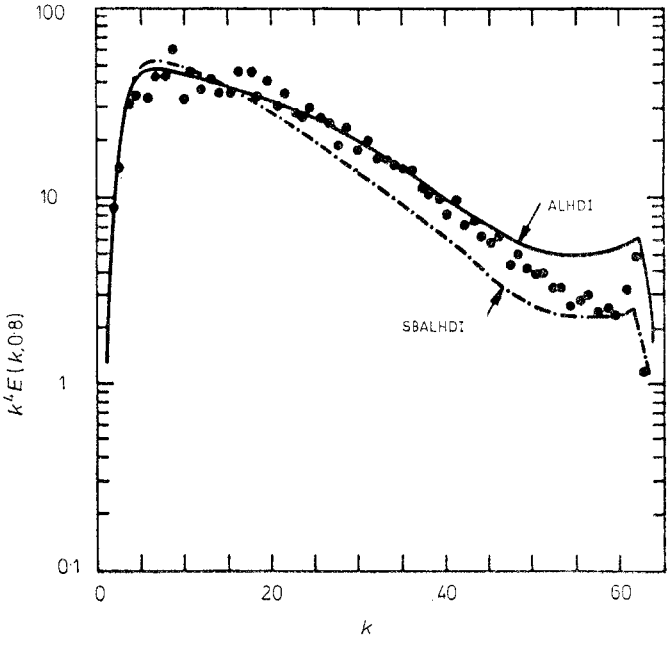

Figure 15. Comparison of a 2D Navier–Stokes decay calculation of $k^4E(k)$ (dots) with two versions of the Lagrangian-history direct interaction approximation (from Herring and Kraichnan 1979).

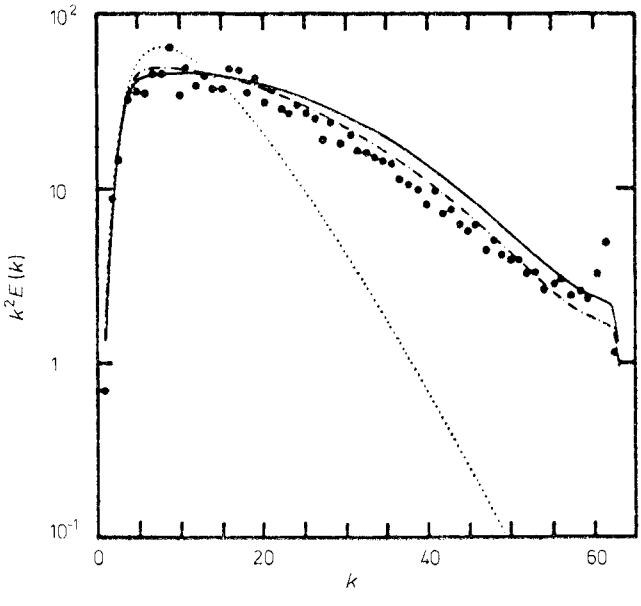

Figure 16. Comparison of a 2D Navier–Stokes decay calculation of $k^2E(k)$ (points) with the results of closure calculations from the same initial spectrum for three different models (from Herring *et al* 1974). Curves as in figure 9.

Not all the closure approximations that have been proposed fit naturally into the form (4.18). Dupree (1974) has described a theory of two-dimensional turbulence based on approximations to two-particle diffusion. A related treatment involving three-point Green functions has been given by Weinstock (1977).

A functional formulation of the closure problem has been given by Martin *et al* (1973) and Phythian (1975a, 1976), who work with generating functionals for the moments. Lundgren (1972) has proposed closures based on partial probability distributions rather than moments. An exact two-dimensional solution forced by white noise is discussed by Thompson (1972).

4.4. Eddy viscosity and sub-grid-scale representations

The concept of eddy viscosity has been highly useful in turbulence theory for visualising and parametrising the transport of turbulent energy both in space and between different scales of motion. More recently, eddy viscosity parameters have been used to represent the effects of sub-grid-scale motions in large-scale computer simulations of flows.

Eddy viscosity representation of the small scales involves an analogy between the dynamical effects of these scales and the effects of thermal agitation. In typical turbulent flows almost all the thermal agitation energy is well-separated in scale from the smallest hydrodynamic scales which are appreciably excited. This permits the accurate representation of molecular viscous and diffusive effects by local differential operators.

In three-dimensional flows the analogy between sub-grid scales and thermal agitation already is imperfect because the turbulent motion in fact has a continuous distribution of scale sizes. This means that the effects of sub-grid scales on explicitly computed scales cannot be accurately represented by a simple differential operator of the form $\nu_{\text{eddy}}\nabla^2$ (Corrsin 1974). In two-dimensional flow, the eddy viscosity concept meets with additional and more severe difficulties associated with the reverse flow of kinetic energy, from small scales to large scales. Molecular viscosity does not exist in a strictly two-dimensional fluid (Dorfman and Cohen 1970). We are not interested here in two-dimensional fluids but rather in the two-dimensional macroscopic hydrodynamics of a three-dimensional fluid. Nevertheless we shall see that the non-existence of molecular viscosity in two dimensions correctly suggests severe difficulties for the eddy viscosity representation of sub-grid scales.

The anomalous nature of transport coefficients in two dimensions shows up already in the equilibrium statistical mechanics of the truncated inviscid system. If the truncation wavenumber is the order of the reciprocal of the mean intermolecular distance, the truncated system is a model of the molecular fluid, with the hydrodynamic modes representing approximate collective coordinates of the molecules. The absence of compressive modes in the model is unimportant here. Renormalised perturbation theory, and in particular the DIA, can be used to compute the effective damping of perturbations of the fluid. If $G(k, t)$ is the mean amplitude of a decaying perturbation of a mode of wavenumber $k \ll k_{\max}$, with $G(k, 0)=1$, then the DIA gives the relaxation equation (Kraichnan 1975)

$$\partial G(k, t)/\partial t + k^2 \int_0^t \eta(t-s) G(k, s)\, \mathrm{d}s = 0. \tag{4.19}$$

In three dimensions the time-lagged damping function $\eta(t)$ goes like $t^{-3/2}$ at large t. Since $G(k, t)$ varies slowly with t for small k, the damping term in (4.19)

may be replaced by $\nu' k^2 G(k, t)$ where $\nu' = \int_0^\infty \eta(s)\, ds$ is the effective viscosity. But in two dimensions it is found that $\eta(t)$ goes like t^{-1} so that the effective viscosity diverges logarithmically and cannot be defined. The divergence is found to arise from low-wavenumber contributions to $\eta(t)$. These results also come from renormalisation group analysis (Forster *et al* 1976, 1977) and corroborate kinetic theory results for two-dimensional fluids.

Closure approximations again provide a natural framework for formulating eddy viscosity representations of small-scale dynamics in non-equilibrium turbulent states where there is a cascade of energy and enstrophy. Let k_m be some arbitrarily chosen wavenumber which may be thought of as dividing explicitly treated scales $k < k_m$ from scales $k > k_m$ which are to be represented by an eddy viscosity. If $k \ll k_m$, and with certain conditions on the shape of the energy spectrum and the behaviour of the relaxation times θ_{kpq}, the contributions to (4.18) from p and/or $q > k_m$ are dominated by the terms proportional to $E(k)$. If we denote all such contributions to (4.8(*b*)) by $T(k|k_m)$ then an effective eddy viscosity at wavenumber k may be defined by

$$\nu(k|k_m) = -T(k|k_m)\,[2k^2 E(k)]^{-1} \tag{4.20}$$

in analogy to the molecular viscosity term in (4.8(*a*)).

If $k \ll k_m$, some calculation (Kraichnan 1976a) yields

$$\nu(k|k_m) = (2\pi/15) \int_{k_m}^\infty \theta_{qqk}[7U(q) + q\, dU(q)/dq] q^2\, dq \qquad \text{(three dimensions)} \tag{4.21(a)}$$

$$\nu(k|k_m) = (\pi/4) \int_{k_m}^\infty \theta_{qqk}(d/dq)\,[q^2 U(q)]\, dq \qquad \text{(two dimensions).} \tag{4.21(b)}$$

Here $U(q)$ represents the excitation per mode ($E(k) = 2\pi k^2 U(k)$ in three dimensions and $E(k) = \pi k U(k)$ in two). With $k \ll q$ the TFM, DIA or LHDIA closures give θ_{qqk} independent of k so that both (4.21(*a*)) and (4.21(*b*)) give k-independent results for $\nu(k|k_m)$ if $k \ll k_m$.

If (4.21(*a*)) is evaluated in the inertial range (4.11) it gives $\nu(k|k_m) \sim \epsilon^{1/3} k_m^{-4/3}$. In the two-dimensional energy-inertial range (4.21(*b*)) gives the same result, but with the difference that $\nu(k|k_m)$ is *negative*. We may note that $q^2 U(q)$ in (4.21(*b*)) is proportional to the enstrophy per mode and decreases with increase of q for any spectrum that falls below enstrophy equipartition. The negative eddy viscosity in two dimensions, of course, reflects the fact that energy flow is to lower rather than higher wavenumbers (Starr 1968).

A physical mechanism for the negative viscosity has been proposed by Kraichnan (1976a). The large scales (wavenumber k) strain the small scales (wavenumber q), drawing them into elongated shapes with constant enstrophy and decreased energy. At the same time a secondary flow associated with the small scales grows on scales $\sim 1/k$ and gives destructive interference with the excitation at wavenumber k, thereby maintaining energy balance. The net result of this process, with stochastic variation of the straining in time taken into account, is the negative viscosity (see Starr 1953, 1968, Krause and Rudiger 1974).

If $k \sim k_m$, the validity of the eddy viscosity concept is weakened by non-local effects in both space and time. The time effects are illustrated by the lag in (4.19). Similar structure in (4.18) is hidden in the θ factors which in the DIA and LHDIA closures involve integrations over past time. The non-local space effects show up, at the least, as k dependence of $\nu(k|k_m)$. If $\nu(k|k_m)$ is evaluated in the enstrophy

inertial range, the fact of zero-energy cascade implies that the negative values of $\nu(k|k_m)$ for $k \ll k_m$ must be suitably balanced by positive contributions at $k \sim k_m$ (we have $k < k_m$ always). This means that a simple approximation of positive eddy viscosity (all k) designed to simulate the cascade of enstrophy to higher wavenumbers does intrinsic violence to the dynamics. This point is developed by Leith (1971), Kraichnan (1976a) and Basdevant *et al* (1978).

If only the enstrophy cascade is considered, a simple positive eddy viscosity coefficient may be appealed to. If k_m is in the enstrophy inertial range, dimensional analysis or an idealised diffusion model implies that this coefficient has the form

$$\nu_{\text{eddy}} \sim \eta^{1/2} k_m^{-2} \tag{4.22}$$

where η is the cascade rate in (4.12) or (4.17) (Leith 1968). A form more appropriate to sub-grid-scale representation in actual computations is

$$\nu_{\text{eddy}} \sim |\nabla\omega| k_m^{-3} \tag{4.23}$$

(Leith 1968) where ω is the local vorticity associated with the explicit scales (see also Smagorinsky 1963).

Basdevant *et al* (1978) give detailed proposals for sub-grid-scale representations that are based on the k-dependent results of the closure approximations and so maintain both energy and enstrophy conservation. It is important to note that even in full detail the closure approximations are at the level of second-order moments and ignore phase coherence effects that may be very important. The closures can be formulated for inhomogeneous flows (e.g. Kraichnan 1972); in this form they would appear to be more suited for simulations of individual realisations than the homogeneous isotropic forms which we have discussed and which are used by Basdevant *et al* (1978). However, inhomogeneity implies very much greater computational difficulty.

In principle the sub-grid scales can be eliminated entirely from the equations of motion if they are unexcited initially. But it is not clear to what extent the extra non-linearity thereby introduced in the equations of motion of the explicit scales can be approximated by a generalised eddy viscosity, or even the full structure of (4.18). The stochastic model representations of the DIA or TFM closures (Kraichnan 1970c, Leith 1971) are equations for amplitudes rather than covariances, although much information is lost by averaging and implicit simple approximation of statistical distributions. These amplitude equations provide, in addition to the effective k-dependent eddy viscosity terms, a random driving term of the explicit scales by the sub-grid scales, a feature that may be more faithful to the actual dynamics. The effects of this driving on ensemble-averaged energy transfer show up in the first term on the right-hand side of (4.18). Rose (1977) has examined such random driving effects in the context of renormalisation group analysis (see also Forster *et al* 1977).

It is probable that the excitation of sub-grid scales by explicit scales and the subsequent reaction of the sub-grid scales on the explicit scales also involves coherent, phase-locked phenomena that are intrinsically unsuited to any statistical treatment.

4.5. Error growth and predictability

Instability is one of the general characteristics of turbulence: the velocity field is sensitive to perturbations even though the averages over an ensemble of realisations

of the velocity may be insensitive. Thus, if two realisations differ initially by a small amount, the difference may grow with time and eventually become the order of the velocity field itself. An alternative statement is that initial error or incompleteness in the specification of the velocity field may grow with time. The importance of this effect in the prediction of meteorological flows was pointed out by Robinson (1967, 1971) and Lorenz (1969). Since then the subject has attracted increasing interest. We shall limit the discussion here to theoretical studies of error growth in homogeneous isotropic turbulence that fall into the general framework of the closure approximations described in §4.3 and to computer simulations of error growth that serve to test the theories.

Let us call the difference between the velocity fields of two realisations the difference or error velocity field. The error dynamics at the statistical level of second-order moments is then described by the covariance or spectrum function of the difference velocity and by the covariance of the velocity of one realisation with that of the other. All the closures described in §4.3 may be used to obtain equations for the evolution of the spectrum function of the error energy (kinetic energy of the error field) (Lorenz 1969, Leith 1971, Leith and Kraichnan 1972, Kraichnan 1970b). The results obtained by the DIA closure have been compared with computer simulations of low-Reynolds-number three-dimensional isotropic turbulence by Herring *et al* (1973). Figures 17 and 18 show the evolution of the total error energy and the error-vorticity spectrum for one of the cases. At higher Reynolds numbers the DIA closure is expected to underestimate the error energy growth because of the lack of discrimination between convection and distortion effects on the small scales, mentioned in §4.3.

Lilly (1972a,b) has studied numerically the growth of error in computer simulations of two-dimensional turbulence. Leith (1971) and Leith and Kraichnan (1972) have used the EDQNM and TFM closures to examine error energy and error enstrophy growth in the energy inertial ranges for both two- and three-dimensional turbulence and for the enstrophy inertial range in two dimensions. In the energy inertial ranges it was found that the time for error energy initially confined to and dominating wavenumbers $k > k_2$ to spread down to and dominate wavenumbers $k_3 \ll k_2$ is $\sim \epsilon^{-1/3} k_3^{-2/3}$, independent of k_2. This is the eddy circulation time for scales with wavenumber k_3. The error propagation time is independent of k_2 because the characteristic dynamical times decrease as k increases. Down propagation of error was again found in the enstrophy inertial range (4.17), the time of propagation from k_2 to $k_3 \ll k_2$ being $\sim \eta^{-1/3} \{[\ln (k_2/k_1)]^{2/3} - [\ln (k_3/k_1)]^{2/3}\}$. An application was made to propagation of errors to larger scales in the atmosphere, in refinement of earlier work by Lorenz (1969).

Simulations to test these results for the asymptotic inertial ranges could be computed only if the range of wavenumbers were limited by some sub-grid-scale parametrisation, which would greatly complicate the test. However, there are some difficulties in principle with using the Eulerian error energy to measure error growth (Leith and Kraichnan 1972). With this measure the random displacement of a small-scale structure by its own size represents a large error, while the dynamical significance may be small. Effects of this kind may result in overestimates of error growth in the inertial ranges by the Eulerian closure approximations.

The instability of individual turbulent realisations to perturbations is in contrast to the expected stability to perturbation of an aptly chosen ensemble of realisations. Leith (1975) has made the interesting suggestion that the stability of the ensemble

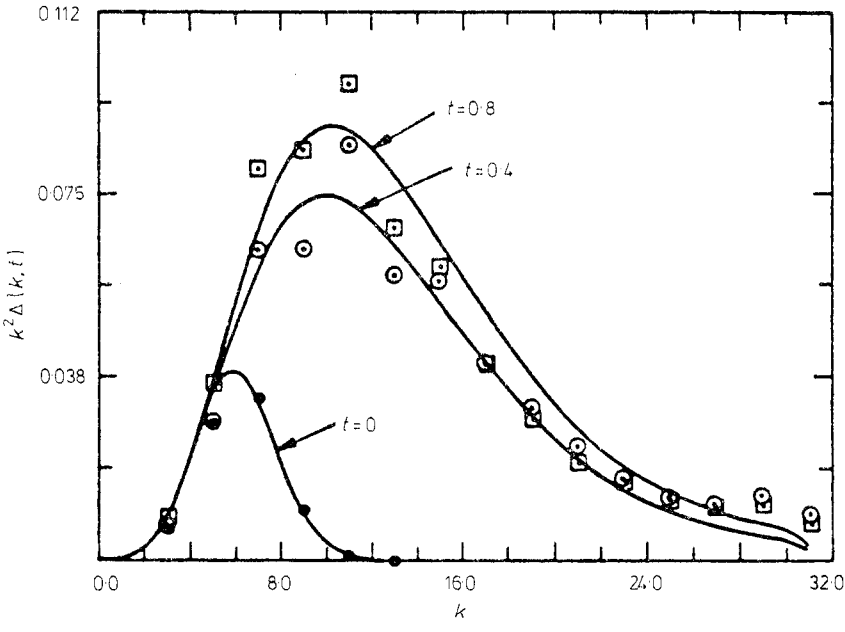

Figure 17. Three-dimensional error vorticity spectrum (points) and its evolution in time, compared with the predictions of the DIA (full curves) at three different times for a typical case (from Herring *et al* 1973).

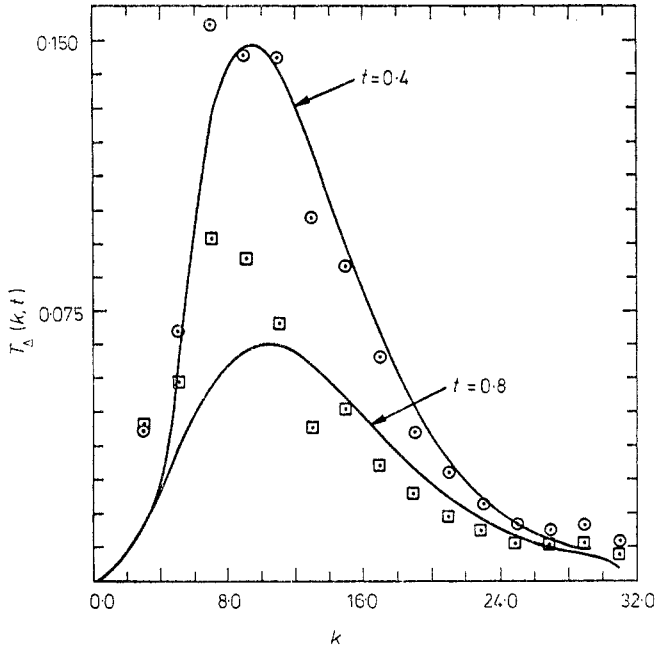

Figure 18. Three-dimensional error transfer spectrum $T_\Delta(k, t)$ and its evolution (points), compared with the predictions of the DIA at two different times, for the same case shown in figure 17 (taken from Herring *et al* 1973).

can profitably be investigated in terms of the fluctuation-dissipation theorem which (for equilibrium ensembles) relates mean response to perturbation and the fluctuations of the unperturbed ensemble. Leith derives this theorem for two-dimensional or geostrophic turbulence, makes an application to climate response, and discusses the implications of the deviation of the actual ensemble from absolute equilibrium.

5. Turbulence on the surface of a rotating sphere

A principal reason for interest in two-dimensional turbulence is the possibility of applying the theory to planetary boundary layers. On a global scale the Earth's atmosphere and oceans are a very thin layer so that it is reasonable to expect two-dimensional motion on scales large (over, say, 100 km) compared to the layer thickness. Observation suggests a degree of randomness in the mesoscale motions which are smaller than the size of the planet but still large compared to the layer thickness.

There are many complicating factors. Winds and currents vary with altitude and depth so that the tangential motion in the mesoscales is z-dependent and not strictly two-dimensional in the sense we have been assuming. Moreover, there are fully three-dimensional motion (e.g. cumulus systems) at small scales, molecular and eddy friction at the surface of land and sea, effects of topographic surface variations, radiant energy inputs which vary diurnally and with cloud cover and surface character, heat of vaporisation and condensation of water, density and salinity variations in the oceans, wave effects at the air–sea interface, temperature and density variations with altitude in the atmosphere, and many others.

The rotation of the Earth plays a crucial role. Uniform rotation of a plane layer of fluid about an axis perpendicular to the plane (z axis) tends to lock the fluid into two-dimensional motion independent of z (Taylor–Proudman theorem) (Proudman 1916, Taylor 1923, Greenspan 1968, Inglis 1975). Perturbations that produce z variation in $\boldsymbol{u}$ (vertical shear) result in inertial waves which represent a balance of acceleration, Coriolis force and pressure and which, even in the linear regime, can give spectral transfer by reflection from the boundaries (Phillips 1963). The Coriolis force in a uniform fluid layer on the surface of a sphere varies with latitude. In the β plane or tangent plane approximation the variation is linear. The variation of Coriolis force gives rise to another set of waves, the Rossby waves, whose wavevectors lie in the surface. A comprehensive treatment of the dynamics of rotating fluids is given by Greenspan (1968).

The non-linear dynamics of a rotating fluid layer with stochastic excitation involves the interplay of these wave processes with the turbulent transfer and distortion processes that occur without rotation, together with whatever internal and boundary damping processes act. The rotation also produces characteristic boundary-layer structures (Ekman spirals) associated with viscous (or eddy viscous) drag.

In what follows we shall describe some studies of idealised turbulence in a rotating fluid layer. With regard to atmospheric and oceanographic applications, the idealisations all fall within the quasi-geostrophic approximation, based upon a local near balance among Coriolis force, centrifugal force, pressure and gravity. A current review of geostrophic turbulence, with emphasis on the relation of theory and observation, is given by Rhines (1979). Our interest here is in the way the basic equilibrium and non-equilibrium analysis of two-dimensional turbulence in §§3 and 4

is altered by rotation, topography and z-dependent flow phenomena. The essential feature of the quasi-geostrophic approximation is that the inviscid equation of motion is of the type (2.14), but with $\omega = -\nabla^2\psi$ replaced by a more general scalar functional of the stream function, the potential vorticity, containing additional terms involving rotation, buoyancy and topographic variation.

Consider first a uniform, thin spherical fluid layer without surface friction and without rotation. Equation (2.14) holds for the flow over the surface and all the general analysis of §§3 and 4 carries over to this geometry, which is topologically equivalent to the cyclic square. The stationary eigenmodes for the stream function are spherical surface harmonics (Platzman 1960, Wiin-Nielsen 1972). Tang and Orszag (1978) have performed numerical simulations of isotropic turbulence decay in this geometry analogous to those of Herring *et al* (1974) for the cyclic square. The results show weaker transfer to high mode numbers in the spherical geometry, a phenomenon which the authors associate with a transfer mechanism (i.e. the coefficients in (3.4)) that is more local than in the plane geometry.

In the spherical layer with rotation (2.14) is replaced by

$$(\partial/\partial t + \boldsymbol{u}.\nabla)\zeta = 0 \tag{5.1}$$

where

$$\zeta = \omega + \Omega^* \cos\phi \tag{5.2}$$

is the potential vorticity. Here Ω^* is the angular rate of rotation of the spherical surface about an axis and ϕ is the latitude. In the β-plane approximation (5.2) is replaced by

$$\zeta = \omega + \beta^* y \tag{5.3}$$

where y is the local North–South coordinate and β^* is the y derivative of the local normal component of the rotation vector. It can be verified by partial integrations, using (2.17), that (5.1) has the constants of motion $\int |\boldsymbol{u}^2|\, \mathrm{d}^2x$ and $\int \zeta^2\, \mathrm{d}^2x$.

The term in Ω^* or β^* gives rise to the Rossby waves which are linear at low amplitude and are modified by and exchange energy with the previously studied turbulent excitations at higher amplitudes. The Rossby waves are dispersive, with frequency inversely proportional to wavenumber. Thus the ratio of eddy circulation frequency ku' (where u' is a typical value of u) to Rossby wave frequency decreases with k. This ratio is a measure of the effective degree of non-linearity. Thus, with suitable excitation, the system can exhibit turbulence almost unaffected by rotation at large k and Rossby waves almost unaffected by turbulence at low k. The qualitative effect of the wave oscillations on the turbulence is inhibition of turbulent transfer, as the random walks of fluid elements are changed to oscillations (Rhines 1975, 1979). The non-linear interactions of the waves with themselves is of a resonant type. Stable soliton waves may be important (Stern 1975, Redekopp 1977, Rhines 1979).

Numerical computer simulations showing the evolution of random waves and turbulence in the β plane have been carried out by Rhines (1975) and Williams (1978). Tang and Orszag (1978) present computer studies of the exact spherical equation (5.1)–(5.2). The simulations are consistent with the qualitative picture stated above.

Holloway and Hendershott (1977) have extended the TFM closure to the system (5.1)–(5.3). They use forms for the relaxation times θ in (4.18) which take into account both the decorrelating effects of wave oscillation on triple correlations and

the resonant interactions of nearly linear waves. A wealth of detailed predictions about the behaviour of transfer functions comes from this analysis.

Variations in the layer thickness (topographical or orographical variations) modify the stationary eigenmodes and their couplings. In a channel of uniform width such variations can couple the vortex motion to the potential flow. In a rotating spherical layer, or the β-plane approximation to it, the dominant effect of slight variations in layer thickness is a coupling of the vortex motion to the uniform part of the Coriolis force. The potential vorticity is

$$\zeta = \omega + h(x, y) \tag{5.4}$$

where

$$h(x, y) = \beta^* y + f_0 d(x, y)/D. \tag{5.5}$$

f_0 is the normal component of the planetary rotation vector at $y=0$, $d(x, y)$ is the variation in layer thickness and D is the mean layer thickness (Holloway and Hendershott 1974, Salmon *et al* 1976).

The system (5.1) and (5.4)–(5.5) has been investigated by computer simulation (Holloway and Hendershott 1974, Bretherton and Haidvogel 1976, Holloway 1978), equilibrium statistical theory (Salmon *et al* 1976, Herring 1977) and closure approximations (Herring 1977, Holloway 1978). The results of these approaches are happily consistent. An equilibrium analysis like that of §3 can be carried out by expanding $h(\boldsymbol{x})$ in the eigenfunctions $\phi_n(\boldsymbol{x})$. Then the equilibrium canonical ensemble based on the constants of motion E and $\int \zeta^2 \, \mathrm{d}^2x$ (Salmon *et al* 1976) yields

$$\langle u_n \rangle = 2\alpha\lambda_n(\beta + 2\alpha\lambda_n{}^2/\rho)^{-1} h_n \tag{5.6(a)}$$

$$\bar{E}_n = \tfrac{1}{2}\langle u_n{}^2 \rangle = \tfrac{1}{2}(\beta + 2\alpha\lambda_n{}^2/\rho)^{-1} + 2\alpha^2\lambda_n{}^2(\beta + 2\alpha\lambda_n{}^2/\rho)^{-2} h_n{}^2 \tag{5.6(b)}$$

where $\omega_n = \lambda_n u_n$ and h_n is the mode amplitude of $h(\boldsymbol{x})$.

The most noteworthy contrast with the results of §3 is the non-zero mean value $\langle u_n \rangle$, correlated with the topography. In states with strong condensation in the lowest modes, this correlation emphasises the largest topographic features. In physical space the correlation expresses conservation of the angular momentum of the fluid as it experiences horizontal divergence or convergence. Anticyclonic flow (clockwise in the Northern hemisphere) is favoured where the layer is thin. Qualitatively similar equilibrium states are predicted by Bretherton and Haidvogel (1976) who use the concept of energy-conserving enstrophy cascade to dissipative large-n modes to support a criterion of minimum enstrophy at given energy.

Both the absolute equilibrium states and cascade transfer phenomena are treated by Herring (1977) who uses the DIA and an extension of the TFM closures and by Holloway (1978) who uses a modified TFM closure. The DIA closure predicts via fluctuation-dissipation relations that the equilibrium states can consist of both a static and a dynamic excitation. In non-equilibrium, transfer processes can maintain static large-scale circulations against frictional forces by means of energy supplied from fluctuating small scales. Zimmerman (1978) infers the latter process by simple perturbation analysis. The cited computer simulations seem to support fairly well the predictions of the absolute equilibrium theory and the closure approximations.

In all the cases considered so far the motion has been purely horizontal with no vertical variation of velocity within the fluid. Charney and Stern (1962) have developed an analogy between purely two-dimensional incompressible flow and three-dimensional quasi-geostrophic flow in which effects of buoyancy due to temperature

differences are taken into account. Under a suitable set of approximations (see, for example, Rhines 1979) and under the assumption that contributions from the boundaries at top and bottom may be neglected, this theory leads to a potential vorticity of the form (Charney and Stern 1962, Charney 1966, 1971)

$$\zeta = \omega - \partial^2\psi/\partial z_*{}^2 = -\nabla^2\psi - \partial^2\psi/\partial z_*{}^2 \tag{5.7}$$

where

$$z_* = zN_s/f_0.$$

z is the vertical coordinate, f_0 is the local vertical component of the planetary rotation vector, and N_s, the Brunt–Väisälä frequency, is a characteristic frequency for the vertical oscillation of air parcels under the action of gravity and buoyancy (with a temperature that varies with z in such a way that the atmosphere is stable to adiabatic displacements). The equation of motion is still (5.1) and ∇ is the horizontal gradient operator. The quadratic constants are $\int \zeta^2 \, \mathrm{d}^3x$ (note that the integration is now three-dimensional) and (in the absence of boundary-term contributions) the energy

$$E = \tfrac{1}{2}\rho \int [|\nabla\psi|^2 + (\partial\psi/\partial z_n)^2] \, \mathrm{d}^3x \tag{5.8}$$

where the final term represents buoyant potential energy and ρ is a mean value for the layer.

Charney (1971) proposes that the system (5.1)–(5.7) can exhibit statistically isotropic turbulent solutions in the x, y, z_* coordinate system and that the similarity arguments that hold in ordinary two-dimensional turbulence carry over to the extent that there is a (log-corrected) k^{-3} spectrum in an inertial range. Moreover, the equilibrium statistical-mechanical analysis of §3 continues to apply, leading to equilibria of the form (3.18(a)) but with the three-dimensional wavenumber playing the role of λ_n.

This proposal has been investigated in detail by Herring (1980) who uses a simplified TFM closure. Herring assumes an initial state that is homogeneous in three dimensions but with vertical–horizontal anisotropy. He finds that high wavenumbers have a weak tendency to isotropy and have asymptotically a log-modified k^{-3} spectrum. Low wavenumbers (large scales) tend instead to a z-independent (barotropic) two-dimensional spectrum. The methods used are an extension of earlier treatments (Herring 1974, 1975) of three- and two-dimensional anisotropic turbulence. Herring notes that the assumed vertically homogeneous initial state is unrealistic in the sense that the motion (5.1) is strictly two-dimensional so that there is no mechanism for homogenising and thus no way to reach such an initial state from more general states.

The Charney–Stern quasi-geostrophic equations embody continuous variation with z (continuous baroclinicity). Models with a finite number of barotropic horizontal layers that can be considered a discrete version of these equations have also been investigated. Rhines (1977) has studied the exchange of energy among modes in a two-layer model by computer simulation. The equilibrium statistical mechanics of the two-layer model has been treated by Salmon *et al* (1976) and a modified EDQNM closure has been formulated for this model by Salmon (1978). The properties of the two-layer model are summarised by Rhines (1979). A prominent feature, consistent with Herring's results for continuous baroclinicity, is that large-scale baroclinic modes tend to pass energy to smaller-scale barotropic modes which in turn pass energy to larger-scale barotropic modes.

It is unclear to what extent the predictions of the Charney–Stern equations are modified by boundary effects at the surface of earth or sea. Blumen (1978a,b) finds

strong influences of the boundaries which, among other effects, modify the asymptotic power laws. It should be remembered that important phenomena, notably the formation of fronts (Hoskins 1976, Andrews and Hoskins 1978), lie outside any analysis that uses statistical homogeneity in the horizontal, whatever is assumed in the vertical. Bretherton (1966a,b) investigates a number of instability processes in quasi-geostrophic flow.

Spectra with an approximate k^{-3} form have been observed in the atmosphere (e.g. Wiin-Nielsen 1972, Julian *et al* 1970, Chen and Wiin-Nielsen 1978). Mercifully we have no space in this review to attempt to analyse the degree of relation these results have to the idealised enstrophy or potential-enstrophy inertial range. Great caution is called for in any such analysis. The observed spectra cover a short range in k while the theory indicates a slow asymptotic approach to the log-corrected k^{-3} behaviour. Moreover, many processes act at once in the atmosphere.

6. Turbulent diffusion

By analogy with molecular diffusion it is plausible that a particle which moves with a turbulent fluid should execute a random walk on scales large compared to the eddy size l and eddy circulation time $\tau = l/v$, where v is a typical velocity value. The effective diffusivity should be $\kappa \sim lv$ and if the particle is started at a random position in a statistically isotropic velocity field at time $t=0$ then any component, say y_1, of the particle displacement $\boldsymbol{y}(t)$ should satisfy $\langle y_1^2 \rangle \sim 2\kappa t$. The largest spatial scales of the turbulence usually dominate v and therefore κ. Thus the condition of a random walk on scales large compared to turbulent scales may be difficult to satisfy since the energy-containing turbulent scales may be the size of the system, particularly in two dimensions.

Taylor (1921) has derived for statistically stationary turbulence the exact result

$$\langle y_1^2 \rangle = \int_0^t \kappa(s)\, \mathrm{d}s \qquad \kappa(t) = D^{-1} \int_0^t U^L(s)\, \mathrm{d}s \qquad (6.1(a, b))$$

where $\kappa(t)$ is a time-dependent diffusivity and $U^L(t) = \langle \dot{\boldsymbol{y}}(t) . \dot{\boldsymbol{y}}(0) \rangle$ is the Lagrangian velocity correlation. D is the space dimensionality. The preceding discussion suggests $\kappa(t)$ approaches a limit $\sim lv$ as $t \to \infty$.

Computer simulations of particle dispersion in a normally distributed velocity field with a compact wavenumber spectrum (Kraichnan 1970a) support Taylor's analysis including the behaviour of $\kappa(\infty)$ for $D=3$. For $D=2$ there are anomalies if the velocity field is frozen in time. In that case a finite fraction of the particles is trapped, since the streamlines must form closed loops in the neighbourhoods of local maxima and minima of the stream function. These anomalies disappear if the normally distributed velocity field decorrelates in time with correlation time $\sim l/v$. They also do not show up in computer simulations of dispersion in truncated $D=2$ Stokes flow with a spectrum corresponding to an absolute equilibrium state of §3 (Salu and Montgomery 1977).

Relative dispersion or diffusion, the statistics of the separation $\boldsymbol{r}(t)$ of a pair of particles that move with the fluid and are randomly placed with separation $\boldsymbol{r}_0 = \boldsymbol{r}(0)$ initially, differs importantly from one-particle diffusion. Relative dispersion is effected by the shear that acts over the separation $\boldsymbol{r}(t)$, rather than the magnitude of the velocity field. If r is smaller than the scale size of the eddies that carry most of the shear then the rate of separation is in proportion to r and $\langle [r(t)]^2 \rangle$ increases

exponentially in stationary turbulence (Cocke 1969, Kraichnan 1974b). If r is larger than the energy-range scale l, then the two particles should diffuse independently so that $\langle r_1^2\rangle \sim 4\kappa(\infty)t$.

Richardson (1926) was the first to study relative dispersion. He proposed that at intermediate scales of separation $\langle r_1^2\rangle$ should grow as if the diffusivity that acted upon it were r-dependent. On the basis of a variety of empirical data ranging from molecular diffusion to diffusion by cyclonic storm systems he proposed that this diffusivity have the form $\mu(r) \propto r^{4/3}$. In the $-5/3$ energy inertial range, Obukhov (1941) used dimensional arguments to obtain the same law, which leads to

$$\langle r_1^2\rangle \sim \epsilon t^3 \tag{6.2}$$

where ϵ is the rate of energy cascade through the inertial range per unit mass and $1/r$ is an inertial-range wavenumber. Richardson came very close to deducing the Kolmogorov spectrum fifteen years in advance. The data base was later significantly enlarged when Richardson and Stommel (1948) published a definitive study of the separation of parsnip-pairs in the sea.

The assumption in (6.2) that the effective shear acting across $\boldsymbol{r}$ arises from eddies of size $\sim r$ is as plausible in the $D=2$ energy inertial range as it is for $D=3$ (we must replace ϵ by $|\epsilon|$ for $D=2$). But in the asymptotic enstrophy inertial range most of the shear at separation r comes from eddies of size $\gg r$. This approximates the situation of spatially uniform random shear so that approximately exponential growth of $\langle r_1^2\rangle$ is to be expected. Neglecting the logarithmic corrections in the enstrophy inertial range, Lin (1972) obtains

$$\ln \langle [r_1(t)/r_1(0)]^2\rangle \sim \eta^{1/3} t \tag{6.3}$$

where η is the enstrophy cascade rate per unit volume. Peskin (1973) argues however that $\langle r_1^2\rangle \propto t^3$ in this range also. Balloon measurements in the atmosphere (Morel 1970, Morel and Larcheveque 1974) perhaps give some support to (6.3), but they do not describe an asymptotic situation.

The relative diffusion in a spatially uniform and randomly-changing-in-time shearing field has an anomaly for $D=2$. If the rate of change of the shear field is very rapid (Kraichnan 1974b) or the shear is piecewise constant in time (Kraichnan 1976a), the average $\langle r_1(t)/r_1(0)]^{-2}\rangle$ decreases with t for $D>2$ but is constant for $D=2$. This implies that the kinetic energy of a blob of vorticity subjected to such shearing remains constant on the average (Kraichnan 1976a). A consequence is that the negative eddy viscosity (4.21(b)) vanishes, if $q^2U(q)$ vanishes at k_m so that the sub-grid-scale excitation is effectively composed of such blobs.

A systematic analytical treatment of one-particle dispersion can be based on the function $G(\boldsymbol{x}, t; \boldsymbol{x}', t')$ which is defined as the probability that a particle which starts at $\boldsymbol{x}', t'$ reaches $\boldsymbol{x}$ at time t. In homogeneous, isotropic, stationary turbulence $G(\boldsymbol{x}, t; \boldsymbol{x}', t') = G(|\boldsymbol{x}-\boldsymbol{x}'|, t-t')$, with $G(x, 0) = \delta(\boldsymbol{x})$. Lagrangian-history-based renormalised perturbation analysis (Kraichnan 1977a) yields the infinite-series differential equation

$$\partial G(x, t)\partial t = \sum_{n=1}^{\infty} K_{2n}(t)\, \nabla^{2n} G(x, t) \tag{6.4}$$

where $K_2(t) = \kappa(t)$ as given by (6.1(b)) and the remaining $K_{2n}(t)$ depend on higher-order Lagrangian moments. Only the $K_2(t)$ term affects $\langle x_1^2\rangle = \int x_1^2 G(x, t)\, \mathrm{d}\boldsymbol{x}$. The higher terms make $G(x, t)$ a non-Gaussian function of x. For $x \gg l$, central-limit arguments imply that $G(x, t)$ is asymptotically Gaussian (Taylor 1921) and this

conclusion is supported by the structure of the higher $K_{2n}(t)$. The summation in (6.4) converges (Kraichnan 1979).

On the other hand, Eulerian renormalised perturbation theory (Kraichnan 1976b, 1977a) yields

$$\partial G(x, t)/\partial t = \int_0^t \mathrm{d}s \int \mathrm{d}\boldsymbol{y} \xi(|\boldsymbol{x}-\boldsymbol{y}|, t-s)\, \nabla^2 G(y, s) \tag{6.5}$$

where

$$\xi(x, t) = D^{-1} G(x, t)\, U(x, t) + \text{higher-order terms} \tag{6.6}$$

with $U(x, t) = \langle \boldsymbol{u}(\boldsymbol{x}, t).\boldsymbol{u}(0, 0)\rangle$. This is a non-local diffusion equation, the non-localness expressing the fact that the mean-free-path and mean-free-time of the diffusion process are finite (Corrsin 1974). In (6.4) the non-localness is expressed both by the Lagrangian averages (which are non-local functionals of Eulerian moments) and the infinite series in powers of ∇^2. Evaluation of $\mathrm{d}\langle \boldsymbol{x}_1^2\rangle/\mathrm{d}t$ from (6.5), with some partial integrations and comparison with (6.1), shows that

$$D^{-1} U^L(t) = \int \xi(x, t)\, \mathrm{d}\boldsymbol{x}. \tag{6.7}$$

A large number of proposals for approximate computation of $\kappa(t)$ and $G(x, t)$ have appeared in the literature. Most of them can be described as truncation of (6.4) or (6.6) at the lowest term, followed by further approximations. Such truncation of (6.6), without further approximation, yields the DIA for $G(x, t)$ (Roberts 1961a,b). This truncation in (6.7) is equivalent to a statistical independence approximation of Corrsin (1959, 1962). Alternatively, (6.4) can be truncated and $U^L(t)$ approximated by a DIA method (Kraichnan 1977b) or by the LHDIA (Kraichnan 1977a). The following is a partial chronological list of papers in which truncation of (6.6) is accompanied by simplifying approximations: Goldstein (1951), Bourret (1960), Roberts (1961a,b), Saffman (1962), Weinstock (1968, 1978), Krasnoff and Peskin (1971), Taylor and McNamara (1971), Montgomery *et al* (1972), Montgomery and Tappert (1972), Montgomery (1975a,b), Lundgren and Pointin (1976) and Salu and Montgomery (1977). Alternative expansion methods and the resulting approximations were explored by Phythian (1975b) and Phythian and Curtis (1978).

Saffman (1962) suggested the approximation of $G(x, t)$ in (6.6) by $\tilde{G}(k, t) = \exp[-k^2 \int_0^t \kappa(s)\, \mathrm{d}s]$, where $\tilde{G}(k, t)$ is the Fourier transform of $G(x, t)$, and then substitution into (6.5) to determine $\kappa(t)$ self-consistently. This and related approximations have been examined by several authors (see Lundgren and Pointin 1976). Salu and Montgomery (1977) take $\tilde{G}(k, t) = \exp[-k^2 \kappa(\infty) t]$ and consider also the possibility of approximating the time dependence of $U(x, t)$ by that of $G(x, t)$. The result is

$$\kappa(\infty) \sim [\int U(k)\, k^{-2}\, \mathrm{d}\boldsymbol{k}]^{1/2} \tag{6.8}$$

where $U(k)$ is the modal intensity $[E(k) \sim k^{D-1} U(k)]$. Simple approximations of this kind impressively reproduce the computer simulations of $\kappa(\infty)$ by Kraichnan (1970a) for diffusion by normally distributed velocity fields. They are inferior to the DIA only in describing transient effects in $\kappa(t)$. Equation (6.8) also describes well the $\kappa(\infty)$ values found by Salu and Montgomery (1977) from simulations of $D = 2$ absolute equilibrium states.

Renormalised perturbation expansions can also be formed for relative dispersion. The DIA approximation has been treated by Roberts (1961a,b) and the LHDIA by Kraichnan (1966). The latter yields

$$\partial P(\boldsymbol{r}, t)/\partial t = \partial[\eta_{ij}(\boldsymbol{r}, t)\, \partial P(\boldsymbol{r}, t)/\partial r_j]/\partial r_i \tag{6.9}$$

where $P(\boldsymbol{r}, t)$ is the probability of a separation r for a pair initially separated by $\boldsymbol{r}_0$ at $t=0$ and $\eta_{ij}(\boldsymbol{r}, t)$ is an r-dependent diffusivity tensor expressed, by the approximation, in terms of Lagrangian velocity covariances. Equation (6.9) is a slight generalisation of the diffusion equation proposed by Richardson (1926). The LHDIA yields (6.2) in a $k^{-5/3}$ energy inertial range. It should yield also exponential-type growth of $\langle r^2 \rangle$ in the enstrophy inertial range, but the calculation has not been performed.

Turbulent diffusion in plasmas is centrally important to the confinement problem in controlled thermonuclear power research. Bohm (1949) proposed, without derivation, that the coefficient of self-diffusion for test particles in a plasma is inversely proportional to the uniform steady magnetic-field strength B. In contrast, conventional Chapman–Enskog theory gives a B^{-2} dependence (e.g. Ferziger and Kaper 1972). Taylor and MacNamara (1971) confirmed the B^{-1} dependence and pointed out that the latter was intrinsic to two-dimensionality regardless of the shape of the electric-field fluctuation spectrum. The Bohm B^{-1} dependence was confirmed even for thermal equilibrium. Three-dimensional treatments which quickly followed (Montgomery *et al* 1972, Okuda and Dawson 1973, Montgomery 1975a) showed that the B^{-1} dependence was associated with excitations that had $\boldsymbol{k}.\boldsymbol{B}=0$, where $\boldsymbol{k}$ is the wavevector of the associated component of the velocity field or electric field, while the B^{-2} dependence for the diffusivity was associated with $\boldsymbol{k}.\boldsymbol{B}\neq 0$. In three dimensions either dependence could dominate under appropriate circumstances.

7. Magnetohydrodynamic turbulence

The addition of electrical conductivity to the properties of a fluid leads to a number of interesting electromagnetic phenomena and associated changes in the nature of fluid turbulence. If the conductivity is infinite the magnetic lines of force associated with currents within or external to the fluid are frozen in the fluid and move with it. The tension associated with the lines of force then adds stiffness to the fluid and gives rise to waves, like those in a tense string, which propagate along the lines of force (Alfvén waves). If the conductivity is finite, there is in addition a diffusion of the lines of force through the fluid, accompanied by dissipation of energy. In general, the conducting fluid exhibits exchange of kinetic energy and magnetic energy and dissipation by both viscosity and electrical resistance.

A uniform magnetic field in the conducting fluid does not affect motion either entirely parallel or entirely perpendicular to the lines of force because in both cases the lines of force are not distorted. Suppose that the fluid is bounded by rigid, slippery, parallel horizontal surfaces and the uniform field points vertically. Purely vertical motion is prevented by the boundaries and purely two-dimensional horizontal motion is unaffected by the magnetic field. Motions with vertical components and motions which are horizontal with vertical gradients distort the lines of force and are broken up both by the ensuing wave radiation and by eddy-current damping (Joule dissipation). Thus the uniform vertical magnetic field favours the pure two-dimensional motion. In this respect it is analogous to rotation about a vertical axis, discussed in §5.

Lielausis (1975), Tsinober (1975) and Volisch and Kolesnikov (1976a,b,c, 1977) describe experiments in which uniform magnetic fields are used to induce two-dimensional or nearly two-dimensional motion in turbulent liquid metals. Some of

the measured spectra suggest the $-5/3$ and -3 asymptotic spectra discussed in §4. However, the dynamic basis is not wholly clear. Alemany *et al* (1979) point out that the Joule damping time is k-independent and thereby may induce a k^{-3} spectrum in three as well as in two dimensions.

The electromagnetic effects on fluid motion are described by adding a ponderomotive or Lorentz-reaction term to (2.42):

$$(\partial/\partial t + \boldsymbol{u}.\nabla) + \boldsymbol{u}\nabla p/\rho = \nu\nabla^2\boldsymbol{u} + (\rho c)^{-1}\boldsymbol{j}\times\boldsymbol{B} \tag{7.1}$$

where c is the velocity of light (we use CGS units) and the current density $\boldsymbol{j}$ and magnetic induction field $\boldsymbol{B}$ are related by $\nabla\times\boldsymbol{B} = 4\pi\mu\boldsymbol{j}/c$ where μ is the magnetic permeability. $\boldsymbol{B}$ is derivable from a vector potential according to $\boldsymbol{B} = \nabla\times\boldsymbol{a}$. We neglect displacement current and assume that the electric field E satisfies $\boldsymbol{j} = \sigma(\boldsymbol{E} + \boldsymbol{u}\times\boldsymbol{B}/c)$, where σ is a scalar conductivity. This implies that $\boldsymbol{E} = -\boldsymbol{u}\times\boldsymbol{B}/c$ if $\sigma = \infty$. Maxwell's induction equation then leads to

$$\partial\boldsymbol{B}/\partial t = \nabla\times(\boldsymbol{u}\times\boldsymbol{B}) + \eta\nabla^2\boldsymbol{B} \tag{7.2}$$

where $\eta = c^2/4\pi\mu\sigma$ is called the magnetic diffusivity (dimensions $\mathrm{L}^2\mathrm{T}^{-1}$). The derivation of these hydromagnetic equations is discussed, for example, by Spitzer (1956). A review of hydromagnetic turbulence theory in three dimensions, with emphasis on the generation of large-scale magnetic fields by turbulent dynamo action, is given by Moffatt (1978). If $\nabla.\boldsymbol{u} = 0$ (we have also $\nabla.\boldsymbol{B} = 0$), (7.1) and (7.2) determine the evolution of $\boldsymbol{u}$ and $\boldsymbol{B}$ from initial values. With $\boldsymbol{j}$ eliminated in favour of $\boldsymbol{B}$, (7.1) takes the form

$$(\partial/\partial t + \boldsymbol{u}.\nabla)\boldsymbol{u} + \nabla p/\rho = \nu\nabla^2\boldsymbol{u} + (4\pi\mu\rho)^{-1}(\nabla\times\boldsymbol{B})\times\boldsymbol{B}. \tag{7.3}$$

There has been little systematic study of compressible magnetohydrodynamic turbulence ($\nabla.\boldsymbol{u} \neq 0$).

Fyfe and Montgomery (1976) have carried out a systematic study of two-dimensional magnetohydrodynamic (MHD) turbulence in which both $\boldsymbol{u}$ and $\boldsymbol{B}$ are confined to the x, y plane and there is no variation in the z direction. In this case $\boldsymbol{j}$, $\boldsymbol{a}$ and the vorticity $\boldsymbol{\omega}$ all reduce to their z components j, a and ω. For either periodic boundary conditions or fields which fall off fast enough at infinity, (7.2) can be 'uncurled' to give

$$(\partial/\partial t + \boldsymbol{u}.\nabla)a = \eta\nabla^2 a \tag{7.4}$$

which is identical with the equation for advection of a passive scalar field with molecular diffusivity.

In three dimensions (7.2) can describe the transfer of energy from the velocity field to large scales of the magnetic field if the velocity field is turbulent with helicity (Moffatt 1978). But in two dimensions (7.4) gives a constraint which prevents such dynamo action. If the boundary conditions are cyclic and the vector potential is expanded as

$$a(\boldsymbol{x}, t) = \sum_{\boldsymbol{k}} a_{\boldsymbol{k}}(t)\exp(\mathrm{i}\boldsymbol{k}.\boldsymbol{x}) \tag{7.5}$$

then (7.4) implies

$$(\partial/\partial t)\sum_{\boldsymbol{k}} |a_{\boldsymbol{k}}(t)|^2 = -2\eta\sum_{\boldsymbol{k}} k^2|a_{\boldsymbol{k}}(t)|^2 \tag{7.6}$$

so that $\Sigma_{\boldsymbol{k}}\, k^{-2}|\boldsymbol{B}_{\boldsymbol{k}}(t)|^2 = \Sigma_{\boldsymbol{k}}\,|a_{\boldsymbol{k}}(t)|^2$ decreases with time, where $\boldsymbol{B}_{\boldsymbol{k}}(t)$ is the Fourier component of the magnetic field. The vector potential must decay, and for finite η and no forcing, the magnetic field must become uniform or zero. However, for a

finite time, the magnetic field may amplify at either the large or small scales. The limits $\eta \to 0$ and $t \to \infty$ are subtle, and may not be interchangeable (Pouquet 1978).

Fyfe and Montgomery (1976) have examined the equilibrium statistical mechanics of the system (7.2) and (7.3) along the lines of §3. An analogous treatment of three-dimensional magnetohydrodynamics has been reported by Frisch *et al* (1975). All the fields may be expanded in Fourier series as (7.5). There are then three quadratic constants of motion ($\nu = \eta = 0$) which survive truncation in wavenumber. They are the total energy E, the integrated square of the vector potential A, and the 'cross helicity' P, given by

$$E = \tfrac{1}{2}\rho \int (B^2/D^2 + u^2)\, \mathrm{d}^2x = \tfrac{1}{2}\rho \sum_k k^{-2} (|j_k|^2 + |\omega_k|^2) \qquad (7.7(a))$$

$$A = \tfrac{1}{2}D^{-2} \int a^2\, \mathrm{d}^2x = \tfrac{1}{2} \sum_k k^{-4} |j_k|^2 \qquad P = \tfrac{1}{2}D^{-1} \int \boldsymbol{u}.\boldsymbol{B}\, \mathrm{d}^2x = \tfrac{1}{2} \sum_k k^{-2} \omega_k j_{-k} \qquad (7.7(b, c))$$

where ω_k and $cj_k(4\pi\mu/\rho)^{-1/2}$ are the Fourier amplitudes of $\omega(\boldsymbol{x})$ and $j(\boldsymbol{x})$, and $D^2 = 4\pi\mu\rho$ (see also Montgomery and Vahala 1978).

A Liouville theorem for the truncated system follows easily from the Fourier transforms of (7.2) and (7.3), which may be written as

$$(\partial/\partial t + \nu k^2)\, \omega_k(t) = \sum_{p+q=k} M_1(\boldsymbol{q}, \boldsymbol{p})\, [\omega_q(t)\, \omega_p(t) - j_q(t)\, j_p(t)] \qquad (7.8(a))$$

$$(\partial/\partial t + \eta k^2) j_k(t) = \sum_{p+q=k} M_2(\boldsymbol{q}, \boldsymbol{p})\, [j_q(t)\, \omega_p(t) - \omega_q(t) j_p(t)] \qquad (7.8(b))$$

where

$$M_1(\boldsymbol{q}, \boldsymbol{p}) = M_1(\boldsymbol{p}, \boldsymbol{q}) = \tfrac{1}{2}\boldsymbol{e}_z.(\boldsymbol{q} \times \boldsymbol{p})\, (p^{-2} - q^{-2}) \qquad (7.9(a))$$

and

$$M_2(\boldsymbol{q}, \boldsymbol{p}) = -M_2(\boldsymbol{p}, \boldsymbol{q}) = \tfrac{1}{2}\boldsymbol{e}_z.(\boldsymbol{q} \times \boldsymbol{p}) |\boldsymbol{p} + \boldsymbol{q}|^2 / p^2 q^2 \qquad (7.9(b))$$

where $\boldsymbol{e}_z$ is a unit vector in the z direction.

The canonical probability density, analogous to that in (3.16), is proportional to $\exp(-\beta E - \alpha P - \gamma A)$ where β again is $1/k_B T$ and α and γ are new temperatures for P and A. This density gives the mean values

$$\langle E \rangle = (1/2\beta) \sum_k (2 + \gamma/k^2\rho\beta)\, (1 + \gamma/k^2\rho\beta - \alpha^2/4\rho^2\beta^2)^{-1} \qquad (7.10(a))$$

$$\langle P \rangle = (\alpha/2\rho\beta) \sum_k (\rho\beta + \gamma/k^2 - \alpha^2/4\rho\beta)^{-1} \qquad (7.10(b))$$

$$\langle A \rangle = \tfrac{1}{2} \sum_k (k^2\rho\beta + \gamma - \alpha^2 k^2/4\rho\beta)^{-1} \qquad (7.10(c))$$

and the mean modal intensities

$$\langle |j_k|^2 \rangle = D^{-1}k^2 \langle |\boldsymbol{B}_k|^2 \rangle = D^{-1}k^4 \langle |a_k|^2 \rangle = k^2(\rho\beta - \alpha^2/4\rho\beta + \gamma/k^2)^{-1} \qquad (7.11(a))$$

$$\langle |\omega_k|^2 \rangle = k^2 \langle |\boldsymbol{u}_k|^2 \rangle = k^2/\rho\beta + (\alpha^2/4\rho\beta^2)\, (\rho\beta/k^2 + \gamma/k^4 - \alpha^2/4k^2\rho\beta)^{-1}. \qquad (7.11(b))$$

The requirement that $\langle |j_k|^2 \rangle$ and $\langle |\omega_k|^2 \rangle$ both be positive for all k selects a unique set of values α, β and γ for given $\langle E \rangle$, $\langle P \rangle$ and $\langle A \rangle$ and implies that $\beta > 0$, but either α or γ may be negative.

Suppose, with reference to §3, that $k_{\min}$ and $k_{\max}$ are the lower and upper truncation wavenumbers and, for simplicity, consider the case $\alpha=0$, which implies $\langle P\rangle=0$. If $k_{\max}\to\infty$, the expectations are finite only if $\beta\to\infty$ and $\gamma\to-\infty$ in such a way that $\beta k_{\min}^2+\gamma=O(1)$. For $k>k_{\min}$, $\beta k^2+\gamma\to\infty$. Thus, the contribution to $\langle A\rangle$ from the lowest mode dominates in the limit while the energy spreads out over the higher wavenumbers up to $k_{\max}$. This recalls the similar behaviour of energy and enstrophy, respectively, in the condensed hydrodynamic equilibria of §3. At high enough k there is approximate equipartition of magnetic and kinetic energy whatever the values of α, β and γ. This can be qualitatively understood by thinking of the high-k excitations as random Alfvén waves (Kraichnan 1965b).

Fyfe *et al* (1977a) have carried out computer simulations of (7.8) using a spectral method of Orszag (1971) and starting from highly non-equilibrium initial conditions. The non-dissipative ($\nu=\eta=0$) runs show large temporal fluctuations in individual

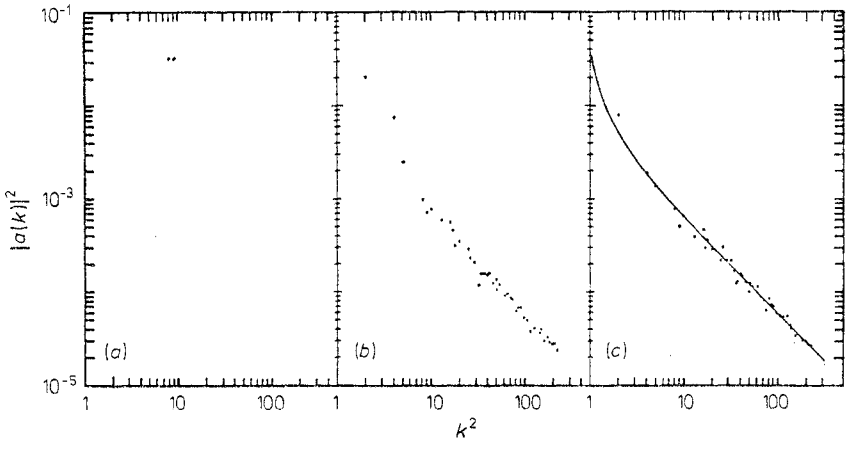

Figure 19. Evolution of a typical 2D non-dissipative vector potential spectrum in MHD (from Fyfe *et al* 1977a). (*a*) shows initial mean square vector potential at $t=0$, and (*b*) and (*c*) show time averaged at later intervals. Full curve is theoretical absolute equilibrium spectrum for these initial conditions.

mode amplitudes after overall evolution seems complete. Time-averaging smooths the spectra considerably, and gives a quite acceptable agreement with (7.11), at least for the case $\langle P\rangle=0$. This suggests that E, P and A are the only isolating constants of motion and that the system is ergodic. Temporal evolution of typical developing spectra are shown in figures 19 and 20.

The analogy of $\langle A\rangle$ and $\langle E\rangle$ in the present hydromagnetic equilibria to $\langle E\rangle$ and $\langle\Omega\rangle$ in the hydrodynamic equilibria of §3 suggests the possibility of dual cascades, like those of §4, with now a cascade of A to low wavenumbers and E to high wavenumbers, as the consequence of the injection of A and E into the system at intermediate wavenumbers by forcing mechanisms. It is important to note that, because of the 'antidynamo theorem' (7.6), a downward cascade of A can take place in the steady state only if a forcing term representing injection of *magnetic* excitation is added to (7.2) or (7.8(*b*)). Moreover, if this excitation is injected only in a band of intermediate wavenumbers, a conservative cascade of A to lower wavenumbers implies zero asymptotic (i.e. $k\to0$) cascade of magnetic *energy*, since $|B_k|^2=k^2|a_k|^2$. Thus there cannot be a steady-state two-dimensional turbulent dynamo which

transforms kinetic energy at intermediate wavenumbers into magnetic energy at much lower wavenumbers or even one which steadily transfers magnetic energy to much lower wavenumbers. However, this restriction is less limiting than might be supposed. Mechanical stirring of a magnetofluid by contact with a solid surface of finite conductivity can*not* be idealised simply by adding a mechanical forcing term into the equation at motion. Any mathematical representation of this process also necessarily includes magnetic forcing of some variety.

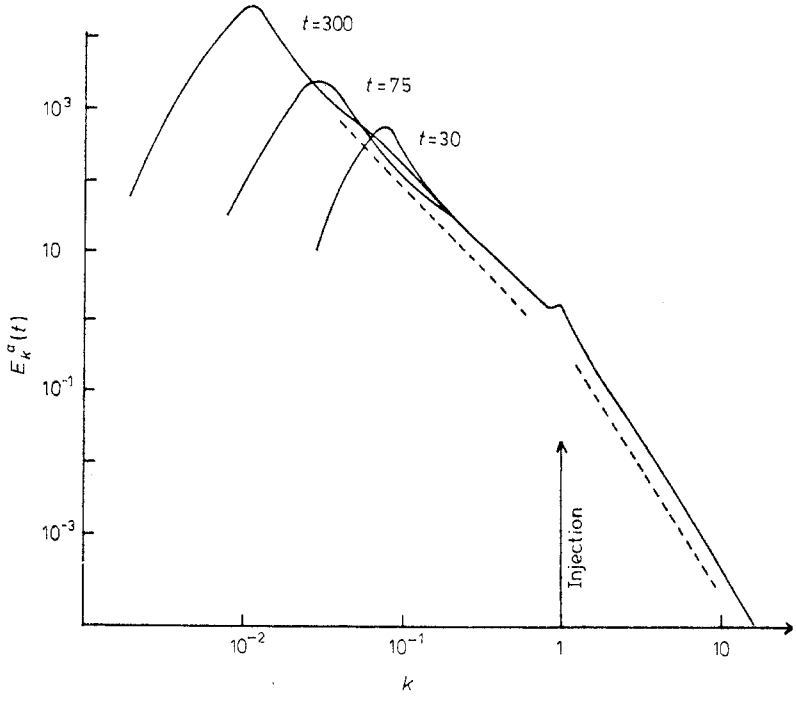

Figure 20. Results of an MHD EDQNM closure calculation for evolving magnetic energy spectrum at three successive times (from Pouquet 1978). Magnetic energy is being continuously injected at $k=1$.

In three dimensions the situation is much different. The three quadratic constants of motion which determine truncated non-dissipative equilibria (Frisch *et al* 1975) are E, P and the magnetic helicity

$$H=\tfrac{1}{2}\int \boldsymbol{a}.\boldsymbol{B}\,\mathrm{d}^3x. \tag{7.12}$$

A is not a constant of motion, and transformation of the kinetic energy of helical motion into the energy of large-scale magnetic fields is possible (Moffatt 1978, Kraichnan 1979).

A paradoxical fact in both two dimensions and three is that the constants of motion of the system with magnetic field do not go over into constants of motion of the purely hydrodynamic system as $\boldsymbol{B}\to 0$. Thus neither P nor A becomes the enstrophy Ω as $\boldsymbol{B}\to 0$ and neither P nor H becomes the hydrodynamic helicity (2.11). The exception is E which goes into the hydrodynamic energy. Instead, as $\boldsymbol{B}\to 0$, the constants involving B also go to zero, while the *rates of change* of the purely hydrodynamic constants of motion go to zero.

If $A(k)$ is the spectrum function of the a fluctuations, satisfying $\int_0^\infty A(k)\,\mathrm{d}k = A$, similarity arguments like those that lead to (4.11) suggest that the spectrum behaviour in an inertial range where A is transferred to lower wavenumbers should have the form in two dimensions

$$A(k) = \text{constant} \times \epsilon_A{}^{2/3} k^{-7/3} \tag{7.13}$$

where ϵ_A is the rate of the conservative transfer of A. These same arguments and dimensional analysis imply a $k^{-5/3}$ spectrum for both magnetic and kinetic energy spectra in the cascade from forcing wavenumbers to higher wavenumbers. However, Kraichnan (1965b) and Kraichnan and Nagarajan (1967) argue that the Kolmogorov similarity scaling is invalid in hydromagnetic turbulence because of decorrelation effects associated with radiation of Alfvén waves which exist as small-scale perturbations on the magnetic lines of force. If such effects are included, the $k^{-5/3}$ spectrum is replaced, in the simplest situation, by a $k^{-3/2}$ spectrum with a coefficient that depends on the level of the mean square magnetic field. Dominance of the high-k dynamics by Alfvén waves also implies approximate equipartition of magnetic and kinetic energy in the energy inertial range.

The cascade of A and E have been investigated both by computer simulation (Fyfe *et al* 1977b) and by an adaptation of the EDQNM closure described in §4.3 (Pouquet 1978). The simulations used a variety of forcing terms added to (7.8) and various values of the Reynolds numbers lu/ν, lu/η, $l\tilde{B}/\nu$ and $l\tilde{B}/\eta$, where u is a characteristic value of u, l is a typical length scale and $\tilde{B}$ is a characteristic value of $B(4\pi\mu\rho)^{-1/2}$. These Reynolds numbers measure the relative size of the linear and non-linear terms in (7.2) and (7.3) and thereby the range of wavenumbers available for inertial-range behaviour. It is plausible, but not established, that a criterion for the natural or spontaneous occurrence of MHD turbulence is the size of the 'Lundquist number' $l\tilde{B}/\eta$. In computing the Lundquist number, we should use only the self-consistently supported part of $\boldsymbol{B}$, i.e. the part which has a curl. Externally imposed uniform $\boldsymbol{B}$ fields will not, in general, lead to turbulent behaviour.

The simulations involve total wavenumber ranges which are too small to test the inertial-range power laws, but do give results that seem consistent with the asymptotic validity of the inertial ranges. Some results of the simulations which seem likely to persist if much larger-scale computations were made are: (i) substantial back-transfer of A to the largest spatial scales; (ii) large fluctuations of the Fourier amplitudes about time-averaged intensity values—more so than in analogous pure Navier–Stokes computations; (iii) very slow evolution of the longest wavelengths of the magnetic field; (iv) a strong tendency toward equipartition of kinetic and magnetic energy at the highest wavenumbers where dissipative effects did not dominate. These characteristics appear also in unforced decay simulations by Orszag and Tang (1978) which have $k_{\max}/k_{\min} = 128$.

The treatment of two-dimensional MHD turbulence by the EDQNM closure (Pouquet 1978) is similar in principle to the earlier treatment of three-dimensional MHD turbulence by Pouquet *et al* (1976). The elementary physical arguments that lead to the $k^{-7/3}$ and $k^{-3/2}$ inertial ranges are built into the relaxation times used by Pouquet in constructing the closure. Thus, as in all such closure analysis, the confirmation of the power laws in the final computations involves circular logic and serves principally to demonstrate a level of self-consistency in the physical and dimensional reasoning, including, most importantly, the convergence of integrals describing the rates of transfer.

Pouquet (1978) has made an interesting and significant conjecture about the intermittency of the small scales of the turbulence described by (7.2) and (7.3) As noted in §4.1, the two-dimensional Euler equations do lead from smooth initial conditions to singularities in finite time, a fact connected with the conservation of enstrophy. In two-dimensional MHD flow, enstrophy no longer is conserved and Pouquet therefore conjectures that such flow is like three-dimensional Euler flow in that singularities do develop in finite time. Orszag and Tang (1978) have investigated this question by computer simulation. Their results (necessarily restricted to finite wavenumber ranges) suggest strongly that singularities do indeed develop in finite time in two-dimensional MHD flow, but that the singularities are less strong than in three-dimensional Euler flow. The results suggest that, in contrast to three-dimensional Euler flow, (7.2) and (7.3) do not lead to finite dissipation rates independent of ν and η as the latter go to zero.

A picture of the small-scale behaviour of (7.2) and (7.3) with effectively very small ν and η may be formulated as a two-step process. In the first step, lines of force are stretched, increasing the magnetic field and its gradients. Taken to the extreme, this generates microscopic 'sheet pinch' configurations—thin current sheets normal to the plane of variation of the field variables—across which the tangential component of magnetic field changes almost discontinuously. These sheet pinches are likely to be unstable against roll-up into vortices which can re-initiate the process. This qualitative picture fails to account, however, for the large regions seen by Orszag and Tang which are relatively free of both magnetic and velocity fields, as if both fields were expelled from the interiors of the regions. A model of the possible singular behaviour to be expected as $\eta \to 0$ has been given by Matthaeus and Montgomery (1979). The model is based upon current filamentation and concentration on sets of decreasing measure near a zero of the magnetic field of the so-called 'x-point' variety (saddle points in a).

A number of variants of two-dimensional and quasi-two-dimensional plasma turbulence have been described in the observational, experimental and theoretical literature with and without a steady perpendicular magnetic field. We have not the space unfortunately even to cite this literature systematically. Instead we briefly call attention to several of the topics.

The electrostatic guiding-centre plasma and its analogy to two-dimensional Navier–Stokes turbulence (e.g. Taylor and MacNamara 1971, Montgomery 1975a,b) has been mentioned throughout this review. The accurate analogy does not extend to dissipative effects.

A precursor of Navier–Stokes enstrophy-cascade theory appears in Chen's (1965) paper on drift-wave turbulence, where a k^{-5} potential spectrum (k^{-3} energy spectrum) is conjectured. Hasegawa and Mima (1978) give a more elaborate theory of drift-wave turbulence, arriving at the equation

$$(\partial/\partial t)\,(\nabla^2\phi - \lambda^2\phi) - (\nabla\phi \times \boldsymbol{e}_z).\nabla\nabla^2\phi = 0 \tag{7.14}$$

for the electrostatic potential ϕ. This differs only by the term in λ (a parameter) from the Euler equation for the stream function (§2). Fyfe and Montgomery (1979) have further explored the direct and inverse cascade behaviour of (7.14). The inverse cascade may be the basic mechanism responsible for the large potential islands that repeatedly occur in plasma confinement experiments.

Fluctuating magnetic fields in the solar wind appear to constitute a quasi-two-

dimensional turbulence somewhat reminiscent of the quasi-geostropic turbulence discussed in §5. There is often an average steady magnetic field with fluctuation vector usually perpendicular to the steady field but with the rate of variation of the fluctuation vector largest parallel to the steady field. The equations of motion simplify considerably in this essentially passively convected regime (see Siscoe *et al* 1968, Belcher and Davis 1974, Barnes 1979).

Kelley and Kintner (1978) argue that the high-latitude magnetosphere of the Earth supports fluctuations in electric field which can be interpreted as a two-dimensional guiding-centre plasma. They measure power spectra which appear to be consistent with the simultaneous existence of $k^{-5/3}$ energy cascade and k^{-3} enstrophy cascade ranges (in terms of the correspondence between guiding-centre plasma and Navier–Stokes flow).

Sudan and Keskinen (1977, 1979) and Barone (1980) examine turbulence in a two-component plasma which exhibits electron density fluctuations in a plane perpendicular to a uniform magnetic field. A two-fluid-model set of equations is handled by the direct interaction approximation. Application is made to fluctuations in the equatorial electrojet.

Electrostatic plasma oscillations in the absence of a steady magnetic field give rise to a kind of turbulence which differs from the fluid turbulence usually studied in that the oscillations are essentially longitudinal (compressive) and rapid linear oscillations typically give time scales small compared to those associated with non-linear transfer. The rapid linear oscillations make numerical simulation more difficult but perturbation-based approximations more solidly based. A large body of work on the weakly non-linear regime is summarised and cited by Kadomtsev (1965), Tsytovich (1970, 1972) and Davidson (1972). Some recent papers dealing with strongly non-linear electrostatic oscillations are Fyfe and Montgomery (1978), Zakharov (1972) and Nicholson and Goldman (1978).

8. Two-dimensional superflow

Onsager (1949) and Feynman (1957) have pointed out that the condition of single-valuedness of the phase of the macroscopic wavefunction requires that vortex motion of a superfluid must involve cores, where the macroscopic wavefunction breaks down, and circulation about these cores which is quantised in multiples of h/m, where h is Planck's constant and m is the mass of a helium atom. In three-dimensional flow the quantised vortices can take the form of rings or they can terminate on the walls of the container. If the core diameter is sufficiently small compared to the radius of curvature along the core axis, the vortices obey Stokes' flow equations modified by a Magnus force due to interaction of the core with the normal fluid component. An excellent review is given by Langer and Reppy (1970). Donnelly and Roberts (1971) and others have constructed detailed theories of the creation, interaction and destruction of the quantised vortices.

Kosterlitz and Thouless (1973) and Kosterlitz (1974) proposed a novel type of phase transition in two-dimensional systems in which the raising of temperature through a critical value T_c results in the dissociation of pairs of vortices with opposite sign. They suggested applications to magnetism, melting and superfluidity in two-dimensional systems. Such transitions were studied by José *et al* (1977) by renormalisation group transformations. Nelson and Kosterlitz (1977) predicted that

vortex pair dissociation results in a universal jump (to zero) of the superfluid mass per unit area when a thin film of ^{4}He on a substrate is raised through T_c, namely

$$(\rho_s/k_B T)_{T \to Tc} = 8\pi(m/h)^2 \tag{8.1}$$

where ρ_s is the superfluid mass per unit area.

Experimental confirmation of (8.1) has been reported by Bishop and Reppy (1978), Rudnick (1978) and Webster *et al* (1979). There has been an explosion of theoretical interest in the Kosterlitz–Thouless transition including papers by Myerson (1978), Nelson (1978), Young (1978) and Donnelly *et al* (1979). Ambegaokar *et al* (1978), Huberman *et al* (1978) and Ambegaokar and Teitel (1979) have studied dissipative phenomena near the transition, which are important in interpreting the experiments. Applications to superconductivity have been proposed by Beasley *et al* (1979), Doniach and Huberman (1979) and Halperin and Nelson (1979). A fascinating extension has been made by Halperin and Nelson (1978) and Nelson and Halperin (1979) who predict a two-stage melting in two-dimensional solids, each stage corresponding to pair disassociation of a particular type of excitation. Some support is reported by Frenkel and McTague (1979) who do computer experiments with a finite set of atoms.

Our discussion will be limited to an attempt to relate the Kosterlitz–Thouless transition in superflowing films to the analysis of vortex dynamics and statistical equilibria of §§2 and 3. There is no universal agreement about some of the basic theoretical questions. It is hoped that the treatment to follow offers a consistent picture within the frame of elementary methods.

Consider then a thin fluid layer of width W and length $L \gg W$ and cyclic boundary conditions on the ends. We start by discussing an ideal inviscid fluid with rigid, slippery boundaries and a perfectly uniform substrate; then we can introduce the effects of interaction with the normal-fluid component, creation and destruction of vortices, and irregularities in the substrate. It is first of all clear from §3 that superflow—that is, macroscopically excited uniform potential flow through the channel—does not represent absolute statistical equilibrium. In absolute equilibrium the potential flow velocity v, which is an independent dynamical coordinate in the formulation of §2.3, has mean square excitation $\langle Mv^2 \rangle = k_B T$, where M is the total mass of the fluid. Thus, as is well known, persistent superflow is a metastable state which is decaying to absolute equilibrium very slowly. The Kosterlitz–Thouless theory then implies that (i) vortex pairs can mediate this decay and (ii) the rate of decay through interaction with vortices is enormously greater for $T > T_c$.

Under the ideal boundary conditions we have assumed there is no interaction between vortex motion and potential flow apart from the trivial convection of the vortex motion along the cyclic channel by v. As noted in §§2.3 and 2.4, this is no longer true if there is irregularity in the edges of the channel. In the present application, irregularities in the substrate contour also act to couple vortex motion and potential flow (in analogy to the orographic variations discussed in §5) and can be expected to be of greater importance. In either case, the stationary eigenfunctions of the vortex flow are distorted and a mechanism exists for transferring the momentum of the potential flow to the walls or substrate despite the fact that we still impose rigid, slippery boundaries. However, this coupling cannot relax v to equilibrium. The reason is that v represents a circulation through the cyclic channel and, by Kelvin's theorem, circulation cannot be altered by boundary forces on an ideal fluid. Relaxation of v requires a mechanism for altering circulation within the fluid. The

circulations of present interest are quantised (including that represented by v) and their alteration therefore implies the creation and destruction of vortices.

We have pointed out in §2.4 that there is no intrinsic momentum associated with a vortex or a vortex pair. There is momentum associated with the creation or destruction of vortices by local disturbance of the fluid but, as noted in §2.4, this momentum again is not uniquely determined by the strength and position of the vortex. In an ideal uniform channel the momentum imparted to the fluid by creation of a vortex depends on whether it is created as part of a plus-minus pair within the fluid or as part of a vortex image pair near the boundary. Surface irregularities provide further complications. In any event the creation and destruction of selectively oriented vortex pairs, or selectively located isolated vortices, can change the net momentum of the fluid Mv. Net momentum is changed if a vortex is created at one edge and subsequently destroyed at the other or if a vortex pair is created in the fluid and destroyed one vortex at each edge. If closely spaced plus-minus pairs are created in the fluid, then the vortices are moved and permuted in any fashion and finally destroyed as closely spaced plus-minus pairs, the result is no net change in momentum (see (2.38) and (2.41)).

Now consider the interaction of a gas of vortex pairs with the normal-fluid component, which is locked to the substrate. Without the interaction a pair aligned across the channel scoots along the channel. If the cores are dragged by the normal component the Magnus force described in §2.4 pushes the cores together. Suppose that in some sense this interaction is sufficiently weak that (with $v=0$ now) the absolute equilibrium states of §3.3 are still relevant. Clearly, to maintain equilibrium, the interaction with the normal component must include, in addition to the drag, some kind of random force that can move cores apart (Ambegaokar *et al* 1978).

If $v\neq 0$ the cores are, in addition, convected by v, which either adds to the scooting velocity through the normal fluid or subtracts from it. The scooting velocity is inversely proportional to the core separation. Thus, in the latter case there will be a critical core separation beyond which v overpowers the scooting velocity and makes the vortices move *backward* through the normal fluid. When that happens the Magnus force *separates* the cores. If separation continues until the vortices are destroyed at the walls there has been a net momentum transfer from fluid to substrate via the drag, which is directed against v.

We are now finally in a position to interpret (8.1). The transition temperature T_c determined by (8.1) is just the transition temperature for $\langle r^2\rangle$ in the dilute vortex gas pair collapse regime, as described after (3.25), namely $\beta\rho q^2/2\pi=4$. As T rises through the transition the number of pairs in equilibrium that have separations greater than the critical separation just described can increase enormously and mediate a sharp rise in the decay rate of v.

The Magnus force and drag dynamics we have described can be interpreted as mediating a quasi-equilibrium of vortex pairs which are created and destroyed in the presence of v. A creation process which adds momentum $\boldsymbol{P}$ to the fluid also adds energy, described by an interaction energy $\boldsymbol{P}.\boldsymbol{v}$, as described after (2.40). For pairs beyond a critical separation this overpowers the interaction energy between the plus and minus vortices, and the Boltzmann factors for the quasi-equilibrium favour pairs whose separation diverges to the width W of the channel (see Myerson 1978). If the quasi-equilibrium is reached as the result of explicitly introduced creation and destruction processes for pairs of all separations and orientations, then the $\boldsymbol{P}.\boldsymbol{v}$ term biases the free energy of creation (Donnelly *et al* 1979).

There are a number of unsettled questions. Does the Kosterlitz–Thouless transition survive, and in what form, when the vortex gas is not dilute so the log potential so important in pair collapse is substantially distorted? What are the effects of substrate irregularity on the transition and (Donnelly *et al* 1979) on vortex nucleation? Dash (1978) raises interesting questions about the very existence of uniform helium films.

9. Concluding remarks

It seems appropriate to end this review by attempting to assess the status and future of the principal research topics which have been discussed. The easiest subject to discuss is the equilibrium statistical mechanics of the inviscid truncated continuum. This is an exactly soluble problem, once the eigenfunctions of Laplace's operator are known in the geometry at hand and, in contrast to three dimensions, the solutions are non-trivial and may be relevant to geophysical phenomena (§§5 and 7).

The equilibrium statistics of the discrete vortex system is not exactly soluble. It differs significantly from that of the continuum by exhibiting pair collapse and supercondensation (if the vortices are assigned finite cores) at the respective temperature ranges that correspond to the lowest and highest energies. To the extent that discrete vortices are regarded as a computational device for continuous flows these phenomena are interesting curiosities, unlikely to affect a well-posed simulation, but the discrete vortices are essential to the physics of superflow and related topics. It is currently of great interest to study further the modifications of dilute-vortex-gas behaviour that accompany finite core structures and, although it lies outside the scope of this review, to understand more solidly how vortex models are based on the underlying quantum dynamics.

The non-equilibrium statistical behaviour of the two-dimensional fluid, including cascade phenomena, is in a much less happy state. The directions of cascade predicted by assuming approach toward equilibrium seem supported by computer simulations and the latter are at least consistent with the asymptotic forms of energy and enstrophy inertial ranges given by simple theory. The closure approximations which are available for semiquantitative prediction of non-equilibrium spectra are not only computationally difficult but fail to provide internal error estimates. They are almost no help with the interesting questions of intermittency and other properties that involve higher statistical structure than spectra.

The self-organising capacities of magnetofluids, in three dimensions as well as in two, are even stronger than they are for Navier–Stokes flow in two dimensions. It appears likely that both kinds of MHD turbulence and its electrostatic kin are to be expected in thermonuclear plasmas. One of the most underdeveloped areas upon which the methods and techniques originating in two-dimensional turbulence theory seem likely to make an impact is that of the control and manipulation of current-carrying fusion plasmas.

At present the most promising tool for progress in understanding the physical phenomena and for guiding theoretical development is probably computer simulation. This is inherently a more powerful tool in two dimensions than in three. It is now possible to perform simulations with effectively the order of a thousand grid points in each direction (Orszag 1976). No simulation calculation unaided by some theoretical apparatus can settle questions of asymptotic high-Reynolds-number behaviour, however.

We lack the courage to make a critical assessment of the future of two-dimensional turbulence theory in the considerable variety of geophysical applications for which it is currently being used. But it does seem proper to stress that great caution must be used when interpreting phenomena of the real world in terms of asymptotic solutions of approximate statistical treatments of idealised theory. In some cases the idealised theory may be more valid in providing a language for discussion rather than a true explanation.

Acknowledgments

This work was supported by the National Science Foundation Global Atmospheric Research Program under Grant ATM-78-09212, the Office of Naval Research under Contract N00014-78-C-0148, the National Aeronautics and Space Administration under Grant NsG-7416, and the Department of Energy under Grant DE-AS05-76ET53045.

We are grateful to a number of colleagues for interactions which aided this review. We want especially to thank (in random order) Edward A Spiegel, Uriel Frisch, David R Nelson, Jackson R Herring, Peter Rhines, Greg Holloway, David E Fyfe, Glenn Joyce, Charles Seyler, Georg Knorr, Thomas S Lundgren, Frederick Tappert, Leaf Turner, Michael E Fisher and Yehuda Salu.

Finally, we wish to thank the National Center for Atmospheric Research at Boulder, Colorado, for valuable technical assistance in the preparation of the manuscript.

References

Alemany A, Moreau R, Sulem P J and Frisch U 1979 *J. Mécanique* **18** 277
Ambegaokar V, Halperin B I, Nelson D R and Siggia E D 1978 *Phys. Rev. Lett.* **40** 783–6
Ambegoakar V and Teitel S 1979 *Phys. Rev.* B **19** 1667–70
Andrews P G and Hoskins B J 1978 *J. Atmos. Sci.* **35** 509–12
Aref H 1979 *Phys. Fluids* **22** 393–400
Aref H and Siggia E D 1980 *J. Fluid Mech.* in press
Barone S R 1980 *Phys. Fluids* **23** in press
Basdevant C, Lesieur M and Sadourny R 1978 *J. Atmos. Sci.* **35** 1028–42
Basdevant C and Sadourny R 1975 *J. Fluid Mech.* **69** 673–88
Batchelor G K 1952 *Rep. Prog. Phys.* **15** 101–41
—— 1953 *Theory of Homogeneous Turbulence* (Cambridge: Cambridge University Press) p186
—— 1959 *J. Fluid Mech.* **5** 113
—— 1967 *An Introduction to Fluid Dynamics* (Cambridge: Cambridge University Press) §§7.3, 7.4
—— 1969 *Phys. Fluids* **12** 233–8
Beasley M R, Mooij J E and Orlando T P 1979 *Phys. Rev. Lett.* **42** 1165–8
Bishop D J and Reppy J D 1978 *Phys. Rev. Lett.* **40** 1727–30
Blumen W 1978a *J. Atmos. Sci.* **35** 774–83
—— 1978b *J. Atmos. Sci.* **35** 784–9
Bogolyubov N N 1946 *J. Phys. USSR* **10** 257–64, 265–74
Bohm D 1949 *The Characteristics of Electrical Discharges in Magnetic Fields* ed A Guthrie and R K Wakerling (New York: McGraw-Hill)
Book D L, McDonald B E and Fisher S 1975 *Phys. Rev. Lett.* **34** 4–8
Bourret R 1960 *Can. J. Phys.* **38** 665–76

Bradshaw P 1976 *Turbulence: Topics in Applied Physics* vol 12 (Berlin: Springer-Verlag) pp1–44, 173–92
Bretherton F P 1966a *Q. J. R. Meteor. Soc.* **92** 325–34
—— 1966b *Q. J. R. Meteor. Soc.* **92** 335–45
Bretherton F P and Haidvogel D 1976 *J. Fluid Mech.* **78** 129–54
Charney J G 1966 *Advances in Numerical Weather Prediction* (Hartford, Conn.: Traveler's Research Center) pp1–10
—— 1971 *J. Atmos. Sci.* **28** 1087–95
Charney J G and Stern M E 1962 *J. Atmos. Sci.* **19** 159–72
Chen F F 1965 *Phys. Rev. Lett.* **15** 381–3
Chen T C and Winn-Nielsen A 1978 *Tellus* **30** 313–22
Cocke W J 1969 *Phys. Fluids* **12** 2488–92
Cook I and Taylor J B 1972 *Phys. Rev. Lett.* **28** 82–4
Corrsin S 1959 *Atmospheric Diffusion and Air Pollution, Advances in Geophysics* vol 6, ed F N Frenkiel and P A Sheppard (New York: Academic)
—— 1962 *Mécanique de la Turbulence* (Paris: Centre National de la Recherche Scientifique) pp27–52
—— 1974 *Adv. Geophys.* **18A** 25–71
Courant R and Hilbert D 1953 *Methods of Mathematical Physics* vol 1 (New York: Interscience)
Dash J G 1978 *Phys. Rev. Lett.* **41** 1178–81
Davidson R C 1972 *Methods in Nonlinear Plasma Theory* (New York: Academic)
DeDominicis C and Martin P C 1979 *Phys. Rev.* A **19** 419–22
Deem G S and Zabusky N S 1971 *Phys. Rev. Lett.* **27** 396–9
Deissler R G 1977 *Handbook of Turbulence* vol 1, ed W Frost and T H Moulden (New York: Plenum) pp165–86
Deutsch G and Lavaud M 1972 *Phys. Lett.* **39A** 253–4
Doniach S and Huberman B A 1979 *Phys. Rev. Lett.* **42** 1169–72
Donnelly R J, Hills R N and Roberts P H 1979 *Phys. Rev. Lett.* **42** 725–8
Donnelly R J and Roberts P H 1971 *Phil. Trans. R. Soc.* A **271** 41–100
Dorfman J R and Cohen E G D 1970 *Phys. Rev. Lett.* **25** 1257–60
Dupree T H 1974 *Phys. Fluids* **17** 100–9
Edwards S F and Taylor J B 1974 *Proc. R. Soc.* A **336** 257–71
Ferziger J H and Kuper H G 1972 *Mathematical Theory of Transport in Gases* (Amsterdam: North-Holland) chap 14, pp423–63
Feynman R P 1957 *Rev. Mod. Phys.* **29** 205–12
Fjørtoft R 1953 *Tellus* **5** 225–30
Fornberg B 1977 *J. Comput. Phys.* **25** 1–31
Forster D, Nelson D R and Stephen M J 1976 *Phys. Rev. Lett.* **36** 867–70
—— 1977 *Phys. Rev.* A **16** 732–49
Forsyth A R 1959 *Theory of Differential Equations* vol 6 (New York: Dover)
Fournier J-D and Frisch U 1978 *Phys. Rev.* A **17** 747–62
Fournier J-D, Frisch U and Rose H R 1978 *J. Phys. A: Math. Gen.* **11** 187–98
Fowler R H 1936 *Statistical Mechanics* (Cambridge: Cambridge University Press) chap 2
Fox D G and Orszag S A 1973 *Phys. Fluids* **16** 169–71
Frenkel D and McTague J P 1979 *Phys. Rev. Lett.* **42** 1632–5
Frisch U and Bardos C 1975 *Global Regularity of the 2-D Euler Equation for Ideal Incompressible Fluids* (Nice: Observatoire de Nice)
Frisch U, Lesieur M and Sulem P-L 1976 *Phys. Rev. Lett.* **37** 895–7
Frisch U, Pouquet A, Léorat J and Mazure A 1975 *J. Fluid Mech.* **68** 769–78
Fyfe D, Joyce G and Montgomery D 1977a *J. Plasma Phys.* **17** 317–35
Fyfe D and Montgomery D 1976 *J. Plasma Phys.* **16** 181–91
—— 1978 *Phys. Fluids* **21** 316–26
—— 1979 *Phys. Fluids* **22** 246–8
Fyfe D, Montgomery D and Joyce G 1977b *J. Plasma Phys.* **17** 369–98
Goldstein S 1951 *Q. J. Mech. Appl. Math.* **4** 129–56
Gonzalez J J and Hemmer P C 1972 *Phys. Lett.* **42A** 263–4
Greenspan H P 1968 *The Theory of Rotating Fluids* (Cambridge: Cambridge University Press)
Hald O H 1976 *Phys. Fluids* **19** 914–5
Halperin B I and Nelson D R 1978 *Phys. Rev. Lett.* **41** 121–4

—— 1979 *J. Low Temp. Phys* **36** 599–616
Hasegawa A and Mima K 1978 *Phys. Fluids* **21** 87–92
Hauge E H and Hemmer P C 1971 *Phys. Norvegica* **5** 209–17
Herring J 1974 *Phys. Fluids* **17** 859–72
—— 1975 *J. Atmos. Sci.* **32** 2254–71
—— 1977 *J. Atmos. Sci.* **34** 1731–50
—— 1980 *J. Atmos. Sci.* in press
Herring J and Kraichnan RH 1972 *Statistical Models and Turbulence* ed M Rosenblatt and C Van Atta (Berlin: Springer-Verlag) pp148–94
—— 1979 *J. Fluid Mech.* **91** 581–97
Herring J, Orszag S, Kraichnan R and Fox D J 1974 *Fluid Mech.* **66** 417–44
Herring J, Riley J J, Patterson G S and Kraichnan R H 1973 *J. Atmos. Sci.* **30** 997–1006
Hinze J 1975 *Turbulence* (New York: McGraw-Hill)
Holloway G 1978 *J. Phys. Oceanogr.* **8** 414–27
Holloway G and Hendershott M 1977 *J. Fluid Mech.* **82** 747–65
Hoskins B J 1976 *Q. J. R. Meteor. Soc.* **102** 103–22
Huberman B A, Myerson R J and Doniach S 1978 *Phys. Rev. Lett.* **40** 780–2
Huggins E R 1970 *Phys. Rev.* A **1** 327–31
Inglis D R 1975 *Rev. Mod. Phys.* **47** 841–7
José J V, Kadanoff L P, Kirkpatrick S and Nelson D R 1977 *Phys. Rev.* B **16** 1217–41
Joyce G and Montgomery D 1972 *Phys. Lett.* **39A** 371–2
—— 1973 *J. Plasma Phys.* **10** 107–21
Julian P R, Washington W M, Hembree L and Ridley C 1970 *J. Atmos. Sci.* **27** 376–87
Kadomtsev B B 1965 *Plasma Turbulence* (Engl. trans. L C Ronson (New York: Academic))
Kelley M C and Kintner P M 1978 *Astrophys. J.* **220** 339–45
Kells L C and Orszag S A 1978 *Phys. Fluids* **21** 162–8
Khinchin A 1949 *Mathematical Foundations of Statistical Mechanics* (Engl. trans. G Gamow (New York: Dover))
Kida S 1975 *J. Phys. Soc. Japan* **39** 1395–404
Knorr G 1968 *Phys. Lett.* **28A** 166–7
Kolesnikov Y B and Tsinober A B 1972 *Magnitnaya Gidrodinamica* No 3 **23** 148–9
Kolmogorov 1941 *C. R. Acad. Sci., USSR* **30** 301, 538
—— 1962 *J. Fluid Mech.* **13** 82
Kosterlitz J M 1974 *J. Phys. C: Solid St. Phys.* **7** 1046–60
Kosterlitz J M and Thouless D J 1973 *J. Phys. C: Solid St. Phys.* **6** 1181–203
Kraichnan R H 1959 *Phys. Rev.* **112** 1181–2
—— 1965a *Phys. Fluids* **8** 575–98
—— 1965b *Phys. Fluids* **8** 1385–7
—— 1966 *Phys. Fluids* **9** 1937–43
—— 1967 *Phys. Fluids* **10** 1417–23
—— 1970a *Phys. Fluids* **13** 22–31
—— 1970b *Phys. Fluids* **13** 569–75
—— 1970c *J. Fluid Mech.* **41** 189–217
—— 1971a *J. Fluid Mech.* **47** 513–24
—— 1971b *J. Fluid Mech.* **47** 525–35
—— 1972 *J. Fluid Mech.* **56** 287–304
—— 1974a *J. Fluid Mech.* **62** 305–30
—— 1974b *J. Fluid Mech.* **64** 737–62
—— 1975 *J. Fluid Mech.* **67** 155–75
—— 1976a *J. Atmos. Sci.* **33** 1521–36
—— 1976b *J. Fluid Mech.* **77** 753–68
—— 1977a *J. Fluid Mech.* **83** 349–74
—— 1977b *J. Fluid Mech.* **81** 385–98
—— 1979 *Phys. Rev. Lett.* **42** 1677–80
Kraichnan R H and Nagarajan S 1967 *Phys. Fluids* **10** 859–70
Krasnoff E and Peskin R L 1971 *Geophys. Fluid Dyn.* **2** 123–46
Krause F and Rudiger G 1974 *Astron. Nachr.* **295** 85–193
Kriegsmann G A and Reiss E L 1978 *Phys. Fluids* **21** 258
Lamb H 1945 *Hydrodynamics* (New York: Dover)

Landau L D and Lifshitz E M 1959 *Fluid Mechanics* (Reading, Mass.: Addison-Wesley)
Langer J S and Reppy J D 1970 *Prog. Low Temp. Phys.* **6** 1
Lee T D 1952 *Q. Appl. Math.* **10** 69
Leith C 1968 *Phys. Fluids* **11** 671
—— 1971 *J. Atmos. Sci.* **28** 145
—— 1975 *J. Atmos. Sci.* **32** 2022–6
—— 1978 *Ann. Rev. Fluid Mech.* **10** 107–28
Leith C and Kraichnan R H 1972 *J. Atmos. Sci.* **29** 1041–58
Leslie D C 1973 *Developments in the Theory of Turbulence* (Oxford: Oxford University Press)
Lielausis O 1975 *Atomic Energy Review* **13** 527
Lilly D K 1969 *Phys. Fluids Suppl.* **II** 240
—— 1971 *J. Fluid Mech.* **45** 395
—— 1972a *Geophys. Fluid Dyn.* **3** 289–319
—— 1972b *Geophys. Fluid Dyn.* **4** 1–28
Lin C C 1943 *On the Motion of Vortices in Two Dimensions* (Toronto: University of Toronto Press)
Lin J T 1972 *J. Atmos. Sci.* **29** 394–6
Lorenz E N 1969 *Tellus* **21** 289–307
Lundgren T S 1972 *Statistical Models and Turbulence* ed M Rosenblatt and C Van Atta (Berlin: Springer-Verlag) pp70–100
Lundgren T S and Pointin Y B 1976 *Phys. Fluids* **19** 355–8
—— 1977a *Phys. Fluids* **20** 356–63
—— 1977b *J. Stat. Phys.* **17** 323–55
McDonald B E 1974 *J. Comput. Phys.* **16** 360–70
Martin P C, Siggia E D and Rose H A 1973 *Phys. Rev.* A **8** 423–37
Matthaeus W H and Montgomery D 1979 *Proc. Scientific Computer Information Exchange Conf.* (Livermore: Lawrence Livermore Laboratory)
—— 1980a *Proc. NY Acad. Sci.* to be published
—— 1980b submitted to *Phys. Fluids*
May R M 1967 *Phys. Lett.* **25A** 282
Merilees P and Warn H 1975 *J. Fluid Mech.* **69** 625–30
Milne-Thompson L M 1960 *Theoretical Hydrodynamics* (New York: MacMillan) 4th edn
Moffatt H K 1969 *J. Fluid Mech.* **35** 117–29
—— 1978 *Magnetic Field Generation in Electrically Conducting Fluids* (Cambridge: Cambridge University Press)
Monin A S and Yaglom A M 1975 *Statistical Fluid Mechanics: Mechanics of Turbulence* vol 1 and 2 (Cambridge, Mass.: MIT Press)
Montgomery D 1971 *Theory of the Unmagnetized Plasma* (New York: Gordon and Breach)
—— 1975a *Plasma physics: Les Houches 1972* ed C deWitt and J Peyraud (New York: Gordon and Breach) pp425–535
—— 1975b *Physica* **82C** 111–24
Montgomery D and Joyce G 1974 *Phys. Fluids* **17** 1139–45
Montgomery D, Liu C S and Vahala G 1972 *Phys. Fluids* **15** 815–9
Montgomery D and Tappert F 1972 *Phys. Fluids* **15** 683–7
Montgomery D, Turner L and Vahala G 1980 *J. Plasma Phys.* to be published
Montgomery D and Vahala G 1978 *J. Plasma Phys.* **21** 71–83
Morel P 1970 *Ann. Géophys.* **26** 815–28
Morel P and Larcheveque M 1974 *J. Atmos. Sci.* **31** 2189–96
Morf R H, Orszag S A and Frisch U 1980 *Phys. Rev. Lett.* to be published
Myerson R J 1978 *Phys. Rev.* B **18** 3204–13
Nelson D R 1978 *Phys. Rev.* B **18** 2318–38
Nelson D R and Halperin B I 1979 *Phys. Rev.* B **19** 2457–84
Nelson D R and Kosterlitz J M 1977 *Phys. Rev. Lett.* **39** 1201–5
Nicholson D R and Goldman M V 1978 *Phys. Fluids* **21** 1766–76
Novikov E A 1974 *Arch. Mech. Warsaw* **26** 741–5
—— 1975 *Zh. Eksp. Teor. Fiz.* **68** 1868–82
—— 1978a *Phys. Atmos. Ocean* **14** 668–71
—— 1978b *Zh. Eksp. Teor. Fiz.* **75** 368–76
Obukhov A M 1941 *Izv. Akad. Nauk SSSR Ser. Geogr. Geofiz.* **5** 453–66

Okuda H and Dawson J M 1973 *Phys. Fluids* **16** 408–26
Onsager L 1949 *Nuovo Cim. Suppl.* **6** 279–87
Orszag S A 1970 *J. Fluid Mech.* **41** 363–86
—— 1971 *Stud. Appl. Math.* **50** 293–327
—— 1974 *Fluid Dynamics: Les Houches 1973* ed R Balian and J-L Peube (New York: Gordon and Breach) pp235–374
—— 1976 *Proc. 5th Int. Conf. on Numerical Methods in Fluid Dynamics* ed A I van der Vouren and P J Zandbergen (Berlin: Springer-Verlag) p32
—— 1977 *Handbook of Turbulence* ed W Frost and T H Moulden (New York: Plenum) chap 10
Orszag S A and Patterson G S 1972 *Phys. Rev. Lett.* **28** 76–9
Orszag S A and Tang C-M 1978 *J. Fluid Mech.* **90** 129–43
Parker R L 1966 *Proc. R. Soc.* A **291** 60–72
Peskin R L 1973 *J. Atmos. Sci.* **30** 733–4
Phillips O M 1963 *Phys. Fluids* **6** 513–20
Phythian R 1975a *J. Phys. A: Math. Gen.* **8** 1423–32
—— 1975b *J. Fluid Mech.* **67** 145–53
—— 1976 *J. Phys. A: Math. Gen.* **9** 269–81
Phythian R and Curtis W D 1978 *J. Fluid Mech.* **89** 241–50
Platzman G W 1960 *J. Meteor.* **17** 635–44
Pointin Y and Lundgren T 1976 *Phys. Fluids* **19** 1459–70
Pouquet A 1978 *J. Fluid Mech.* **88** 1–16
Pouquet A, Frisch U and Léorat J 1976 *J. Fluid Mech.* **77** 321–54
Pouquet A, Lesieur M, André J C and Basdevant C 1975 *J. Fluid Mech.* **72** 305–19
Proudman J 1916 *Proc. R. Soc.* **92** 408–24
Redekopp L G 1977 *J. Fluid Mech.* **82** 725–45
Rhines P 1975 *J. Fluid Mech.* **69** 417–43
—— 1977 *The Sea* vol 6 (New York: Wiley) pp189–318
—— 1979 *Ann. Rev. Fluid Mech.* **11** 401–41
Richardson L F 1926 *Proc. R. Soc.* A **110** 709–37
Richardson L F and Stommel H 1948 *J. Meteor.* **5** 238–40
Roberts P H 1961a *J. Fluid Mech.* **11** 257–83
—— 1961b *Can. J. Phys.* **39** 1291–9
Robinson G D 1967 *Q. J. R. Meteor. Soc.* **93** 490–518
—— 1971 *Q. J. R. Meteor. Soc.* **97** 300–12
Rose H A 1977 *J. Fluid Mech.* **81** 719–34
Rose H A and Sulem P-L 1978 *J. Physique* **39** 441–84
Roshko A 1976 *AIAA J* **14** 1349–57
Rudnick I 1978 *Phys. Rev. Lett.* **40** 1454–5
Saffman P G 1962 *Appl. Sci. Res.* A **11** 245–55
—— 1971 *Stud. Appl. Math.* **50** 377–83
—— 1977 *Structure and Mechanics of Turbulence, Lecture Notes in Physics* vol 76, ed H Fiedler (Berlin: Springer-Verlag)
Saffman P G and Baker G R 1979 *Ann. Rev. Fluid Mech.* **11** 95–122
Salmon R 1978 *Geophys. Astrophys. Fluid Dyn.* **10** 25–53
Salmon R, Holloway G and Hendershott M C 1976 *J. Fluid Mech.* **75** 691–703
Salu Y and Montgomery D 1977 *Phys. Fluids* **20** 1–3
Salzberg A and Prager S 1963 *J. Chem. Phys.* **38** 2587
Seyler C E Jr 1974 *Phys. Rev. Lett.* **32** 515–7
—— 1976 *Phys. Fluids* **19** 1336–41
Seyler C E Jr, Salu Y, Montgomery D and Knorr G 1975 *Phys. Fluids* **18** 803–13
Smagorinsky J 1963 *Mon. Weather Rev.* **91** 99–164
Sommerfeld A 1950 *Mechanics of Deformable Bodies* (Engl. trans. G Kuerti (New York: Academic))
Spitzer L 1956 *Physics of Fully Ionized Gases* (New York: Interscience)
Starr V P 1953 *Tellus* **25** 233–46
—— 1968 *Physics of Negative Viscosity Phenomena* (New York: McGraw-Hill)
Stern 1975 *J. Marine Res.* **33** 1–23
Sudan R N and Keskinen M J 1977 *Phys. Rev. Lett.* **38** 966–70
—— 1979 *Phys. Fluids* **22** 2305–14

Sulem P-L and Frisch U 1975 *J. Fluid Mech.* **72** 417–23
Tang C-M and Orszag S A 1978 *J. Fluid Mech.* **87** 305–19
Taylor G I 1921 *Proc. London Math. Soc. Ser. 2* **20** 196–212
—— 1923 *Proc. R. Soc.* **104** 213–8
Taylor J B 1972 *Phys. Lett.* **40A** 1–2
Taylor J B and McNamara B 1971 *Phys. Fluids* **14** 1492–9
Tennekes H and Lumley J L 1972 *A First Course in Turbulence* (Cambridge, Mass.: MIT Press)
Thompson P D 1972 *J. Fluid Mech.* **55** 711–7
Tolman R C 1938 *Principles of Statistical Mechanics* (Oxford: Oxford University Press) chaps 3 and 5
Tsinober A B 1975 *Magnitnaya Gidrodinamika* No 1, 7–22
Tsytovich V N 1970 *Nonlinear Effects in Plasma* (Engl. trans. J S Wood (New York: Plenum))
—— 1972 *An Introduction to the Theory of Plasma Turbulence* (Oxford: Pergamon)
Volish A D and Kolesnikov Y B 1976a *Dokl. Akad. Nauk SSSR* **229** 573–4
—— 1976b *Magnitnaya Gidrodinamika* No 3, 25–8, 141–2
—— 1976c *Magnitnaya Gidrodinamika* No 4, 47–52
—— 1977 *Magnitnaya Gidrodinamika* No 1, 35–8
Webster E, Webster G and Chester M 1979 *Phys. Rev. Lett.* **42** 243–6 (erratum **42** 412)
Weinstock J 1968 *Phys. Fluids* **11** 354–7
—— 1977 *Phys. Fluids* **20** 1631–50
—— 1978 *Phys. Fluids* **21** 887–90
Weiss N O 1966 *Proc. R. Soc.* A **293** 310
Wiin-Nielsen A 1972 *Meteorologiske Annaler* **6** 107–24
Williams G P 1978 *J. Atmos. Sci.* **35** 1399–426
Wolibner W 1933 *Math. Z.* **37** 698–726
Young A P 1978 *J. Phys. C: Solid St. Phys.* **11** L453–5
Zakharov V E 1972 *Zh. Eksp. Teor. Fiz.* **62** 1745–59
Zimmerman J T F 1978 *Geophys. Astrophys. Fluid Dyn.* **11** 35–47